

## Article

# Experimental Research Studies on Seismic Behaviour of Confined Masonry Structures: Current Status and Future Needs

Juan Jose Pérez Gavilán Escalante <sup>1</sup>, Svetlana Brzev <sup>2,\*</sup>, Eric Fernando Espinosa Cazarin <sup>1</sup>, Sara Ganzerli <sup>3</sup>, Daniel Quiun <sup>4</sup>  and Matthew T. Reiter <sup>5</sup>

<sup>1</sup> Institute of Engineering, Universidad Nacional Autónoma de México, Mexico City 04510, Mexico; jperezgavilan@eiingen.unam.mx (J.J.P.G.E.); eespinosac@iingen.unam.mx (E.F.E.C.)

<sup>2</sup> Department of Civil Engineering, University of British Columbia, Vancouver, BC V6T 1Z4, Canada

<sup>3</sup> Department of Civil Engineering, Gonzaga University, Spokane, WA 99258, USA; ganzerli@gonzaga.edu

<sup>4</sup> Department of Engineering, Pontificia Universidad Católica del Perú, San Miguel, Lima 15088, Peru; dquiun@pucp.edu.pe

<sup>5</sup> School of Civil and Environmental Engineering, Cornell University, Ithaca, NY 14850, USA; mtr68@cornell.edu

\* Correspondence: sbrzev@mail.ubc.ca

**Abstract:** Confined masonry (CM) is a construction system that consists of loadbearing masonry wall panels enclosed by vertical and horizontal reinforced concrete confining elements. The presence of these confining elements distinguishes CM from unreinforced masonry systems, and makes this technology suitable for building construction in regions subject to intense seismic or wind activity. CM construction has been used in many countries and regions, and has performed well in past earthquakes. The purpose of this paper is to review experimental research studies related to the seismic in-plane and out-of-plane behaviour of CM structures. The authors identify the key design and construction parameters considered in previous research studies and perform statistical analyses to establish their influence on the seismic performance of CM walls. For the purposes of this study, the authors compiled databases of previous experimental studies on CM wall specimens, which were used for statistical analyses. Finally, the paper discusses research gaps and the need for future research studies that would contribute to the understanding of seismic behaviour and failure mechanisms of CM walls.

**Keywords:** confined masonry; seismic behaviour; experimental database; in-plane shear behaviour; in-plane flexural behaviour; out-of-plane seismic effects



**Citation:** Pérez Gavilán Escalante, J.J.; Brzev, S.; Espinosa Cazarin, E.F.; Ganzerli, S.; Quiun, D.; Reiter, M.T. Experimental Research Studies on Seismic Behaviour of Confined Masonry Structures: Current Status and Future Needs. *Buildings* **2023**, *13*, 1776. <https://doi.org/10.3390/buildings13071776>

Academic Editor: Marco Di Ludovico

Received: 27 May 2023

Revised: 22 June 2023

Accepted: 29 June 2023

Published: 12 July 2023



**Copyright:** © 2023 by the authors. Licensee MDPI, Basel, Switzerland. This article is an open access article distributed under the terms and conditions of the Creative Commons Attribution (CC BY) license (<https://creativecommons.org/licenses/by/4.0/>).

## 1. Introduction

Confined masonry (CM) systems consist of load-bearing masonry walls which are constructed first, one floor at a time, followed by cast-in-place reinforced concrete (RC) tie-columns. Finally, RC tie beams are constructed on top of the walls, simultaneously with the floor/roof slab construction. Horizontal and vertical RC confining elements (tie beams and tie-columns) provide confinement to the masonry walls and contribute significantly to their lateral load resistance due to in-plane and out-of-plane seismic actions. Key concepts related to design and construction of CM structures are presented elsewhere [1–3].

The first reported use of CM construction was in the reconstruction of buildings destroyed by the 1908 Messina, Italy earthquake (M 7.2), which caused over 70,000 fatalities. The evidence from numerous past earthquakes affecting some of the most seismically prone areas of the world confirmed good performance of CM structures that were designed and constructed according to the codes [3,4]. Although CM buildings experienced damage in a few severe earthquakes, such as the 2010 Maule, Chile earthquake (M 8.8), the collapse of these buildings has rarely occurred, and the number of fatalities and volume of overall losses have been small given the earthquake intensity [5]. Many earthquake engineers

believe that CM technology represents a viable alternative to the new construction of inadequately engineered reinforced concrete (RC) frames with masonry infills and/or unreinforced masonry (URM) construction. The detailing of reinforcement in CM structures is simpler compared to in RC frames, because more advanced design procedures and careful detailing of reinforcement in beams and columns is needed to achieve ductile seismic performance of RC frames. CM construction is clearly superior in terms of seismic performance compared to URM construction, due to the presence of RC confining elements. A few international initiatives have been directed at promoting CM construction for application in seismically prone countries and regions without prior experience related to CM technology [6].

CM construction has been practised in a number of European countries (Italy, Slovenia, Croatia, North Macedonia, Romania, and Serbia), as well as in Latin America (Mexico, Chile, Peru, Colombia, Argentina, and Venezuela), the Middle East (Iran, Algeria, and Morocco), South Asia (Indonesia), and the Far East (China). The combined population of countries in which CM construction has been practised is over 3.5 billion (nearly one-half of the world's population) and spans five continents [7]. Examples of global CM applications have been documented by Brzev and Mitra [1]. A review of international seismic design codes and guidelines for CM buildings was presented by Brzev et al. [8]. Based on the review of global CM design and construction practices, it can be concluded that the differences are not significant. The main source of variation is related to the application of different masonry units, ranging from solid clay bricks to multi-perforated clay blocks (also known as modular blocks) and hollow/solid concrete blocks. The size of masonry units, often limited by local masonry manufacturing practices, influences the wall thickness and the size of RC confining elements. Secondly, the type of masonry unit also influences the interface between masonry wall and adjacent RC tie-columns (toothing or reinforcing bars). Since different construction practices may influence the seismic behaviour of CM walls, the results of statistical analysis of experimental data based on the testing of CM specimens constructed using different masonry units need to be used to establish various prediction models.

This paper presents an overview of previous experimental research studies related to the behaviour of CM wall structures subjected to the effects of axial loading, flexure and shear due to in-plane and out-of-plane seismic actions and complements previous review studies on the behaviour of CM structures under in-plane seismic actions [9]. Comprehensive research studies on seismic behaviour of CM structures performed mainly in Latin American countries, e.g., Mexico, Peru, and Chile from the 1960s to the present were considered in this study. The authors also acknowledge the contributions to research and the state of practice of CM construction by researchers from other Latin American countries not included in the paper, e.g., Argentina, Colombia, Venezuela, etc. Selected experimental studies performed in other countries and regions have also been considered in this paper. The following text provides a historic overview of research studies on structural and seismic performance of CM structures from Mexico, Peru, and Chile.

Formal investigations on the behaviour of masonry structures in Mexico began after the 1957 earthquake. Early research studies were focused on axial strength of masonry walls [10], the effect of eccentric axial forces [11,12], and ductility [11,13]. Subsequently, extensive research efforts have been directed towards studying the mechanical properties of masonry components [14], cracking of walls due to differential settlements [15], and the behaviour of walls under cyclic loading [16]. The results of previous Mexican research studies were summarised in a report, which also included some post-earthquake observations and design recommendations [17]. A major analytical research study was subsequently performed [18].

The performance of high-strength reinforcing bars for masonry walls was studied [19,20], along with different reinforcing strategies [21–23]. Expressions for estimating the contribution of horizontal reinforcement were proposed based on the Mexican research studies [24–27]. Strategies for the retrofitting and design of CM shear walls with external

welded wire mesh were explored [28–30]. In 1991, the National Centre for Disaster Prevention (CENAPRED) was created in Mexico City. New facilities included the fully equipped Structures Laboratory donated by the Japanese government, which greatly enhanced experimental research capabilities. In 1997, the first shaking table in Mexico, donated by the Kajima Technical Research Institute of Japan, was inaugurated at UNAM (4 m × 4 m dimensions, five degrees of freedom, 20-ton load capacity), and the first CM building model was tested in 1999 [31].

The results of previous investigations culminated in the development of a new design code for CM structures [32]. Active research in the subsequent years led to the development of subsequent edition of the code in 2017 [33,34]. Shear strength design provisions for CM walls were fully revised based on several research studies [35–39]. The contribution of joint reinforcement to the shear resistance of CM walls was also studied [40,41]. Design expressions for masonry walls supported by beams and the related numerical models were developed [42–44]. A state-of-the-art approach for analysis and design of masonry structures, including CM structures, was presented in major publications [45,46]. Shaking-table investigations have continued to produce much-needed data on the seismic behaviour of mid-rise CM structures [47–49]. Performance of CM walls under out-of-plane lateral loading and the corresponding design approaches have been extensively studied in recent years [50].

The first application of CM construction in Peru was reported in the 1940s. Experimental testing of masonry wall specimens started after the inauguration of the Structures Laboratory of the Catholic University of Peru (PUCP) in 1979 [51]. Professor Angel San Bartolomé conducted several experimental studies on CM walls, including the effect of horizontal reinforcement and the level of axial load on the response of walls subjected to lateral cyclic loading, as well as the effect of in-plane slenderness [52,53]. Shaking-table testing of a half-scale three-storey CM building was performed [54]. Another study was focused on the comparison of behaviour of CM walls with toothed masonry-concrete interface versus the walls with horizontal steel dowels. The study was motivated by the good performance of CM walls with horizontal dowels in the 1985 Llolleo, Chile earthquake. The Japan–Peru Centre for Seismic Research and Disaster Mitigation (UNI-CISMID) was inaugurated in 1989 and included a strong wall facility, which enabled pseudo-dynamic testing of multi-storey CM walls [55]. A historic overview of research and code development related to CM structures in Peru was presented by Quiun and Santillán [56].

CM construction has been practiced in Chile since the 1930s, and has demonstrated good seismic performance in numerous damaging earthquakes [5,57]. Experimental studies on 22 CM wall specimens subjected to in-plane reversed cyclic loading performed in the 1990s were used to develop an analytical model for predicting nonlinear behaviour of CM structures [58]. Another experimental study was performed on CM walls with openings subjected to reversed cyclic loading and it involved the testing of 16 full-size specimens. A few research studies have been performed focusing on the effect of wall density on the seismic vulnerability of CM buildings in Chile [59,60], and the prediction of seismic displacement demands in CM structures [61].

The paper presents a review of previous experimental research studies related to the behaviour of CM wall structures subjected to axial loading, flexure, and shear due to in-plane and out-of-plane seismic actions. Experimental databases were compiled and analysed to identify relevant design and construction parameters and their influence on the seismic behaviour of CM buildings. A few other important design and construction aspects, such as the influence of masonry materials, the effect of openings in CM walls, and the interface between the masonry and adjacent RC confining elements, are also discussed. This paper is focused on engineered CM structures designed according to the applicable codes and guidelines, as opposed to non-engineered CM construction practices, which are not compliant with the design codes/guidelines, but are found in many countries.

## 2. In-Plane Shear Behaviour

CM walls subjected to in-plane lateral loads most often experience behaviour leading to a diagonal tension shear failure mechanism [62]. This mechanism is characterised by the development of inclined cracks in the masonry walls that ultimately propagate into the RC confined elements and culminate in failure [3] (Figure 1). It is important to note that some codes, e.g., the Mexican [33] and Peruvian [63] ones, define the shear strength of CM walls without horizontal reinforcement as the strength at the onset of cracking (stage 1), while the maximum shear strength while considering steel contribution (stage 2) is used for the design of walls with horizontal reinforcement. The shear strength of a CM wall,  $v_R$ , is determined as the sum of several components, including masonry,  $v_m$ , axial stress,  $v_p$ , and horizontal reinforcement,  $v_s$ , as follows:

$$v_R = v_m + v_p + v_s \quad (1)$$

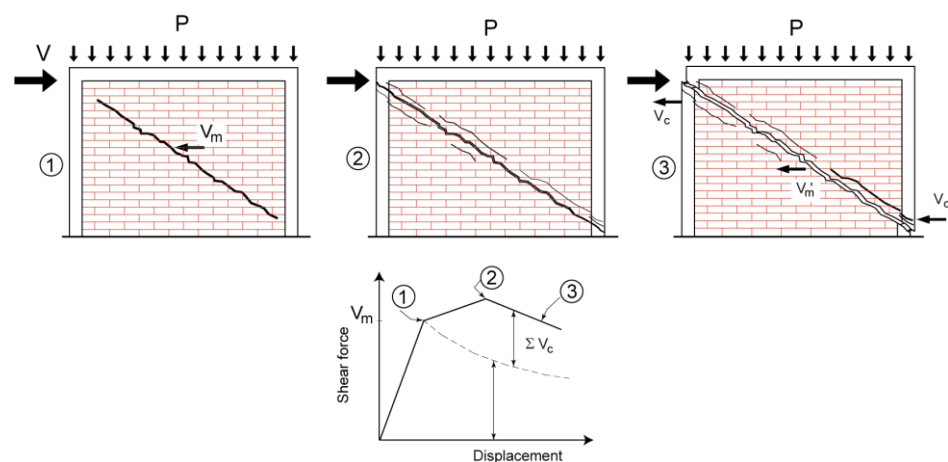


**Figure 1.** Mechanism of shear resistance for a CM wall panel: (1) the onset of diagonal cracking; (2) maximum shear strength; and (3) failure (reprinted from [3] with permission of the publisher, the Earthquake Engineering Research Institute). Note that the force–displacement curve shows a CM wall (solid line) and a URM wall (dashed line).

A review of the key parameters influencing the shear strength of CM walls is presented in this section, primarily based on the findings of previous international research studies. The authors also performed a statistical analysis using a database compiled by Treviño [64], which contains detailed data on 104 CM wall specimens from 26 experimental studies performed in Mexico, Peru, Venezuela and Chile [13,16,65–88] (see Tables A1 and A2 in Appendix A for more information). The test specimens were subjected to either monotonic or reversed cyclic lateral loading, subjected to different axial stress levels, with different wall dimensions, masonry material properties (masonry units and mortar), as well as RC tie-column materials and reinforcement. All of the specimens included in the database were solid walls (i.e., without openings). The experimental data were used to establish relationships between different specimen design parameters and masonry strength, using a simple univariate analysis.

### 2.1. Masonry Component

It has been recognised by numerous researchers that several parameters influence the shear strength of unreinforced masonry,  $v_m$ , including the wall's aspect ratio ( $H/L$ ), shear–moment interaction, and the level of axial stress. For the purpose of this study, the masonry component of shear strength can be presented in the following form:

$$v_m = av'_m f \quad (2)$$

where  $a$  is an empirical constant, which is usually in the range from 0.3 to 0.5 (based on previous research studies),  $v'_m$  is the diagonal compression strength, and  $f$  is a factor that considers the wall's aspect ratio.

### 2.1.1. The Effect of Masonry Tensile Strength

The notion that the shear strength of a wall at the onset of cracking is related to the tensile strength of the masonry and the corresponding axial stress is based on the stress analysis at the section located at the centre of the wall [89] (Figure 2). Shear strength is calculated by setting the principal tensile stress to be equal to the tensile strength of the masonry,  $f_t$ , which can be determined experimentally. In a hypothetical situation, a wall is not subjected to axial compression, and the shear strength of the masonry depends only on the tensile strength of the masonry. The shear strength of the masonry,  $v'_m$ , can be determined by performing diagonal compression tests. Alternatively, it can be estimated as a function of  $\sqrt{f_m}$ , where  $f_m$  denotes the compression strength of the masonry (which can be determined based on either the gross or net area of the section).

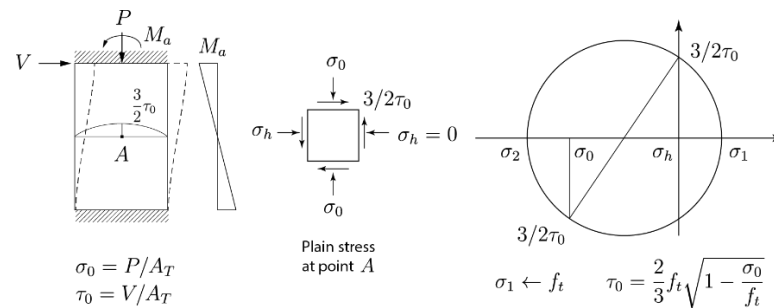


**Figure 2.** Masonry shear strength  $\tau_0$  as a function of the axial stress  $\sigma_0$ ; diagonal tension shear mechanism.

The above-mentioned experimental database [64] was used to establish a relationship between the CM shear strength,  $v_R$ , and the compression strength of the masonry,  $f_m$ , as shown in Figure 3. It was shown that the following power function

$$v_R = a_1 f_m^{a_2} \tag{3}$$

offers the best fit for the input data, with  $a_1 = 0.19$  and  $a_2 = 0.52$ . Note that the exponent  $a_2 = 0.52$  shows that the masonry shear strength is directly proportional to the square root of the compressive strength of the masonry,  $f_m$ ; this is similar to the findings of previous studies on RM walls [90].

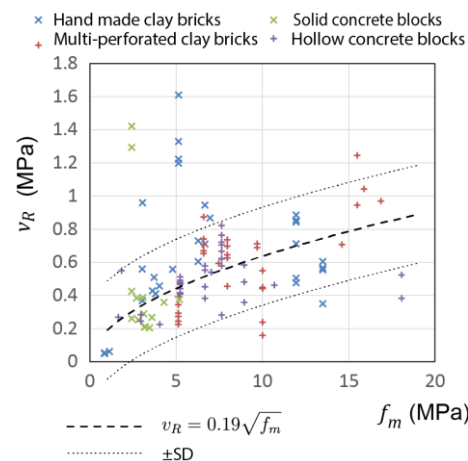


**Figure 3.** Relation between CM shear strength,  $v_R$ , and the masonry compressive strength,  $f_m$  (data from [64]).

The above equation can be presented in a form suitable for design applications, as follows:

$$v_R = 0.19\sqrt{f_m} \quad (4)$$

### 2.1.2. The Effect of Wall Aspect Ratio

An equation for the  $f$  factor, can be presented in the following form

$$f = b - c \cdot \frac{M}{V \cdot L}; \quad \frac{M}{V \cdot L} < 1 \quad (5)$$

where  $b$  and  $c$  are empirical constants determined through experimental studies. For example, D'Amore and Decanini [91] analysed the results of past experimental studies on 58 CM wall specimens with aspect ratios ranging from 0.62 to 2.95; of these, 39 specimens were subjected to reversed cyclic loading and 19 specimens were subjected to monotonic loading. The results indicated that shear resistance of CM walls should be reduced for slender walls ( $H/L > 1$ ) in order to take into account shear–moment interaction. They proposed a factor similar to the one defined in Equation (5), where  $b = 1.35$  and  $c = 0.35$ .

Alvarez [92] analysed the experimental results for 17 walls tested under reversed cyclic lateral loading in Mexico, Peru, and Chile. It was argued that, since the aspect ratio changes the internal stress distribution in a wall, it can be expected that the shear strength of walls with different aspect ratios should be different. The research study also confirmed that flexural deformation was more significant in slender walls, and that the shear strength can be expected to decrease with increasing aspect ratio, even when the failure mechanism does not change. The study also indicated an increase in the shear strength of walls with lower aspect ratios. Based on the findings of the study, Alvarez proposed an  $f$  factor similar to that in Equation (5); however, the aspect ratio  $H/L$  was used instead of the shear span ratio  $M/VL$ , and the following coefficients were used:  $b = 1.35$  and  $c = 0.35$ .

The following equations were proposed by Pérez Gavilán, Flores, and Alcocer [35] based on the results of an experimental research program performed on CM walls:

$$\begin{aligned} f &= 1.55 & h_e/L < 0.2 \\ f &= 1.69 - 0.69(h_e/L) & 0.2 \leq h_e/L \leq 1 \\ f &= 1 & h_e/L > 1 \end{aligned} \quad (6)$$

It can be seen that, according to the proposed equation, the values  $b = 1.69$  and  $c = 0.69$  should be used in Equation (5). The  $f$  factor, as presented above, was incorporated in the latest Mexican masonry design code [33] as a multiplier in the shear resistance equation for CM walls. However, in the formula in the Mexican code, the  $f$  factor is also applied to the axial stress component, that is,  $(av'_m + d\sigma_0) \cdot f$ , where the axial component  $d\sigma_0$  will be discussed later in this section. The experimental results and the proposed formula are plotted in Figure 4. The CM specimens at the ultimate stage of testing are shown in Figure 5.

Marques and Lourenço [9] also reviewed test data from previous research studies and confirmed the effect of aspect ratio on the shear strength of masonry; however, the effect of wall aspect ratio was considered an independent term, as opposed to a multiplier for the overall shear strength, which is used in the Mexican masonry code [33] and in design provisions for reinforced masonry (RM) walls in several international design codes. Past research studies have shown that shear span ratio ( $M/VL$ ) is a more useful parameter than the aspect ratio ( $H/L$ ), because it is able to account for different boundary conditions when  $M/V$  is considered to be the effective wall height, see Figure 6 [35]. Note that  $V$  is the applied shear force,  $M$  is the bending moment acting on the wall section under consideration (usually located at the base of the wall), and  $L$  denotes the length of the wall.

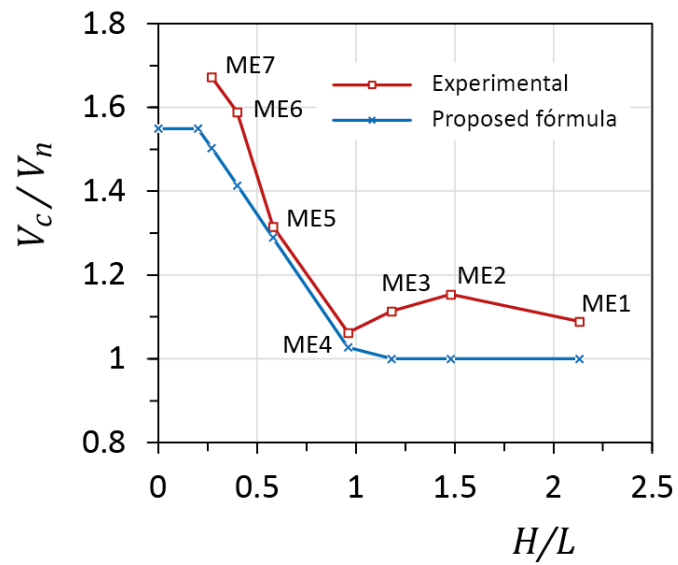


Figure 4. Experimental versus predicted shear resistance at the onset of cracking (adapted from [35]).

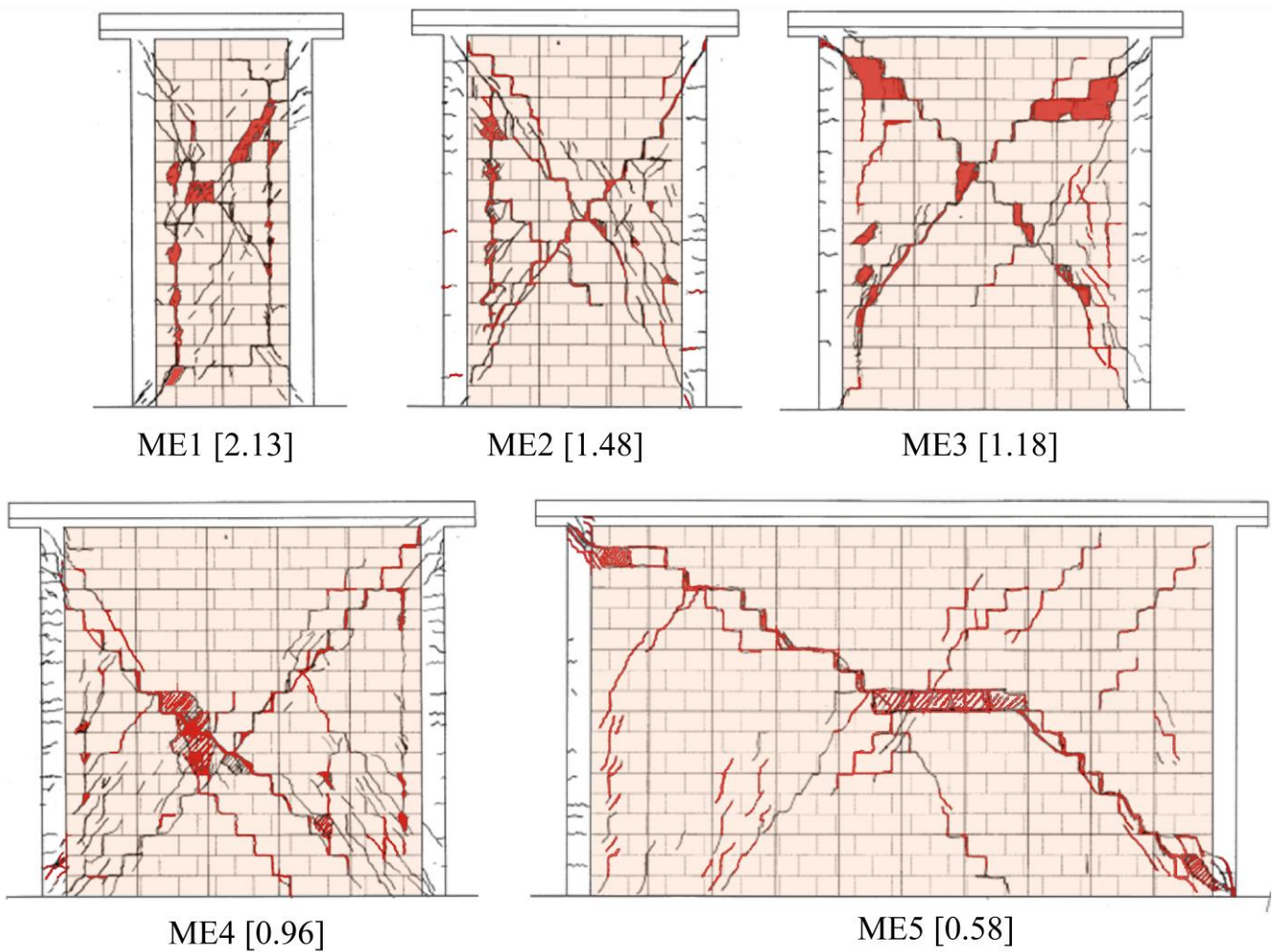
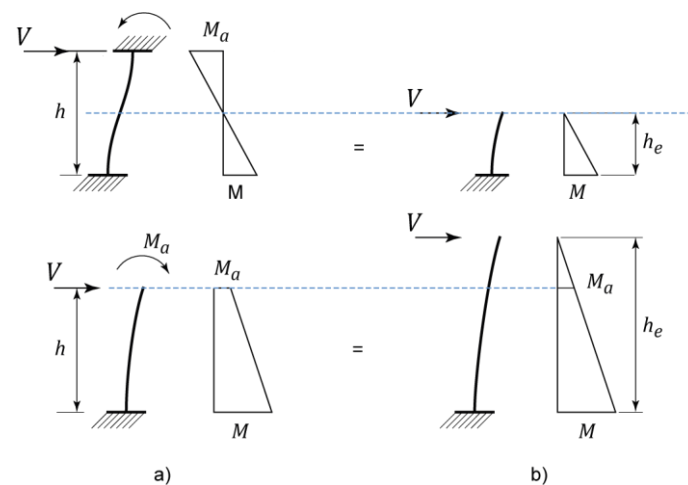


Figure 5. Damage patterns for various test specimens at the end of the test (the corresponding aspect ratios are shown in brackets) (adapted from [35]).



**Figure 6.** Effective height for different boundary conditions: (a) actual boundary conditions and (b) the corresponding effective heights  $h_e/L = M/VL$  (adapted from [35]).

### 2.1.3. Shear–Moment Interaction

Boundary (end support) conditions in masonry shear walls may range from a cantilever condition (fixed at the base and free at the top), which corresponds to single-curvature bending, to a fixed–fixed condition (i.e., with both ends fixed), which corresponds to double-curvature bending (see Figure 6). It appears that the presence of a bending moment at the top causes a decrease in the shear resistance of a masonry wall. Unfortunately, experimental research evidence related to this topic is very limited, at least in the context of CM walls. The Peruvian masonry design code [63] included a reduction in the shear strength for slender walls ( $H/L > 1$ ) due to the moment at the top of the wall, based on the results of a numerical study [93].

Based on a review of the experimental data related to 58 CM walls, D’Amore and Decanini [91] proposed a factor to account for shear–moment interaction in walls with aspect ratio  $H/L > 1$ . The proposed factor resulted in a decrease in the shear strength due to an increase in the bending moment at the top.

The effect of shear–moment interaction was examined in an experimental study on five fully grouted RM walls with  $H/L = 1$  [94]. The results indicated the effect of  $M/VL$  ratio on the shear resistance and ductility of the test specimens (Figure 7a). The specimen with  $M/Vd_v = 1.2$  (corresponding to  $M/VL = 1.25$ , solid line) attained a shear capacity that was by approximately 25.0% higher than the corresponding capacity of an otherwise identical specimen with  $M/Vd_v = 1.8$ . It was also observed that the specimen with a lower shear capacity demonstrated a somewhat higher ductility.

Pérez Gavilán [39] proposed an approach for reducing the shear strength of CM walls, based on the hypothesis that diagonal cracking occurs when a threshold lateral displacement is attained, regardless of whether the lateral displacement is due to lateral force, bending moment, or both. An experimental study on six CM wall specimens subjected to reversed horizontal cyclic loading and bending moment at the top was performed to verify the proposed hypothesis. The ratio of the shear resistance with a moment on top of the wall,  $V_c$ , and the shear resistance without moment at the top (cantilever condition),  $V_n$ , is shown on the vertical axis in Figure 7b, while the aspect ratio of the wall ( $w$ ) is shown on the horizontal axis. The key parameter affecting the extent of reduction in shear strength is a normalised moment  $\beta$  (ratio of bending moment at the top of the wall and the moment corresponding to the fixed–fixed condition). Note that  $\beta = -1$  corresponds to the fixed–fixed condition (double-curvature bending), while  $\beta = 0$  corresponds to the cantilever condition. Figure 7b shows the results for single curvature bending. The results also depend somewhat on the ratio of the moduli of rigidity and elasticity for masonry  $G/E$ , which ranged from 0.2 to 0.4 (see dashed and solid lines on Figure 7b). It can be

seen from the diagram that  $V_c/V_n$  ratio rapidly increases when aspect ratio ( $w$ ) is less than 1.0 (squat walls); therefore, the effect of shear–moment interaction is insignificant for squat walls. However, a significant decrease in the  $V_c/V_n$  values can be observed when  $w$  increases from 1.0 to 3.0; this effect is particularly pronounced for higher  $\beta$  values (1.0 to 2.0), which may correspond to walls in multi-storey buildings. Based on the analyses of several real-life structures, the results of another research study [95] pointed out that shear–moment interaction term may be important for squat walls with aspect ratios in the range from 0.5 to 1.0. Note that slender walls are usually not affected by shear–moment interaction because they typically experience double-curvature bending.

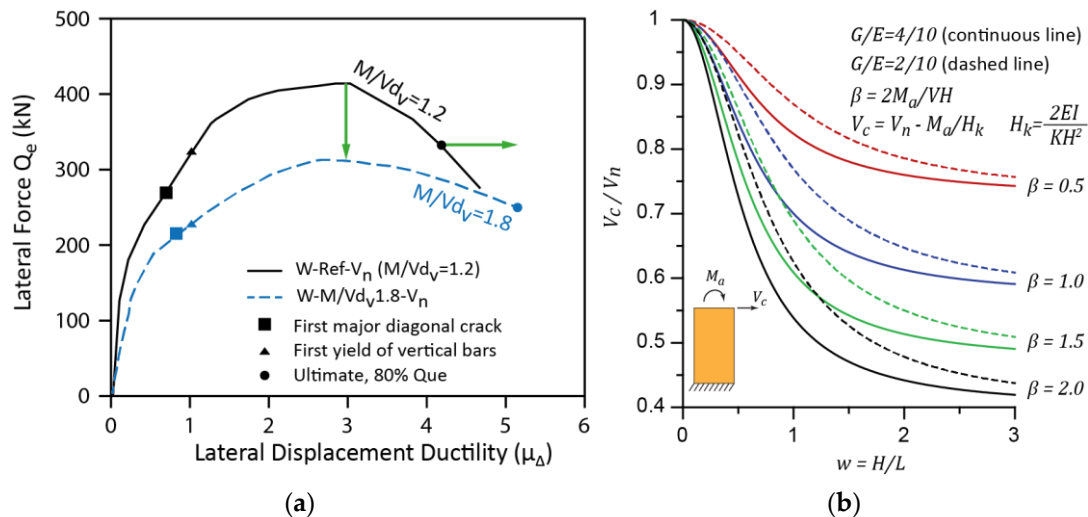


**Figure 7.** Moment–shear interaction in masonry walls: (a) the effect of shear span ratio on the shear resistance of RM walls (adapted from [94]) and (b) the effect of moment at the top on the normalised shear resistance of CM walls with different aspect ratios (adapted from [39]).

## 2.2. The Axial Stress Component

An interaction between compression and shear stresses in masonry walls is well established [96]. Low to moderate axial compression enhances the shear strength of masonry walls by delaying the onset of cracking in the wall, because axial compression causes a decrease in the magnitude of principal tensile stress. An experimental study on RM wall specimens [97] showed that a relatively modest increase in axial compression stress from 0 to 2.5% of the masonry compression strength  $f_m$  resulted in an increase in the wall shear resistance of more than 20%. It was also observed that RM walls subjected to higher axial compression stresses had a reduced post-cracking deformation capacity, thereby resulting in a more brittle failure mechanism. Based on the statistical analysis of test data on RM shear walls, Anderson and Priestley [98] recommended taking the axial stress component of the masonry shear strength to be 25% of the applied axial stress due to wall self-weight and tributary load from the floors and roof; this was incorporated in the Canadian masonry design code CSA S304-14 [99]. Several research studies on RM shear walls have confirmed a positive effect of axial compression on the masonry shear resistance. In the post-cracking stage, axial compression in the wall causes a delay in the initiation of diagonal cracks, controls the crack width, and improves the force transfer through an aggregate interlocking mechanism [97,100].

According to the New Zealand masonry code (NZS 4230 2004) [101], which is mostly focused on the design of RM walls, axial compression is transmitted from the top to the base of an RM wall by means of a compression strut inclined under an angle  $\alpha$  with regard to the wall axis, with a magnitude that depends on the boundary conditions (cantilever/fixed). The horizontal component of the strut force ( $\tan \alpha \cdot \sigma_0$ ) is taken as the axial stress component of the wall's shear resistance.

The axial stress component of the shear strength for a CM wall has been found to have a significant effect on its shear strength [9,13,102], and can be presented as follows:

$$v_p = d\sigma_0 \quad (7)$$

where  $d$  is an empirical constant, usually in the range from 0.2 to 0.4, but it may be taken to be equal to 0.4, while  $\sigma_0$  denotes the axial stress applied to the wall.

An experimental database [64] was used to establish a relationship between the CM shear strength  $v_R$  and compressive stress  $\sigma_0$ , as shown in Figure 8. It should be noted that 104 data points were considered; of these, 48 points corresponded to specimens that were not subjected to axial compression. It was shown that the following linear function

$$v_p = d_1\sigma_0 + d_2 \quad (8)$$

offers the best fit for the given data when  $d_1 = 0.3952$  (rounded to 0.40) and  $d_2 = 0.4743$  (rounded to 0.47). Note that the independent term  $d_2$  denotes an average shear stress resistance of the CM wall without axial stress.

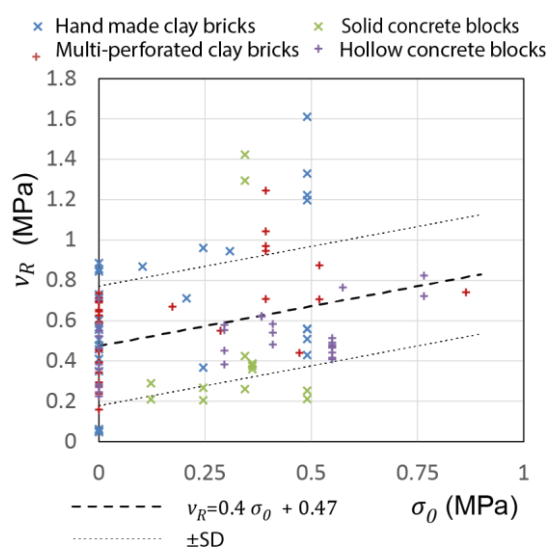


**Figure 8.** The effect of axial stress on the masonry shear strength in CM walls based on statistical analysis of experimental data [64].

### 2.3. Contribution of Horizontal Reinforcement

CM walls may include horizontal reinforcement, usually in the form of ladder-type wire, known as joint reinforcement (JR), which is anchored into the RC tie-columns. The contribution of the reinforcement to the shear strength of a CM wall,  $v_R$ , can be presented as follows:

$$v_s = e\rho_h f_{yh} \quad (9)$$

where  $e$  is an empirical constant,  $\rho_h$  is the horizontal reinforcement ratio, and  $f_{yh}$  is the steel yield strength for JR. For RM walls, the value of  $e$  is typically in the range from 0.4 to 0.8 [99,101,103]. It should be noted that in RM walls, the main horizontal reinforcement contributing to the shear resistance comes in the form of reinforcing bars, similar to those used in RC structures, although JR may also be provided for non-structural purposes. In Mexico, ladder-type JR is no longer used, because it was shown that welded cross wires tended to fail, and small-diameter, high-strength bars ( $f_{yh} = 600$  MPa) are currently used.

Several researchers have proposed mechanical models for predicting the contribution of horizontal reinforcement to CM shear strength [104,105]; however, the accepted model is still mostly empirical, that is, it is based on the experimental evidence [16,25,26,90,106–108].

The contribution of horizontal reinforcement to the shear strength of RM and CM walls was determined based on the assumption of a single diagonal crack inclined under a  $45^\circ$  angle with respect to the horizontal axis [98]. It is considered that horizontal reinforcement is engaged in resisting internal tensile stresses in the wall only after the first crack extends in an incline relative to the reinforcement [107]; this was verified by measuring tensile strain in the JR in an experimental study [40]. When a CM wall experiences the sliding failure mode, JR is no longer effective at resisting shear stress, but it could enhance the wall's lateral drift capacity [49]. A review of the results of previous experimental studies on CM walls showed that JR does not seem to increase their ductility [109].

Matsumura [90] suggested that the contribution of horizontal reinforcement in RM walls depends on the masonry compression strength,  $f_m$ . The same finding was later confirmed by an experimental research study on CM walls, which also revealed an upper limit for the amount of JR (expressed as a function of the  $f_m$ ), beyond which it is not possible to attain a further strength increase [40]. As a consequence, CM walls with a low masonry compression strength,  $f_m$ , may experience only a marginal increase in shear strength due to the use of JR. However, JR could be effective at increasing their displacement capacity.

An experimental database [64] was used to estimate the contribution of JR to the shear strength of the steel component of CM, as shown in Figure 9. It should be noted that 104 data points in total were considered in the statistical analysis; of these, 69 points corresponded to specimens without JR.

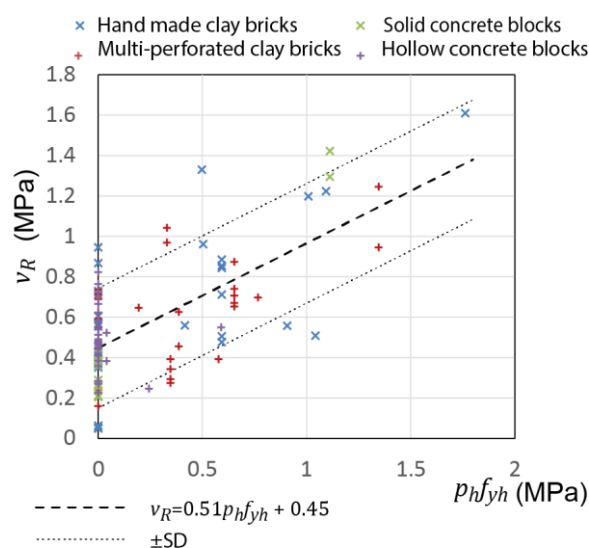


**Figure 9.** The effect of horizontal joint reinforcement (JR) on CM shear strength (based on the experimental database [64]).

It was shown that the following linear function provided the best fit:

$$v_s = e_1 \rho_h f_{yh} + e_2 \quad (10)$$

where  $e_1 = 0.5186$  (rounded to 0.51) and  $e_2 = 0.447$  (rounded to 0.45); hence, 0.5 is recommended as a reasonable value for  $e_1$  in Equation (10).

#### 2.4. The Effect of RC Tie-Columns

RC tie-columns are important components of CM walls, and influence their in-plane shear strength and lateral displacement capacity. Research studies have shown that the tie-columns prevent wall disintegration and provide additional shear capacity in the post-cracking stage. Borah, Kaushik and Singhal [110] performed an experimental study on six half-scaled CM wall specimens subjected to reversed cyclic loading to examine the effect of the amount of longitudinal reinforcement in RC tie-columns on the shear and lateral

displacement capacity of CM walls. The longitudinal reinforcement ratio in tie-columns ranged from 0.7% to 1.0%. The results indicated a significant increase both in the shear and displacement capacity by more than 40% in non-squat CM wall specimens, while in the squat specimens there was no significant difference in shear capacity, but the displacement capacity doubled in the specimen with a higher longitudinal reinforcement ratio.

Based on the statistical analysis of the experimental test data, several researchers concluded that longitudinal reinforcement in tie-columns has a significant effect on the CM shear resistance [24,102,111,112]. Marques and Lourenço [9] also analysed a significant amount of test data, but did not establish a significant relation between the tie-column longitudinal reinforcement and the shear resistance of CM walls.

The main design parameters related to RC tie-columns are longitudinal reinforcement ratio  $\rho$ , steel yield strength  $f_y$ , and concrete compressive strength  $f'_c$ . Using the same parameter ( $\sqrt{\rho f_y f'_c}$ ) as Riahi, Elwood and Alcocer [102], the following linear model was fitted to predict the shear strength of CM walls based on the available data:

$$v_R = f_1 \sqrt{\rho f_y f'_c} + f_2 \tag{11}$$

The regression analysis showed that  $f_1 = 0.029$  and  $f_2 = 0.1647$  offer the best fit. A chart presenting the test data and the fitted model is shown in Figure 10. The diagram shows that longitudinal reinforcement in RC tie-columns has a significant influence on the shear strength of CM walls.

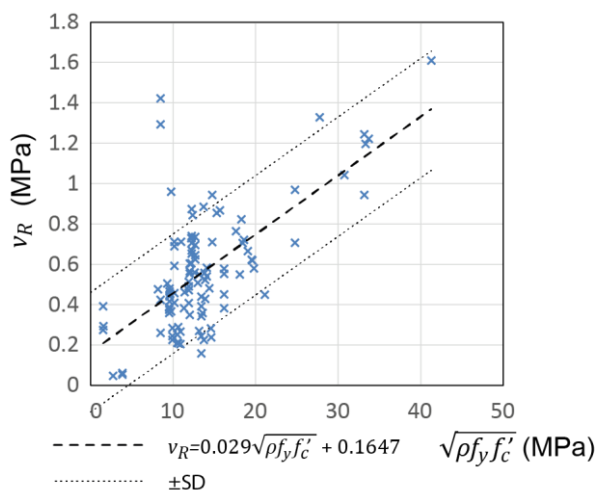


Figure 10. The effect of RC tie-columns on the shear strength of CM walls (experimental data [64]).

### 2.5. Multivariate Model

A multivariate linear model was created to identify the statistical significance of the key variables discussed in this section and their corresponding coefficients, i.e.,  $v_m$ ,  $\sigma$ ,  $H/L$ ,  $\rho_h f_{yh}$  and  $\sqrt{\rho f_y f'_c}$ . The products  $v_m \times H/L$  and  $\sigma \times H/L$  were initially also considered, because the factor  $f$  depends on the  $H/L$  ratio and is usually applied when the masonry shear strength,  $v_m$ , and axial stress,  $\sigma_0$ , are considered together; however, these variables were ultimately omitted from the model, because their influence was very small. The multivariate analysis, carried out using the STATA statistical analysis program, resulted in the following model:

$$v_R = a v_m + b \sigma + c \frac{H}{L} + d(\rho_y f_{yh}) + e \sqrt{\rho f_y f'_c} \tag{12}$$

The results are presented in Table 1, showing the coefficients for each variable, the Pearson’s significance  $p$ , where the variable is indicated to be statistically significant when  $p < 0.05$ , and 95% Confidence Interval.

**Table 1.** Multivariate analysis of shear strength,  $v_R$ .

Variable	Coef.	$p$	95% Confidence Interval	
$v_m$	$a = 0.31$	<0.001	0.19	0.43
$\sigma$	$b = 0.26$	0.001	0.12	0.41
$H/L$	$c = -0.11$	0.002	-0.18	-0.04
$p_h f_{yh}$	$d = 0.39$	<0.001	0.30	0.48
$\sqrt{\rho f_y f'_c}$	$e = 0.001$	0.001	0.0004	0.0016

$R^2 = 0.726$ .

It can be seen from the table that the correlation coefficient is  $R^2 = 0.726$ , which indicates a satisfactory prediction, and that all variables are statistically significant. A negative  $c$  value indicates that the shear strength decreases with aspect ratio. The same model, as described in Equation (12), was developed using  $\sqrt{f'_m}$  instead of  $v_m$ , which resulted in a coefficient  $a = 0.06$  and the  $R^2 = 0.67$ . It can be concluded that  $v_m$  is a better predictor of shear strength,  $v_R$ , than  $\sqrt{f'_m}$ .

It should be noted that the proposed multivariate model is different from the models developed by other researchers, e.g., a model by Marques and Lourenco [9] developed based on an experimental database of 104 CM wall specimens. These models are similar in that they take into account the effect of masonry shear strength, axial compression stress in the wall, and aspect ratio; however, the proposed model also takes into account the effect of horizontal wall reinforcement and the amount of longitudinal reinforcement in RC tie-columns, while [9] accounts for a ratio between the masonry wall area and the total CM wall area. Another model, developed by Riahi, Elwood, and Alcocer [102], is based on a regression analysis of an experimental database consisting of 102 CM wall specimens, and considers the effect of masonry shear strength, axial compression stress, and the effect of longitudinal reinforcement in RC tie-columns. The model does not take into account the influence of wall aspect ratio and horizontal wall reinforcement, since the results of the regression analyses indicated that their influence was insignificant. It should be noted that the experimental data used for all three models included research from different countries and regions, with the greatest number of studies (and their corresponding data points) coming from Latin American countries; this can be attributed to the significant scale of experimental research studies in that region.

## 2.6. Lateral Displacement/Drift Capacity

CM walls, when subjected to in-plane lateral loads, usually demonstrate a shear-dominant behaviour; this can be attributed to the relatively low aspect ratio, absence of horizontal reinforcement, and a design approach that does not require the development of a flexural failure mechanism. It is well established that a shear-dominant failure mechanism is force controlled and is characterised by a limited lateral displacement/drift capacity. However, RM shear walls with shear-dominant behaviour have demonstrated a significant displacement/drift capacity beyond the cracking stage, as shown by previous experimental studies [97,107,113]; this can be partially attributed to the presence of horizontal reinforcement in these walls.

Pérez Gavilán [109] reviewed the results of five experimental studies from Mexico employing 26 full-size CM wall specimens that were subjected to reversed cyclic loading [26,35,40,41,65]. The specimens were constructed using different types of masonry unit, including solid clay bricks, multi-perforated clay blocks, and hollow concrete blocks. The majority of the specimens were reinforced with horizontal JR according to the requirements of the Mexican masonry code [32]. Lateral drift ratios were determined for each specimen at the following critical stages (see Figure 1): the onset of cracking, peak shear capacity ( $\gamma_R$ ), and the ultimate drift capacity ( $\gamma_U$ ) at failure, which corresponds to the force at 80% of peak capacity. The drift ratios at the peak shear capacity ( $\gamma_R$ ) varied from 0.24 to 1.0%,

while the maximum drift capacity ( $\gamma_U$ ) ranged from 0.40 to 2.06%. The study showed that the drift capacity was significantly influenced by the presence of horizontal reinforcement and the type of masonry unit. It was observed that the specimens constructed using hollow concrete blocks demonstrated lower drift capacity than other specimens.

Figure 11 shows the drift ratios at peak strength ( $\gamma_R$ ) for the specimens from the experimental database [64], with a mean drift capacity of 0.49%.

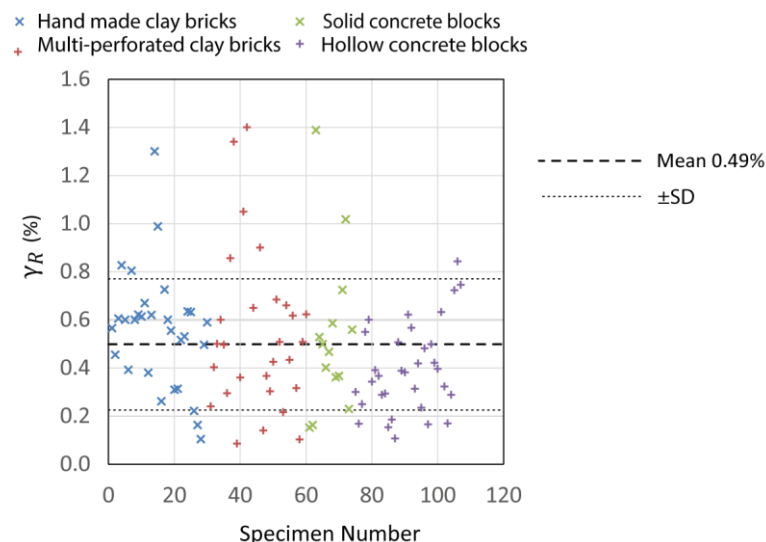


**Figure 11.** Drift ratios at peak strength ( $\gamma_R$ ) based on the experimental data [64].

Several authors have proposed a reduction in the masonry shear strength based on the requirement for ductility in RM shear walls [98,114]. Note that RM shear walls are usually designed to achieve a flexural failure mechanism, in which a plastic hinge develops at the base of the wall. In such a scenario, flexural–shear cracks widen after a few loading cycles, which causes a decrease in the wall shear resistance due to a loss of aggregate interlock shear mechanism. The same phenomenon was reflected in the conceptual model for concrete shear strength proposed by the Applied Technology Council [115], but it is not representative of CM walls. Although the CM walls may attain high ductility [109], these walls usually experience shear failure. Riahi, Elwood and Alcocer [102] observed an inverse relationship between the displacement ductility and the peak shear strength in CM walls; however, it was observed that the ductility depends on the type of masonry unit.

### 3. Behaviour of CM Walls Subjected to Combined Axial Compression and In-Plane Flexure

CM walls subjected to combined axial and in-plane lateral loading usually do not develop a flexural failure mechanism, because the diagonal tension shear mechanism which was discussed in the previous section is the most prevalent. The design of CM walls for flexure under seismic conditions is different from the seismic design of RM shear walls, which are explicitly designed to experience flexural failure according to the Capacity Design approach, e.g., in the USA, Canada, and New Zealand [101]. Design provisions are also based on extensive research studies on the flexural behaviour of these walls in the countries in which RM construction has been practised [98,116,117]. The flexural strength of CM shear walls can be estimated based on the assumptions of flexure theory, such as the plane deformation of the horizontal section of a wall, and an equivalent rectangular stress block simulating the distribution of compression stresses. This section discusses the behaviour of CM walls when subjected to combined axial load and flexure, based on the evidence from experimental studies, and approaches for estimating their strength for design purposes.

### 3.1. Experimental Research Studies

Yielding of the longitudinal reinforcement, development of horizontal cracks in RC tie-columns and concrete crushing at their base are characteristic for flexure-dominant behaviour in CM walls (Figure 12a). In slender walls (with an aspect ratio of 1.0 or higher) vertical cracks develop close to the interface between the masonry panel and adjacent RC tie-columns [118]. The cracks occurred due to the bond pattern used and the non-uniform vertical deformation of the wall. Vertical cracks in slender walls were also reported in [35] (damage patterns for specimens ME1 and ME 2 are shown in Figure 5). The specimens attained high levels of displacement ductility, ranging from 5.65 to 10.45 (ductility was determined according to [119]). As expected, it was observed that the flexural strength increased with increasing axial stress level, as expected.

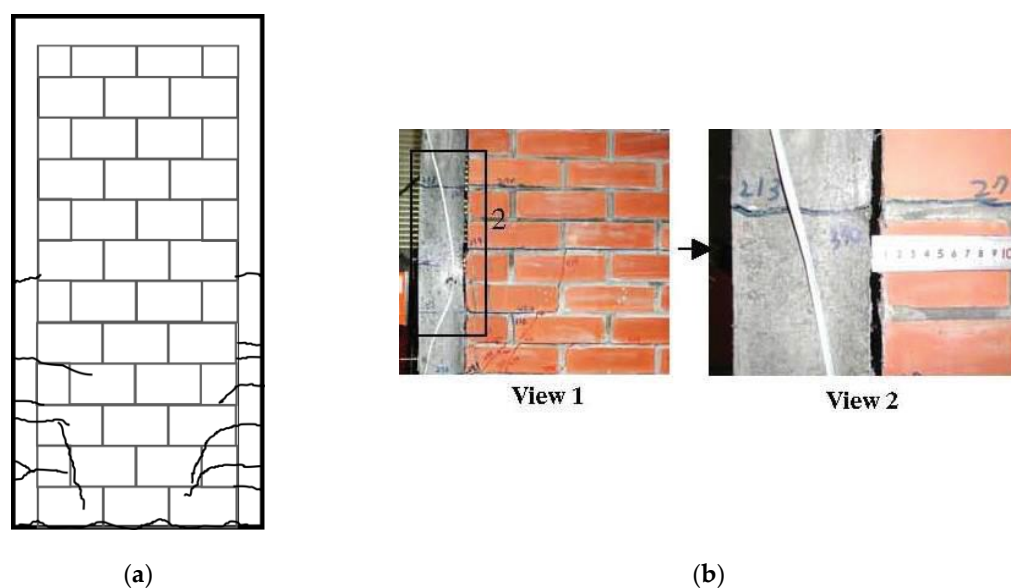


**Figure 12.** Flexural behaviour of CM shear walls observed in experimental studies: (a) damage pattern in specimen M5 at a displacement ductility of 6.0 (adapted from [118]), and (b) separation of RC tie-columns from the masonry panel and horizontal cracks [120].

Yoshimura et al. [120] identified the separation of RC tie-columns from the masonry panel as the cause of early failure of CM walls subjected to intense earthquakes (Figure 12b). They conducted an experimental study to investigate the performance of CM walls with two types of reinforcement aimed at preventing the separation of tie-columns from masonry panels. The program included 28 full-size wall specimens; of these, eight specimens had U-shaped steel reinforcing bars (dowels) extending from the wall into the tie-columns, another eight specimens had straight horizontal dowels, while the remaining specimens had no horizontal reinforcement at the interface. The boundary conditions were fixed–fixed (causing double-curvature bending) or cantilever (single-curvature bending). In addition, the specimens were subjected to two different levels of axial load.

The researchers classified failure modes into flexural failure, diagonal tension shear failure, and combined shear and flexural failure. Of the 28 specimens, 13 specimens were designed to experience flexural failure; however, only five specimens failed via pure flexure. One experienced combined shear and flexural failure, two experienced a flexure–sliding failure, and four specimens underwent shear failure. The flexure–shear mode of failure was expected for two specimens, but those walls experienced shear failure. In contrast, the researchers predicted that 13 specimens would experience shear failure, but 10 specimens experienced shear failure, while the remaining specimens experienced a flexure–sliding failure. It should be noted that the specimens were designed according to the Japanese masonry code.

The specimens with cantilever boundary conditions initially showed flexural behaviour, but ultimately experienced either sliding or shear failure. Unreinforced CM walls with fixed–fixed boundary conditions and without dowels at the tie-column-to-masonry-panel interface did not experience separation of RC tie-columns from the masonry panel, but the specimens with the cantilever boundary conditions and without dowels showed signs of separation. The study showed that the dowels (U-shaped or straight bars) were effective at preventing the separation of tie-columns from the masonry panels.

Meli and Salgado [13] carried out one of the first experimental studies on the behaviour of CM walls subjected to lateral loading. The study included 46 CM specimens subjected to monotonic static loading; of these, five specimens experienced flexural failure (#502, #512, #513, #514, and #517). All walls had a cantilever boundary condition, but they were subjected to different levels of applied axial compression. The specimen dimensions (length  $\times$  width) were 2 m  $\times$  2 m, and hollow concrete blocks were used for construction. RC tie-columns were in the form of two 9.5 mm diameter longitudinal reinforcement bars, made of steel with 420 MPa nominal yield strength. The relatively low longitudinal reinforcement ratio in the tie-columns was most likely responsible for the flexure-dominant behaviour and failure in these walls. The experimental results, in the form of lateral-force-versus-drift ratio, are presented in Figure 13. It can be seen from the chart that the specimens subjected to higher axial load (e.g., #513 and #514) demonstrated higher shear capacity compared to the specimens with lower axial stress levels (e.g., specimens #502 and #517).

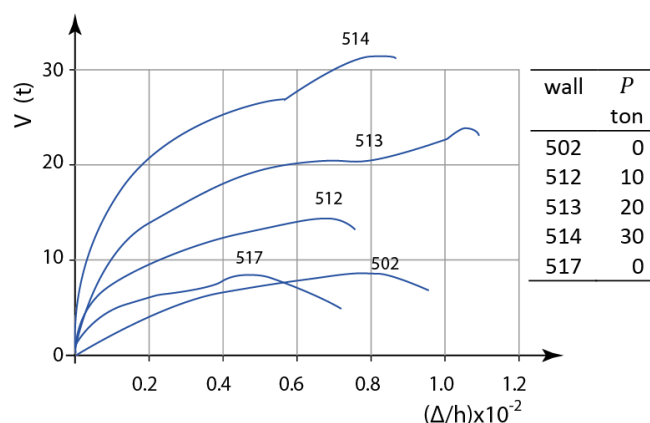


**Figure 13.** Shear-force-versus-drift ratio for the CM wall specimens with flexure-dominant behaviour (adapted from [13]).

Two research studies involved the performance of shaking table tests on CM building models with walls designed to undergo flexural failure [54,121]. San Bartolome et al. [54] tested a three-storey, half-scale CM building model that experienced flexural cracking at the base of the walls due to the yielding of the vertical reinforcement in the tie-columns, until ultimately the walls experienced shear failure. Bustos et al. [121] tested a two-storey, half-scale CM building model. The response was initially characterised by flexural cracking at the base of the tie-columns, followed by sliding cracks in the lower portion of the walls on the first storey level, but the model ultimately experienced a flexural failure mechanism.

Varela-Rivera et al. [122] tested seven CM wall specimens made of autoclaved aerated concrete (AAC) units. Three specimens (M5 to M7) were identical, and were designed to experience flexural behaviour, but were subjected to different axial compression stresses. The walls had an aspect ratio of 2.26 and were subjected to different axial compression stresses: 0.24, 0.47 and 0.71 MPa. The performance of these specimens was characterised by the yielding of the longitudinal reinforcement, and the appearance of horizontal cracks near the base and inclined shear cracks that eventually propagated through the tied columns before failure took place. As expected, the flexural strength of the walls increased with increasing axial stress level. Flexural strength predictions based on the equivalent rectangular stress

showed excellent agreement with the experimental results. It was also observed that the ductility increased with decreasing axial compression stress.

In another experimental study, specifically focused on the flexural behaviour of CM walls [118], six CM wall specimens were constructed using multi-perforated clay blocks with different aspect ratios (1.1, 1.5 and 2.4) and axial stress levels (0.24, 0.47, and 0.71 MPa). Longitudinal reinforcement in the tie-columns was in the form of a single 9.5 mm diameter steel bar with a nominal yield strength of 412 MPa, but no transverse reinforcement was provided. The flexural strength predictions were made based on the flexural theory, with a rectangular stress block for the compression zone and considering the effect of strain hardening in tension steel, and were in excellent agreement with the experimental results. It should be noted that in all cases, the neutral axis depth at the ultimate stage was rather small (it was located within the tie-column).

### 3.2. Estimating the Moment Resistance of CM Walls Subjected to a Combination of Axial Load and Flexure

Based on the results of their experimental study, Meli and Salgado [13] proposed Equation (13) for predicting the moment resistance,  $M_R$ , of CM walls subjected to axial load,  $P$ , using a few simplifying assumptions. For example, it was assumed that longitudinal reinforcement in tie-columns would yield both tension and compression (Figure 14).

$$M_R = A_s f_y d' + P \frac{d'}{2} \quad (13)$$

where  $A_s$  is the area of longitudinal reinforcement in RC tie-columns,  $f_y$  is steel yield strength,  $d'$  is the distance between the longitudinal reinforcement centroids of the tied columns, and  $P$  is the axial force.

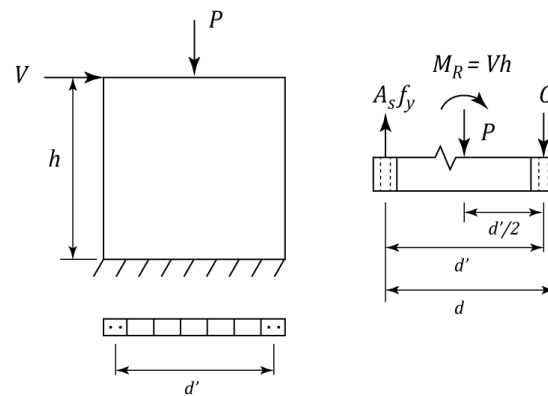


**Figure 14.** Moment resistance for CM walls subjected to combined axial load and flexure (adapted from [13]).

Subsequently, the same researchers [15] proposed a set of Equations (14)–(16) for the moment resistance of CM walls subjected to axial load and flexure, as follows:

$$M_R = M_0 + 0.28Pd' \quad \text{if } P \leq P_R/3 \quad (14)$$

$$M_R = (1.5M_0 + 0.14Pd) \left(1 - \frac{P}{P_R}\right) \quad \text{if } P > P_R/3 \quad (15)$$

$$M_0 = A_s f_y d' \quad (16)$$

where  $d$  is the effective length of the wall section (distance from the centroid of tension steel to the extreme compression fibre), and  $d'$  is the distance between the longitudinal reinforcement centroids of the tie-columns. Note that  $P$  is the applied axial force, while  $P_R$  is the axial load resistance.

The above equations were later incorporated into the Mexican masonry code, with a few changes in the coefficient values, e.g., the value 0.28 in Equation (14) was changed to 0.30, while the value 0.14 in Equation (15) was changed to 0.15 [32,33].

Marques and Lourenço [9] performed a review of moment resistance ( $M_R$ ) design equations from the Mexican masonry design code. They concluded that the equations provide a good estimate when the wall aspect ratio is equal to 1.0, but the estimates are less accurate for other aspect ratio values. They proposed an alternative, Equation (17), based on the flexure theory adapted from Tomažević [123], which is applicable to the CM walls subjected to low axial stress levels. A uniform stress distribution based on the equivalent rectangular compression stress block was assumed for the compression zone of the wall section, with the stress intensity to be determined based on the lesser of design compressive strength for masonry or concrete.

Neutral axis depth,  $x$ , is determined from Equation (18) assuming that longitudinal steel in tie-columns  $A_s$  yields in tension (yield strength  $f_y$ ), but the contribution of longitudinal reinforcement in compression has been ignored, as follows:

$$M_R = A_s f_y (d - 0.4x) + P \left( \frac{L}{2} - 0.4x \right) \quad (17)$$

$$x = \frac{P + A_s f_y}{0.8 \eta_f f'_m t} \quad (18)$$

where  $L$  and  $t$  denote the wall length and thickness, respectively, and  $\eta_f$  is the multiplier for the equivalent rectangular stress block, taken to be equal to 0.85. The proposed equation was verified for 13 CM wall specimens on the basis of three experimental studies.

### 3.3. The Effect of Axial Stress and Wall Aspect Ratio ( $H/L$ )

The effect of the axial stress and wall aspect ratio on the flexural strength of CM walls was studied by analysing results for eight wall specimens from two experimental research studies performed in Mexico, as shown in Figure 15 [13,122]. It can be seen from the chart that normalised moment resistance increased with increasing level of axial stress, which is in line with the design equations for walls subjected to relatively low levels of axial stress; however, it appears that the effect of higher axial stress levels is more significant in slender walls, e.g., for an  $H/L$  value of 2.38.

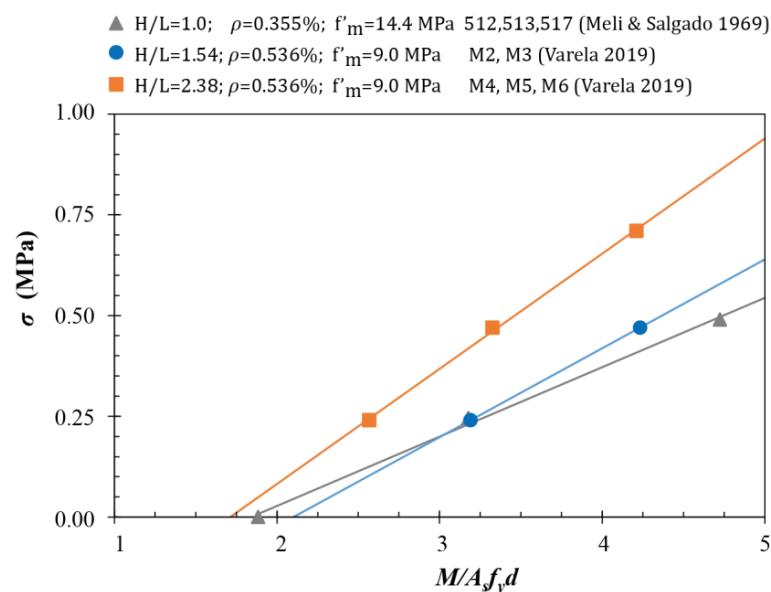


**Figure 15.** A relation between the normalised moment resistance and axial stress for 8 CM test specimens [13,122].

### 3.4. Key Factors Influencing the Occurrence of Shear- and Flexure-Dominant Failure in CM Walls

A discussion related to the shear and flexural behaviour of CM walls due to in-plane seismic actions was presented in the previous sections. The criteria for the occurrence of failure mechanisms (flexural or shear) in CM walls are important for both researchers and design engineers. Formally, flexural failure is achieved when the following condition is met:

$$\frac{M_R}{M_V} < 1.0 \quad (19)$$

where  $M_R$  is the moment resistance of the wall and  $M_v = V_R H$  is the overturning moment due to the wall's shear resistance,  $V_R$ . Observations from previous experimental studies indicate that walls subjected to lateral loading may simultaneously experience damage patterns characteristic of both flexure- and shear-dominant behaviour. The predominant damage pattern may be either diagonal tension cracking (shear related) or a flexure-related damage pattern, such as horizontal cracking and toe-crushing. The predominant damage pattern and failure mechanism depend on the ratio of flexural and shear resistance, as shown in Equation (19), and a combination of damage patterns characteristic of both mechanisms may be expected when the ratio is close to 1.0.

A parametric study was performed to identify the key parameters and to quantify the effect of different combinations of parameters on the occurrence of a shear- or flexure-dominant failure mode, the results of which are presented in Figure 16. Shear and flexural resistance values were determined using the following equations:

$$V_R = v_R t L \quad (20)$$

$$M_R = A_s f_y d' + 0.3 P d, \quad (21)$$

where  $v_R$  was obtained by applying the regression model discussed in Section 2.5. Flexural resistance  $M_R$  was calculated based on the Mexican code discussed earlier in this section (for  $P/P_R < 1/3$ ), where  $d' = L - h_c$ ,  $d = L - h_c/2$ ,  $h_c$  is the tie-column length parallel to the wall length, and  $P = \sigma t L$ .

The six charts presented in Figure 16 are organised into two parts (Figure 16a and Figure 16b, respectively). For analyses performed in Figure 16a, the longitudinal reinforcement ratio in the tie-columns is constant:  $\rho = 0.01583$  (4 #3 bars), while for the charts shown in Figure 16b, the axial stress value is constant:  $\sigma = 0.5$  MPa. The charts were produced for three different horizontal reinforcement ratios:  $p_h f_{yh} = 0.3, 0.6, 0.9$  MPa.

Each chart shows a relationship between the masonry compression strength  $f'_m$  and the  $H/L$  ratio, depending on other relevant parameters. It can be seen that the curves (characterised by  $M_R/M_v = 1$ ) divide each chart into two regions, namely, (i)  $M_R/M_v < 1$ , associated with flexural failure, and (ii)  $M_R/M_v > 1$ , associated with shear failure. Three curves are shown on each chart. For the charts shown in Figure 16a, each curve corresponds to a different axial stress  $\sigma = 0.1, 0.2, 0.3$  MPa, while for the charts shown in Figure 16b, the curves correspond to different longitudinal reinforcement ratios in tie-columns:  $\rho = 0.00396$  (one #3 bar),  $0.00792$  (two #3 bars), and  $0.01583$  (four #3 bars). Note that the analyses were performed assuming a tie-column size of  $12 \times 15$  cm. The diagonal compression stress  $v_m$  was approximated using linear interpolation for the corresponding  $f'_m$  values. For example, for  $f'_m = 3$  MPa, the corresponding  $v_m = 0.3$  MPa, while for  $f'_m = 14$  MPa, the corresponding  $v_m = 1$  MPa. This substitution allowed the use of a single material strength parameter,  $f'_{m'}$ , in the analyses. Since the  $M_R/M_v$  ratio depends on  $H$  and  $t$  (or  $H$  and  $L$ ) independently, the charts were produced for  $H = 250$  cm (storey height).

The study showed that the following five parameters govern the occurrence of the flexural and shear failure mechanisms: axial stress,  $\sigma$ , shear and compression strength of the masonry, expressed in terms of  $f'_{m'}$ , the amount of horizontal reinforcement,  $\rho_h f_{yh}$ , wall aspect ratio,  $H/L$ , and tie-column longitudinal reinforcement ratio,  $\rho$ . The most influential parameter related to flexural failure appears to be the amount of horizontal

reinforcement, followed by the strength of the masonry and the wall aspect ratio. As expected, slender walls tend to undergo flexural failure, and higher masonry strength also promotes flexural failure.

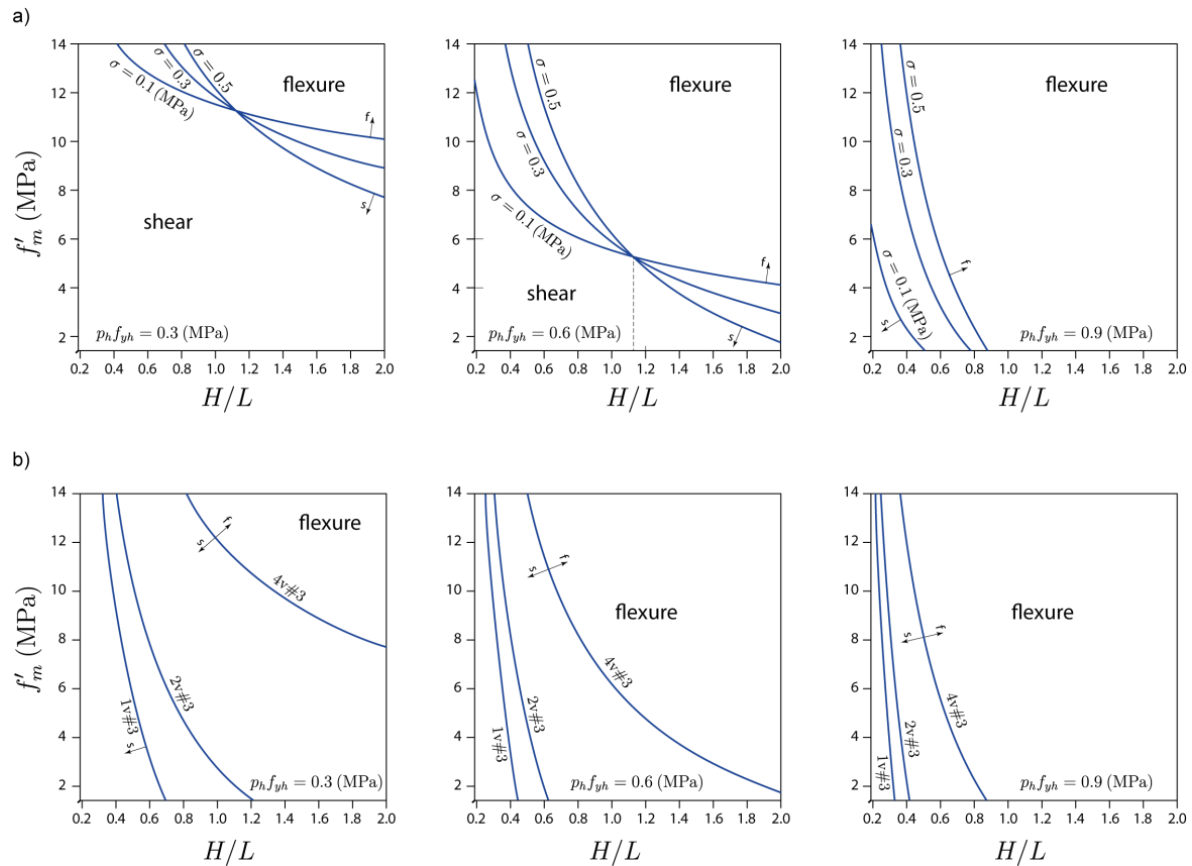


**Figure 16.** Key parameters that influence the occurrence of flexural or shear failure with variable amount of horizontal reinforcement  $\rho_h f_{yh}$ : (a) constant ratio of longitudinal reinforcement in tie-columns ( $\rho = 0.01583$ ), and (b) constant axial stress ( $\sigma = 0.5$  MPa).

It can be seen from the charts that axial stress has a smaller impact on the failure mechanism (shear- or flexure-dominant). It was observed that an increase in axial stress causes an increase in both shear and flexural wall strengths, but to a different extent. It can be seen from Figure 16a that on each chart there is a “critical”  $H/L$  ratio value, close to 1.0, which varies with the amount of horizontal reinforcement and determines whether changes in axial stress will cause flexural or a shear failure. For example, when  $\rho_h f_{yh} = 0.6$  MPa, the critical aspect ratio is  $H/L = 1.12$ . Considering the curve corresponding to  $\sigma = 0.3$  MPa as a reference, it can be observed that when the axial stress increases from 0.3 to 0.5 MPa, flexural failure can be expected for walls with  $H/L > 1.12$ , because the shear resistance increases more rapidly than the flexural resistance, but the opposite is true for walls with  $H/L < 1.12$ . Furthermore, walls with the critical value of aspect ratio do not change their failure mechanism depending on the level of axial stress.

Longitudinal reinforcement ratio  $\rho$  causes an increase in both the flexural and shear resistance of CM walls; however, in this case, it is evident that the rate at which the flexural resistance increases is much higher than that of the shear resistance. This implies that an increase in the longitudinal reinforcement ratio promotes shear failure. The effect of longitudinal reinforcement ratio,  $\rho$ , is less important when the horizontal reinforcement ratio,  $\rho_h f_{yh}$ , increases.

As previously described, under certain circumstances, it is possible to modify the behaviour of CM walls to obtain flexural failure instead of shear failure. It is well known that the flexural failure mechanism is more desirable in terms of ductility and deformation

capacity than shear failure. Figure 17 shows the envelopes of the hysteresis curves obtained from reversed cyclic testing of four CM walls; of these, two specimens demonstrated a shear-dominant behaviour [35], while the remaining specimens demonstrated a flexure-dominant behaviour [118]. The envelopes shown in black colour represent the specimens with an  $H/L$  value close to 1.0, while the envelopes shown in blue colour represent walls with an the  $H/L$  value of 2.0 or higher. It can be observed that the specimens that demonstrated shear behaviour had significantly lower deformation capacity compared to those that exhibited flexure-dominant behaviour. CM walls in taller buildings need to be designed to achieve flexure-dominant behaviour, which is in line with new design trends focused on resilience.

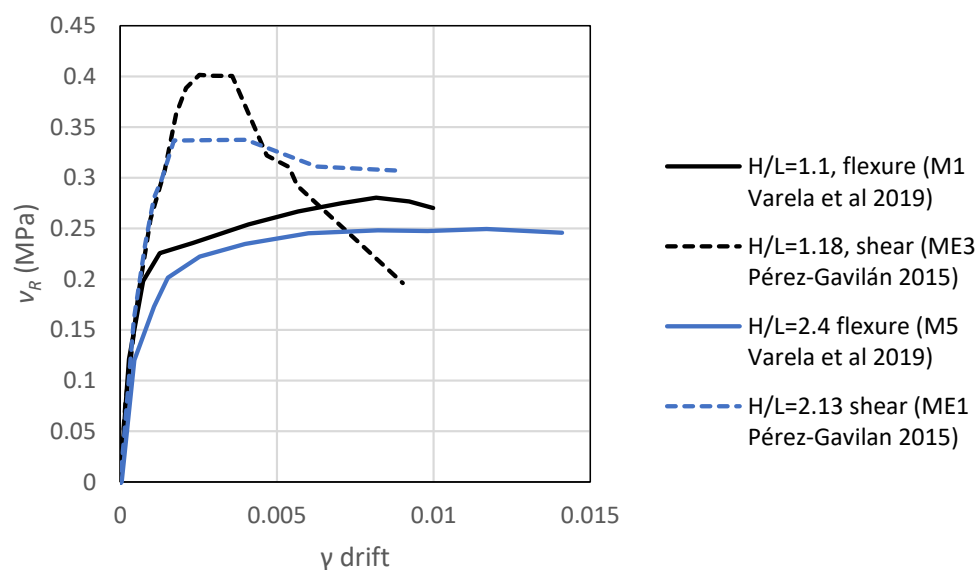


**Figure 17.** Comparison of the shear strength vs. drift envelope for CM specimens with flexure- [118] and shear-dominant [35] behaviour.

#### 4. Behaviour of CM Walls Subjected to Combined Axial Load and OOP Lateral Loading

There is scarce evidence regarding the performance of CM walls subjected to OOP ground shaking. CM walls were exposed to the effects of damaging earthquakes in Indonesia and did not experience significant OOP damage, despite the typical storey height being close to 3 m and wall thickness being only 110 to 120 mm, corresponding to a relatively large slenderness ( $h/t$  ratio of 25 to 30). A number of CM walls experienced OOP damage due to the 2010 Maule, Chile earthquake (M8.8) [124]. The failure was most pronounced on upper floor levels, e.g., the top floor of a building with a wooden roof structure in Cauquenes (Figure 18). The same building also experienced significant in-plane damage in CM walls in the longitudinal direction, and had to be demolished.

In this section, the behaviour of CM walls subjected to OOP loading is discussed, which depends on several factors, including the boundary conditions, wall aspect ratio,  $h/L$ , slenderness ratio,  $h/t$ , axial compression level, the stiffness of the RC confining elements, and the type of loading (static/dynamic). It should be noted that in this section, height  $h$  denotes the unsupported wall height between two horizontal supports (floor/roof); this is different from in discussions related to in-plane seismic loading (Sections 2 and 3), where  $H$  denoted overall wall height. The main focus of the present discussion is on the behaviour of CM walls under OOP seismic loading, which is different from the response of URM walls. The authors acknowledge the extensive previous experimental and analytical research studies related to the OOP response of URM walls; however, further discussion of this is beyond the scope of this paper.

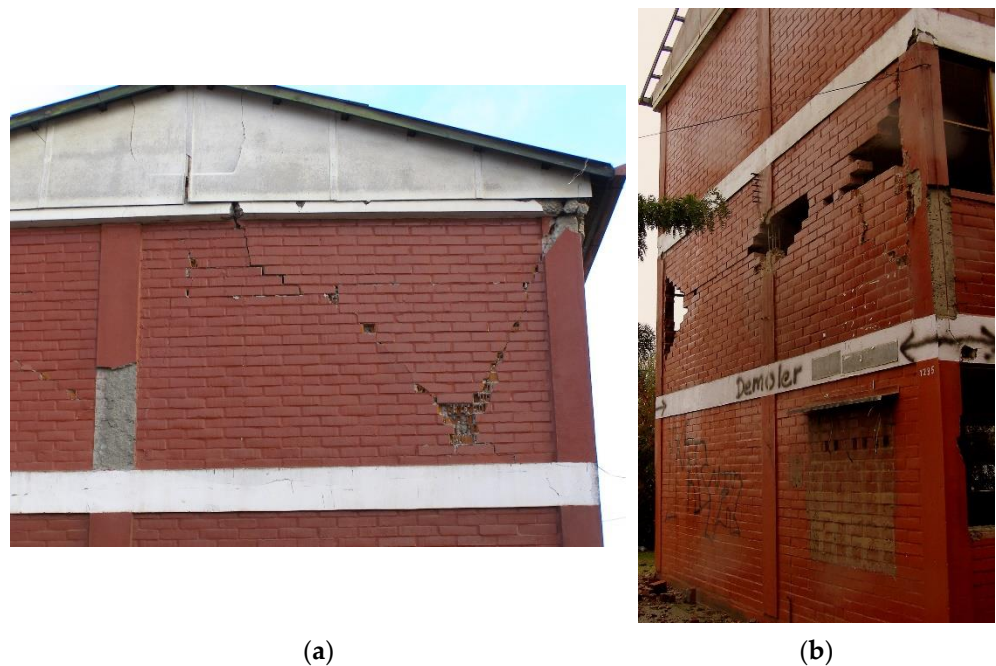


**Figure 18.** Damaged CM walls due to OOP seismic effects during the 2010 Maule, Chile earthquake: (a) damage pattern on the top floor of a building with a flexible timber roof; and (b) damaged walls on the second floor of the same building (credit: S. Brzev).

#### 4.1. Approaches for Estimating the OOP Capacity of CM Walls

Existing approaches for estimating the capacity of masonry walls subjected to gravity and OOP lateral loads are based on different assumptions and result in significantly different predictions, as discussed in this section.

##### 4.1.1. Elastic Flexural Theory

The simplest approach, adopted by several masonry design codes (e.g., [63]), is based on the elastic flexural theory, and the OOP wall capacity depends on the tensile or compressive strength of the masonry (as explained in [96]).

The flexural tensile strength approach considers an elastic uncracked wall section and assumes that the cracking moment corresponding to the flexural tensile strength in the tension zone of the wall has been reached. The wall's flexural capacity is a product of normal stress due to gravity load and the section modulus of the net cross-sectional area for OOP flexure. Consequently, a higher masonry flexural tensile strength normal to the bed joints results in an increase in the wall's flexural capacity.

An alternative approach is based on flexural compression capacity, and assumes that the flexural tensile strength has been attained, that is, that the wall has been cracked. The flexural capacity depends on the resulting masonry stress in the compression zone and the eccentricity of the axial load.

These approaches are based on the following assumptions: (i) the wall spans vertically; (ii) there is no gap between the top of the wall and the floor; and (iii) axial load, which contributes to an increased flexural capacity, is present. These approaches result in conservative estimates of OOP capacity that are significantly lower than the corresponding predictions based on the arching mechanism concept.

##### 4.1.2. Arching Mechanism

An arching mechanism may develop in masonry walls that possess rigid supports, in which translation and rotation at the supports are fully restrained. The concept of the arching mechanism was originally developed for URM walls [125], but it has been extended to masonry infills in RC frame structures ([126–128]), as well as in CM walls [50].

According to the concept of the arching mechanism, two or more rigid segments form in cracked masonry walls subjected to combined gravity loading and OOP lateral pressure with unsupported height/storey height ( $h$ ) and length ( $L$ ). It is expected that horizontal cracks develop at both the mid-height of the wall (interface cracks) and at the top/bottom supports (boundary cracks). Increasing lateral loading at the post-cracking stage causes a rotation of rigid segments and lateral displacements at the mid-height of the wall. As a result, the wall acts as a three-hinged arch (see Figure 19a). The thrust forces ( $T$ ) (also known as strut forces) induce high compression stresses at the hinges (clamping points). The following two failure mechanisms are possible: (i) crushing and (ii) lateral instability (“snap through” mechanism). Crushing may take place at the cracked interface, provided that compressive stress at the clamping points reaches the masonry compressive strength,  $f'_m$ . The ultimate lateral pressure,  $w$ , can be determined from equilibrium of the horizontal component of the thrust force and the lateral pressure, as follows (Figure 19b):

$$\frac{wh}{2} = 2T \sin \gamma \quad (22)$$

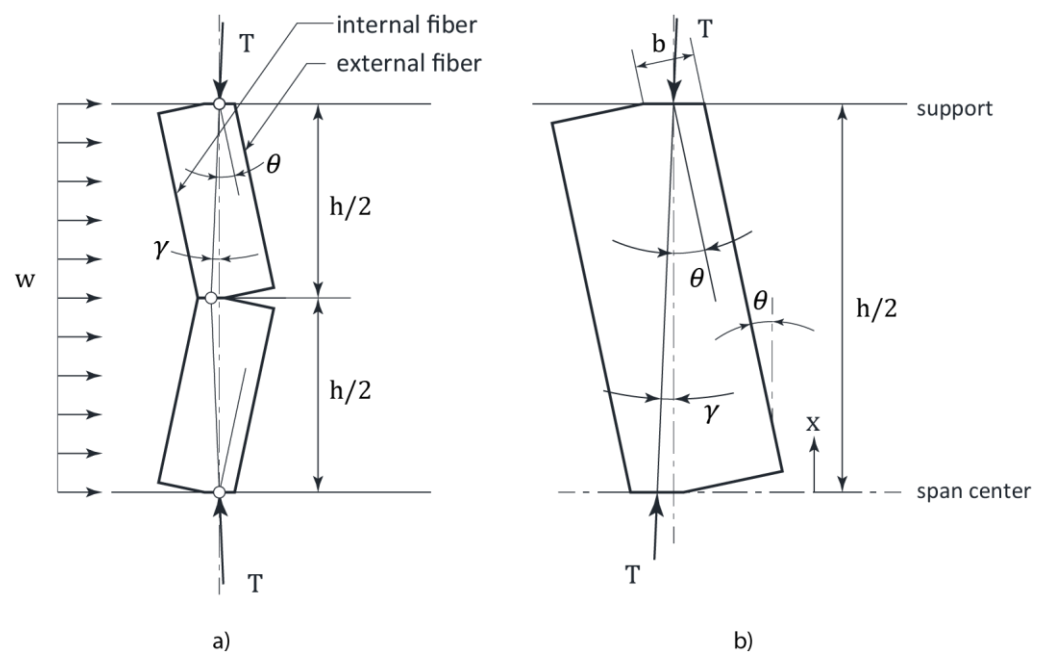


**Figure 19.** Arching mechanism in masonry walls: (a) a three-hinged arch and (b) a rigid segment subjected to thrust forces (adapted from [127]).

#### 4.1.3. Experimental Research Studies

Previous experimental research studies have shown that a form of the arching mechanism that is characterised by crushing occurs in walls with relatively low slenderness ( $h/t$ ) ratios. For masonry infills and CM walls, additional factors that determine the chances for crushing at the wall boundaries include the stiffness of the vertical RC elements and the compressive strength of the masonry. Experimental studies have shown that masonry infill walls with rigid boundary frame elements may also be subject to the crushing failure mechanism [128]. An alternative form of the arching mechanism, lateral instability due to excessive horizontal displacements, may be expected in slender walls and/or walls with flexible supports. The wall segments eventually reach an unstable position that culminates in a “snap through” failure.

The experimental and analytical research evidence related to the behaviour of CM walls subjected to OOP loading is limited. The majority of experimental studies were performed by the same research group in Mexico, by subjecting CM wall specimens to monotonically increasing uniform pressure [50,129–133]; however, in one test, cyclic OOP

load was applied to the top of the specimen [134]. Based on the results of their experimental studies, the researchers developed a one-way spring strut arching method to estimate the OOP strength of CM walls, taking into account the flexibility of the confining elements [50] and the applied axial compression stress (Figure 20). Subsequently, the method was generalised in the form of a bi-directional compression strut mechanism that also took into consideration the torsional stiffness of the RC elements [132].

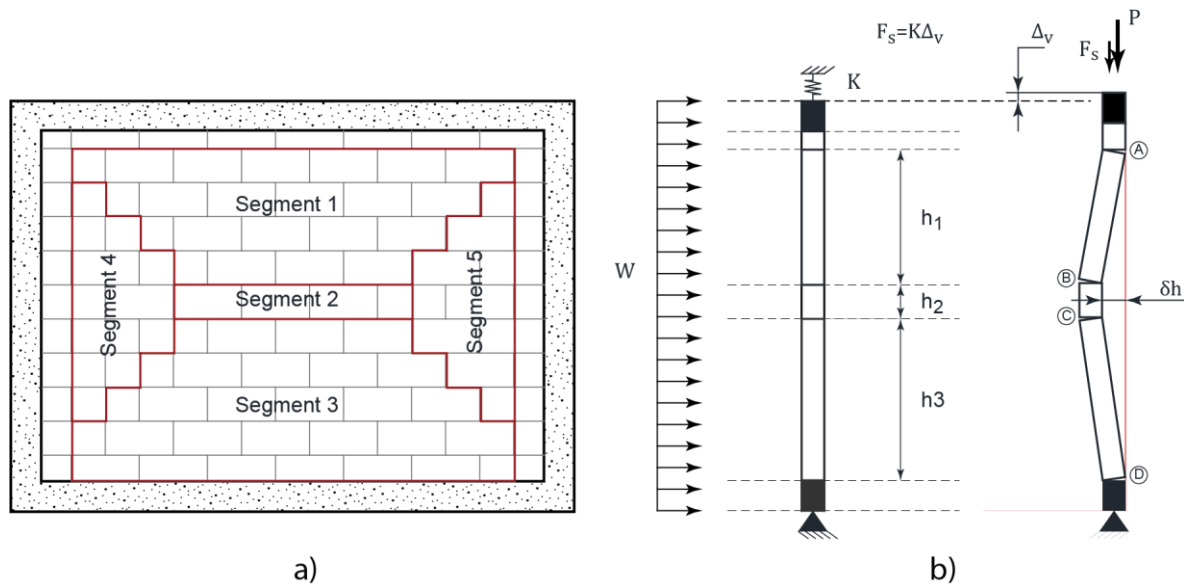


**Figure 20.** Failure mechanism for CM walls subjected to monotonic OOP pressure: (a) cracking pattern and (b) one-way strut analytical model that takes into account the flexibility of the supports (adapted from [50]).

The proposed method built on the arching mechanism concept previously applied to masonry infills in RC frames [127], but is different in the assumptions related to the boundary conditions. The method applied to RC frames with infills assumed rigid boundary conditions due to robust beam and column elements, while the bi-directional compression strut mechanism considers the flexible support provided by the RC confining elements.

Based on a review of previous experimental studies, the authors of this paper compiled a database of 32 CM wall specimens from six experimental studies [50,129–131,133,134]. In five studies, the specimens were subjected to monotonic static loading, which was applied via air bags. In one case, a cyclic OOP lateral load was applied to the top of the specimen [134]. The key design parameters for these specimens are summarised in Table 2, while more detailed information on each specimen is presented in Table A3, Appendix A. It can be seen from the table that the specimens were characterised by  $h/L$  ratios ranging from 0.5 to 2.5, while the  $h/t$  ratio ranged from 12.0 to 25.0.

#### 4.2. Effect of Wall Slenderness ( $h/t$ ) Ratio

Restrictions on wall slenderness expressed in terms of the height-to-thickness ratio,  $h/t$ , are prescribed by design codes to prevent damage and/or instability as a result of OOP seismic actions [8]. It appears that the majority of the tested CM specimens were characterised by slenderness ratios lower than the limits set by international codes.

Based on an analysis of the experimental database, 26 out of the 32 specimens were characterised by an  $h/t$  ratio in the range from 18 to 25. An analysis of the test results for specimens with  $h/t$  values in the range from 12.0 to 25.0 showed a significant scatter with respect to ultimate pressure. There is no clear trend for the relationship between ultimate OOP pressure,  $w_{u}$ , and  $h/t$  value, as shown in Figure 21.

**Table 2.** Summary of experimental studies on the OOP behaviour of CM walls.

Study	# of Specimens	Masonry Unit Type	$h/L$	$h/t$	$t$ (mm)	$f_m$ (MPa)	$w_u$ (kPa)	Key Parameters
Varela-Rivera et al. [129]	6	HCB	0.49	11.7	150	3.07	[13.1, 14.3]	Boundary conditions (supported on 3 or four sides)
Varela-Rivera et al. [50]	6	HCB	[0.74, 0.95]	[18.1, 24]	120 & 150	[2.84, 2.85]	[8.79, 17.83]	Variables: $H/L$ , $H/t$ , and in-plane stiffness of confining elements
Varela-Rivera et al. [130]	3	HCB	0.73	18	150	[2.64, 2.84]	[8.79, 18.91]	Variable axial compression level
Moreno-Herrera et al. [133]	8	HCB2 MPB SB	[0.73, 0.94]	23–24.4	113–120	[3.72, 6.48]	[7.33, 18.06]	Variables: axial compression and masonry unit types
Navarrete-Macias et al. [134]	5	HCB	0.73–1.8	21.3	120	Average 6.48	[8.43–14.07]	Variables: axial stress and $H/L$ Cyclic lateral load on top
Varela-Rivera et al. [131]	4	HCB	1.40 & 2.04	18.7	145	3.3	[19.72, 38.32]	$H/L > 1.0$ ; variable axial compression

Notes: HCB = hollow concrete blocks with three cells; HCB2 = hollow concrete blocks with two cells; MPB = multi-perforated clay blocks; SB = solid bricks.

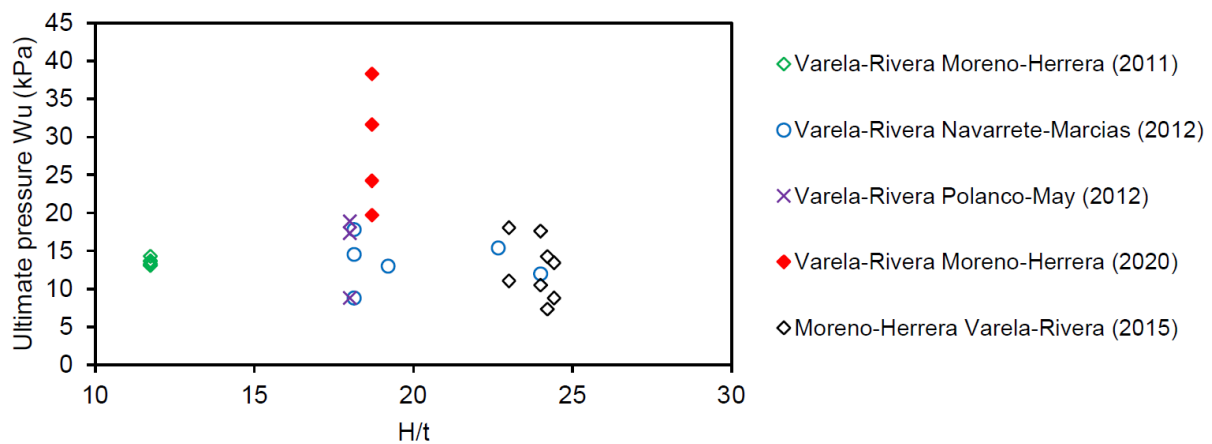


**Figure 21.** Ultimate OOP pressure versus  $h/t$  ratio for the 32 CM wall specimens included in the experimental database [50,129–131,133,134].

A few analytical models consider slenderness ratio ( $h/t$ ) as the main parameter for predicting the OOP strength of masonry walls. The charts presented in Figure 22, developed on the basis of the analytical model proposed by Angel et al. [127], show a variation in the OOP ultimate pressure depending on the slenderness ratio ( $h/t$ ), the masonry compressive strength  $f'_m$ , and the ultimate masonry compression strain,  $\epsilon_{cu}$ . The predictions appear to be on the conservative side compared to the reported experimental data on CM walls [50,129–131,133,134] for  $h/t$  values less than or equal to 25.

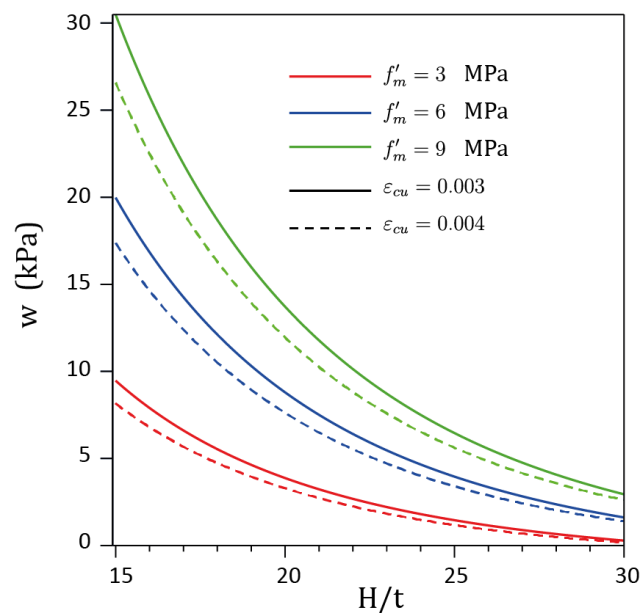


**Figure 22.** Prediction of the ultimate lateral pressure depending on the wall slenderness ratio,  $h/t$ , masonry compression strength  $f'_m$ , and the ultimate masonry strain  $\epsilon_{cu}$ , based on the model by Angel [127].

Tu et al. [135] performed an experimental study that involved the testing of two single-storey CM structures that were subjected to OOP excitation using a shaking table. The results showed that the resulting OOP lateral force for the less slender specimen B2 ( $h/t = 14.4$ ) was six times higher than that for the more slender specimen B1 ( $h/t = 29.5$ ); this is in agreement with the analytical results shown in Figure 22. For example, the curve corresponding to  $f'_m = 9$  MPa and  $\epsilon_{cu} = 0.003$  shows that when the slenderness ratio is

increased from 15 to 30, there is an increase in the corresponding ultimate pressure from 5.0 to 30.0 kPa.

The effect of slenderness on the OOP behaviour of CM walls and RC frames with infills was studied on three half-scaled CM wall specimens that were subjected to in-plane reversed cyclic loading and subsequent OOP vibrations induced via shaking table [136]. The more slender specimen, S1<sub>WF</sub> ( $h/t = 22.7$ ) with a weak RC frame, similar to a CM wall without toothing, exhibited bed-joint sliding masonry failure, which ultimately led to the formation of plastic hinges at the ends of the tie-columns and shear failure at the wall mid-height. On the other hand, a less slender specimen with a more robust RC frame, S3<sub>SF</sub> ( $h/t = 11.0$ ), experienced uniformly distributed cracking over the masonry panel and sliding over two distinct horizontal planes. It was observed that the less slender specimen demonstrated superior performance compared to the otherwise similar more slender specimen.

#### 4.3. Effect of Wall Aspect Ratio ( $h/L$ )

The majority (23 out of 32) of the tested CM wall specimens subjected to uniform OOP pressure were squat walls with an aspect ratio ( $h/L$ ) lower than 1.0 (see Table 2). The results showed that the ultimate pressure values ranged from 8.79 to 18.91 kPa, with an average value of 13.42 kPa (solid line) and a standard deviation of 3.15 kPa (dashed lines) (Figure 23). Varela-Rivera et al. [131] also performed a study on non-squat CM walls (aspect ratios of 1.4 and 2.0) subjected to different levels of axial compression. It was observed that the ultimate pressure increased with increasing aspect ratio (Figure 24).

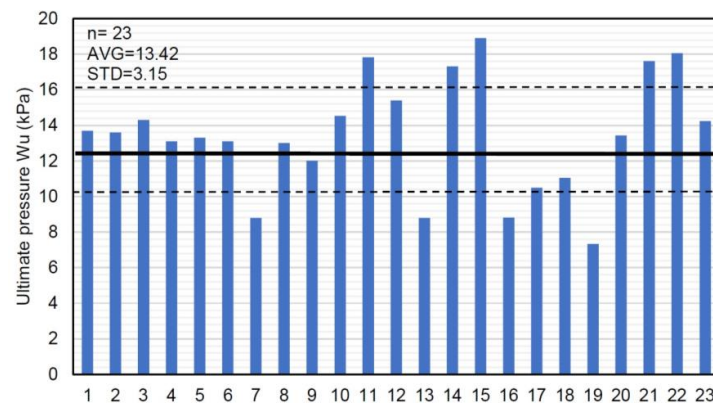


**Figure 23.** Effect of wall aspect ratio ( $h/L$ ) on the OOP behaviour of CM walls: ultimate pressure values for squat CM wall specimens (experimental database included in Table A3).

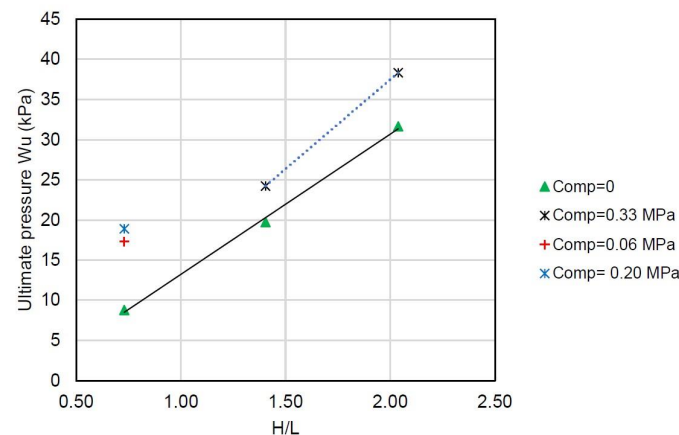


**Figure 24.** The effect of  $h/L$  ratio and axial compression on the ultimate pressure for CM wall specimens (data from [130,131]).

#### 4.4. Effect of Axial Compression

Varela-Rivera et al. [130] studied the effect of axial compression on the behaviour of CM walls subjected to uniform OOP pressure. Three full-scale squat CM wall specimens with an  $h/L$  ratio of 0.73 were subjected to different levels of axial compression ranging from 0 (specimen S-1) to 0.2 MPa (specimen S-3), corresponding to 8% of the masonry compression strength  $f'_m$ . The results showed that the specimens with the application of axial compression achieved approximately double the lateral pressure achieved by specimen S-1, without axial compression. Varela-Rivera et al. [131] also studied the effect of axial compression on the behaviour of CM walls by testing four non-squat wall specimens (aspect ratios of 1.4 and 2.0). All specimens were supported on four sides. Two specimens were subjected to a low axial compression of 0.33 MPa (less than 10% of the masonry compression strength  $f'_m$ ), while the remaining two specimens were not subjected to axial compression. For the specimens with the same  $h/L$  ratio (1.4 or 2.0), it was observed that the ultimate pressure increased by 15–20% with increasing axial compression level. The results for selected specimens are presented in Figure 24.

#### 4.5. Effect of the Stiffness of RC Confining Elements

The stiffness of CM confining elements is an important parameter influencing the seismic response of CM walls subjected to OOP seismic effects; however, its effect has not been extensively studied. It has been well established that CM walls subjected to monotonic OOP loading behave similarly to two-way slabs subjected to uniform gravity loading. A common design approach for URM walls subjected to OOP uniform pressure is similar to that for the design of two-way slabs subjected to a uniform gravity load [96]. Experimental studies (e.g., [50]) have shown that the OOP failure mechanism for CM walls also depends on the stiffness of RC confining elements. The failure of CM walls with stiff RC confining elements is characterised by masonry crushing (e.g., specimen E-4, see Figure 25a). Alternatively, a “snap through” failure mechanism characterised by large OOP displacements may be expected in CM walls with flexible RC confining elements, e.g., specimen E-1, see Figure 25b. Figure 25c shows a difference in the ultimate pressure and OOP displacements for the two specimens. It can be seen from the chart that specimen E-4 (crushing failure) attained higher ultimate pressure and smaller lateral displacements than specimen E-1 which underwent “snap through” failure. It can be observed from the chart that the approximate difference in their ultimate displacements was on the order of 40%.

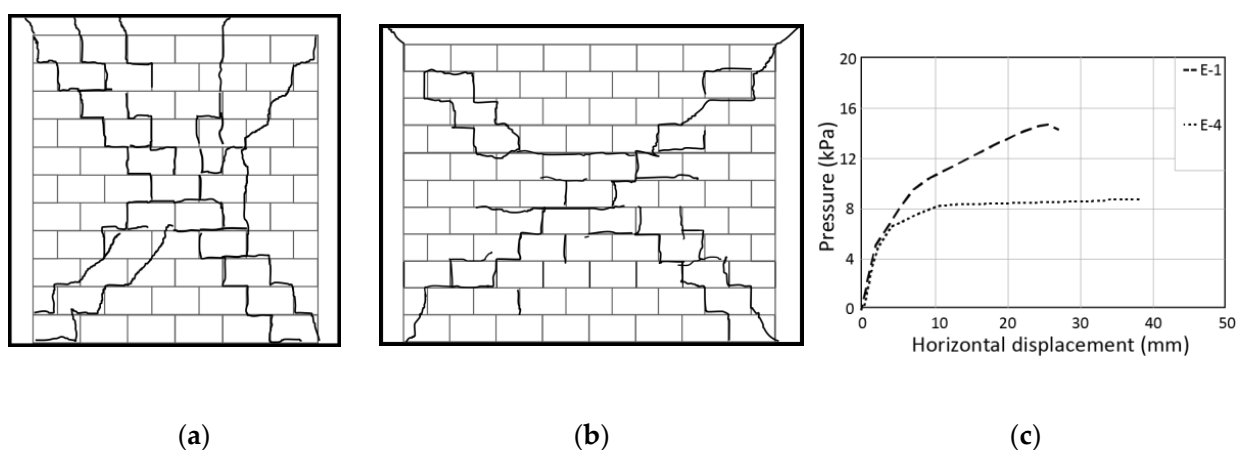
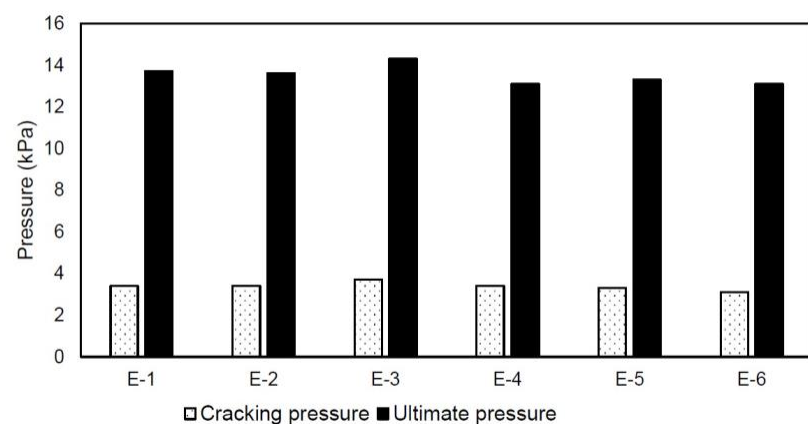
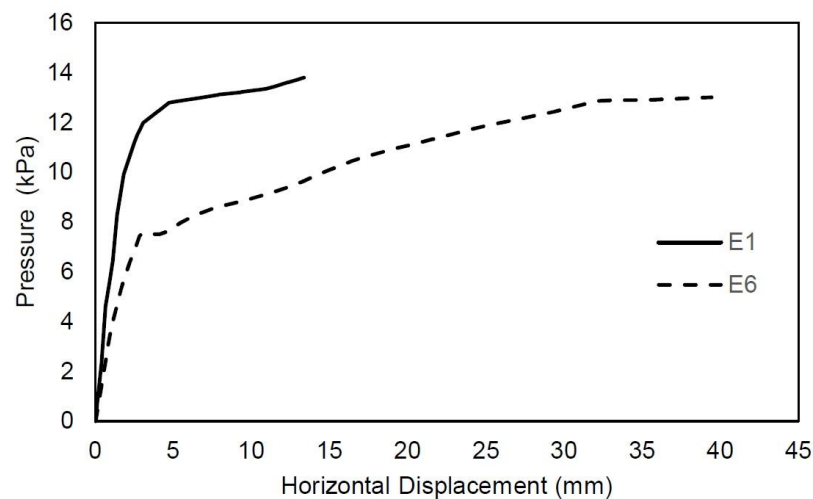


**Figure 25.** Effect of in-plane stiffness of RC confining elements on the OOP behaviour of CM walls (adapted from [50]): (a) specimen E-4 underwent masonry crushing failure; (b) specimen E-1 was subject to a “snap through” failure mechanism; and (c) lateral pressure versus horizontal OOP displacements for specimens E-1 and E-4.

In CM walls supported on all four sides, RC tie-beams are cast integrally with RC floor slabs. In an alternative design scenario, a CM wall can be supported on three sides, while its top edge is supported by an RC tie-beam; this is characteristic of flexible (e.g., wooden) floor or roof diaphragms (see Figure 18a). The effect of the stiffness of confining elements was investigated through an experimental study on six full-size CM wall specimens subjected to increasing monotonic uniform lateral pressure applied via air bags [129]. The specimens were supported on either three or four sides. Figure 26a shows that the magnitude of ultimate pressure was very similar for all specimens (with differences within 10%). Although the magnitude of ultimate pressure was similar for specimens supported on three and four sides, a somewhat different behaviour was observed in the post-cracking stage for specimen E-1 (supported on four sides) compared to specimen E-6 (supported on three sides) (see Figure 26b). In all cases, the ultimate pressure was approximately four times higher than the cracking pressure, which indicates a significant reserve in post-cracking strength.



(a)



(b)

**Figure 26.** The OOP behaviour of CM wall specimens under different support conditions: (a) histogram showing the ultimate and cracking pressures for all specimens (data from [129]); and (b) OOP pressure vs. horizontal displacement curves for specimen E-1 supported on four sides and specimen E-6 supported on three sides (adapted from [129]).

Although the results of the experimental studies mentioned in this section are valuable, it is important to note that the studies were performed on single wall panels, which is an

idealised scenario. In real buildings, several adjacent wall panels exist at the same floor level, as well as on different floors. Therefore, it is important to take into account the effect of the stiffness of RC confining elements on the OOP capacity of CM walls.

#### 4.6. Difference between Monotonic Static Loading and Dynamic/Seismic Loading

In the majority of previous experimental studies on CM walls subjected to OOP loading, the specimens were subjected to increasing monotonic pressure applied by means of air bags [50,129–131,133]. The reported failure mechanism for CM wall specimens supported on four sides was similar to that found in two-way slabs subjected to gravity loading, as shown in Figure 27a [129].

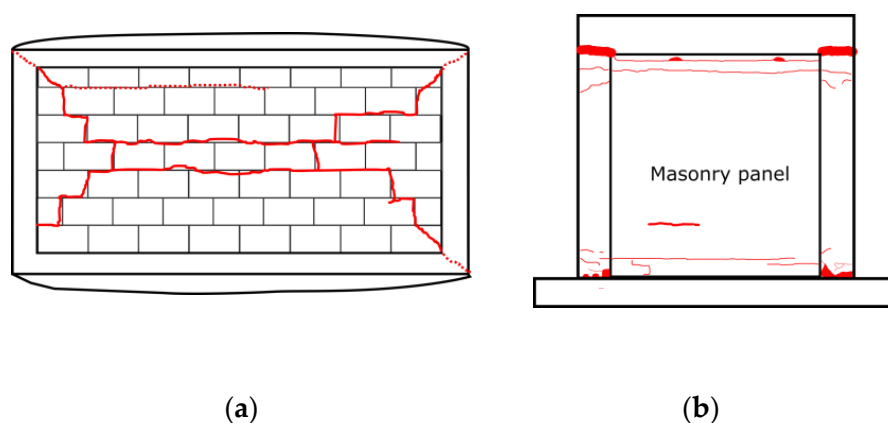


**Figure 27.** Failure mechanisms for CM walls subjected to OOP loading: (a) monotonic static testing via air bags (adapted from [129]) and (b) dynamic testing via shaking table (adapted from [135]).

However, a study performing testing on single-storey CM buildings using a shaking table [135] showed that CM wall specimens subjected to OOP dynamic excitation developed horizontal cracks close to the wall-to-tie-beam interface at the top of the wall, as well as at the base of the wall (Figure 27b). These cracks extended into the RC tie-columns at higher shaking intensities.

Air bags produce a nearly uniform pressure, which may be appropriate for simulating the effect of wind loading on wall specimens; however, seismic inertial forces cannot be adequately simulated by means of uniform pressure. A simple explanation can be provided by considering the dynamics of a single-degree-of-freedom (SDOF) system [137]. When a structure is idealised as an SDOF system, the equivalent static force  $F$  may be expressed as follows:

$$F = Kx = M \psi \frac{L}{m} A \quad (23)$$

where  $K$  and  $M$  represent stiffness and mass, respectively, and  $A$  is ground pseudo-acceleration. Note that the displacement  $x$  is equal to the product of a shape function,  $\psi$ , which is independent of time but depends on the boundary conditions, and  $z$ , a time-dependent scalar which corresponds to the displacement of a SDOF model, as follows:

$$x = \psi z \quad (24)$$

For a simply supported wall spanning the vertical direction,  $\psi$  could be a parabolic or a sinusoidal function with zero displacement at the base and the top, but it cannot be a constant. The difference in shape for the load distribution over the wall height should be incorporated into the results of experimental and analytical studies in which the OOP wall capacity is determined on the basis of the uniform load distribution. A significant decrease in capacity (by more than 20%) was obtained for the model subjected to a non-uniform pressure distribution.

## 5. Factors Related to the Design and Construction of CM Walls

The behaviour of CM buildings subjected to seismic loading is influenced by factors related to the architectural planning of these buildings, such as size and the location of openings. The effect of openings (doors and windows) is relevant for all types of masonry wall structures, as well as RC frame structures with masonry infills. Construction issues, such as the presence and type of tothing along the masonry-to-RC-tie-column interface, are also important, and influence the seismic behaviour of these structures. Finally, the type and mechanical properties of the masonry materials, especially the masonry units and mortar, are also very important. This section presents an overview of research studies related to these important topics and their findings.

### 5.1. Openings in CM Walls

Experimental studies and post-earthquake building surveys have shown that the size, location, and shape of openings significantly influence the behaviour of CM walls. Most importantly, openings cause a decrease in the lateral strength of CM walls and their effectiveness during earthquakes [3]. Several past earthquakes have shown that masonry walls with unconfined openings experience more damage than solid walls, as illustrated in Figure 28.



**Figure 28.** Damage sustained by the Candelabro Hotel building in the 2007 Pisco, Peru earthquake (M 8.0): (a) damage to masonry piers, showing the absence of vertical RC confining elements in longitudinal wall; and (b) undamaged solid CM walls in the transverse wall (photos: D. Quiun).

A few past experimental studies have been performed focusing on the seismic response of CM walls with openings. Yanez et al. [138] tested 16 full-size CM wall specimens under reversed cyclic loading. Of these, eight specimens were constructed using multi-perforated clay blocks, while the remaining specimens were constructed using hollow concrete blocks. There were four types of specimens: two types with window openings, one type with door openings, and a solid wall (without openings). The results showed a significant decrease in the peak strength for the specimens with openings, and the extent of the decrease was dependent on the size of the openings. The specimens with a large window opening with an area accounting for more than 25% of the CM panel area showed the highest strength decrease (40–50% relative to the corresponding solid specimens). An important finding was related to the effect of opening size on the stiffness decrease: the specimens with small openings, having an area of up to 11% of the CM panel area, did not experience a decrease in stiffness compared to the solid specimens. The results also showed that all specimens

attained lateral drifts of 2.0% or higher at the ultimate stage. The onset of cracking occurred at drifts of 1.5% or less. The failure mechanisms of the CM specimens with openings tested in this study are illustrated in Figure 29.

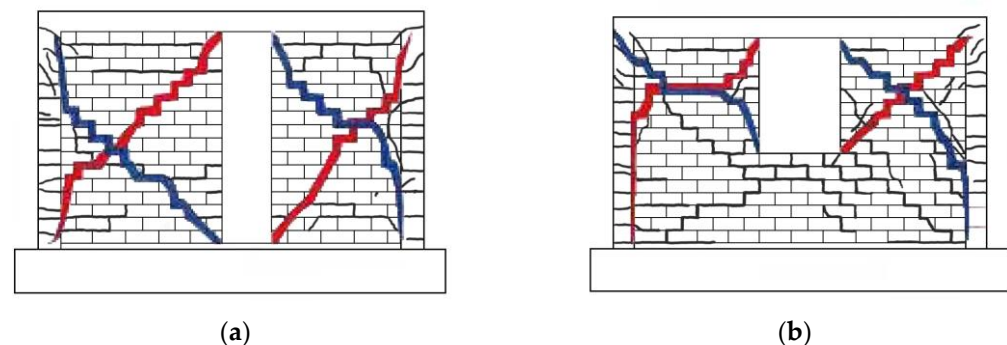


**Figure 29.** Failure mechanisms of CM walls with openings, showing crack patterns for alternative loading directions: (a) door openings and (b) window openings (adapted from [138]).

The provision of RC confining elements around openings is essential for preventing extensive damage or collapse due to in-plane and out-of-plane earthquake effects [1]. Kuroki et al. [139] performed an experimental study on 10 half-scale CM wall specimens to study the effect of openings on the behaviour of CM walls subjected to reversed cyclic loading. The specimens were constructed using full-size solid clay bricks and cement mortar, and the corresponding masonry compressive strength was relatively high (10.4–18.1 MPa). Out of 10 specimens, five specimens had window openings and four specimens had door openings. Of the five specimens with window openings, three had a centrally located window, while two specimens had an eccentrically located window (adjacent to the tie-column). The authors varied the confining arrangement around the openings—some specimens had only vertical confining elements, while others had both vertical and horizontal confining elements. Vertical confining elements around openings consisted of a vertical steel bar enclosed by a continuous spiral tie. Horizontal confining elements were reinforced with four steel bars enclosed by closely spaced ties. The results showed that specimens with unconfined window openings underwent a significant decrease in terms of shear strength, ranging from 15 to 40%. The extent of the decrease was dependent on the location of the opening: the specimens with a centrally located window experienced a smaller decrease compared to the specimens with eccentrically located windows. The results also showed that a specimen with a centrally located opening confined by horizontal and vertical elements attained a higher ultimate strength but lower ductility when compared to an otherwise similar specimen that was confined by vertical elements only. The study showed that the specimens with openings and confining elements showed higher capacity compared to otherwise-similar specimens without openings. Another experimental study [140] confirmed the importance of vertical confining elements around the openings.

Singhal and Rai [141] performed an experimental study on four half-scale CM wall specimens with openings to study the effect of different confining arrangements. The specimens were originally subjected to in-plane reversed cyclic loading and subsequently to OOP shaking table testing. The results showed confinement around the openings to have a beneficial effect on the behaviour of the test specimens in terms of the extent of damage, ultimate strength and displacement/drift potential. The specimen without confining elements (SI-O<sub>2WA</sub>) experienced severe cracking in the spandrels and piers, and its ultimate shear strength was 25% lower compared to the specimen with vertical confining elements (SC-O<sub>2WB</sub>). It should be noted that, despite the severe damage, the specimen did not experience failure, and a drift of 2.2% was attained (the same as the specimens with confining elements at the openings). The specimen with both horizontal and vertical RC confining elements (SC-O<sub>2WC</sub>) around the openings showed the best performance in terms of strength, cracking distribution, and cumulative energy dissipation (Figure 30).

The specimen with vertical confining elements around the openings attained the same ultimate drift as the specimen with horizontal and vertical confining elements (2.2%), but it underwent severe damage in the piers and confining elements at a drift demand of 1.4%. It should be noted that it is common CM construction practice in many countries and regions, including Latin America, Europe, etc., to provide only vertical confining elements around openings in CM structures. A performance comparison of the various specimens is presented in Figure 31.

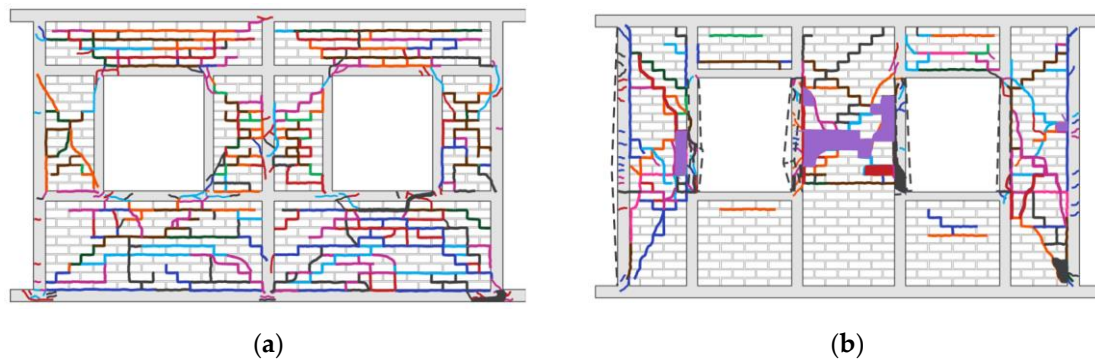


**Figure 30.** Damage of CM wall specimens with openings (adapted from [141]): (a) continuous horizontal RC sill and lintel band and discontinuous vertical confining elements and (b) continuous tie-columns and discontinuous horizontal confining elements.

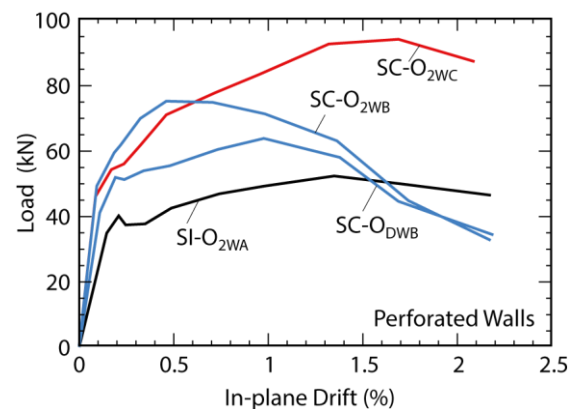


**Figure 31.** Comparison of force-versus-drift envelope for CM specimens with and without openings (adapted from [141]).

Tu et al. [142] performed a study on two CM full-size wall panels with unconfined openings subjected to reversed cyclic loading. The masonry was constructed using solid clay bricks. Specimen CW had a window opening, while specimen CD had a door opening. Both specimens exhibited shear-dominated behaviour, characterised by cracking in the wall piers. The CW specimen showed a higher peak strength (609.6 kN) than the CD specimen (487.2 kN); this can be attributed to the diagonal strut action in the CW specimen being more effective due to the presence of a rigid parapet (i.e., the windowsill). Both specimens attained a maximum drift of approximately 0.58%.

Qin et al. [143] performed an experimental study on four full-size CM wall panels constructed using sintered insulated shale (SIS) blocks, which are similar to the multi-perforated clay blocks used in Latin America and Europe. The specimens were subjected to reversed cyclic loading. One of the specimens was a solid panel, two specimens had window openings, and one specimen had a door opening. The openings were not confined. The specimens demonstrated shear behaviour, characterised by the diagonal cracking of masonry piers and spalling of the SIS blocks, and horizontal cracking in RC tie-columns.

The results showed a significant drop in peak strength (by 25–40%) for the specimens with openings when compared to the solid specimen.

Okail et al. [144] tested six CM specimens, of which two had openings, while the remaining four specimens were solid. Five specimens were constructed using single-wythe solid clay bricks, and one specimen was constructed using hollow concrete blocks (CMUs). The specimens were subjected to monotonic lateral loading. The specimen with a window opening showed a shear behaviour, with diagonal cracks extending over the entire wall height, in a similar manner to the solid specimen. Since the opening was relatively small, with an area on the order of 7% of the overall panel area, it did not significantly affect peak strength (the decrease was approximately 17%). However, the specimen with a door opening exhibited a significant decrease in peak strength—by approximately 43%—compared to the solid specimen.

Several researchers have attempted to quantify the effect of openings on the peak strength of CM walls. Yanez et al. [138] considered parameter  $A_r$  (referred to as  $\alpha$  in their study), which denotes a ratio between the area of an opening ( $A_0$ ) and the area of a CM panel ( $A_p$ ), that is,  $A_r = A_0/A_p$ . The same parameter was considered by other researchers in the context of RC frames with masonry infills with openings, as reported by Singhal and Rai [141]. Riahi, Elwood and Alcocer [102] proposed an equation to estimate the strength reduction factor for CM walls with openings (1–2.2  $A_r$ ). Yanez et al. [138] considered another parameter, B (referred to as  $\beta$  in their study), which is a ratio of the net cross-sectional area of CM panel (including confining elements and masonry portion without openings) and the gross area of CM panel. They examined a relationship between the parameter B and the strength decrease in CM wall specimens with openings.

Based on the experimental database of 38 CM wall specimens from the experimental studies discussed in this section (presented in Table A4, Appendix A), the authors attempted to correlate the factors  $A_r$  and B, discussed above, with a ratio of peak strength ( $H_o/H$ ) between the CM wall specimens with openings ( $H_o$ ) and the corresponding solid specimens (H). The results are presented in Figure 32. It can be seen from Figure 32a that the proposed strength reduction equation [102] was conservative, and underestimated the peak strength for the majority of CM wall specimens. The chart shown in Figure 32b shows a scatter of peak strength ratios for different B values.

## 5.2. Tothing

CM walls require adequate connection between a masonry panel and the adjacent RC confining elements. Such a connection may be attained by constructing the masonry wall first and leaving a toothed (also known as “zig-zag”) vertical edge at both wall ends (Figure 33). Subsequently, concrete is poured into the tie-columns between the toothed edges; finally, concrete is poured in tie-beams on top of the walls (these tie-beams are usually cast integrally with the floor slabs). The same construction process is repeated for all walls at each floor level. The construction challenges usually associated with toothed connections include the presence of air voids within a tie-column due to the difficulty with which fresh concrete flows inside the teeth, and cracking/damage of masonry teeth due to the vibration or consolidation of the fresh concrete in the tie-columns. The toothed portion of a masonry wall is prone to damage, because tooth size is usually small (equal to one-half or one-quarter of a brick length), and also because the available space for concrete consolidation between the tie-column reinforcement and masonry units is limited.

An alternative type of masonry-to-tie-column connection consists of horizontal steel bars (dowels) provided at a regular spacing at the interface between the tie-columns and the masonry wall (Figure 34). The construction process is similar to that explained for a toothed connection, except that a masonry wall is constructed with vertical straight edge at both ends; subsequently, short horizontal steel bars (dowels) are embedded in mortar bed joints with a length of 400 mm or more to assure adequate bar development length, and are anchored into the tie-column with a 90-degree hook (in the case of a wall end). In interior walls, straight dowels can be extended into adjacent wall panels. The dowels are

typically in the form of 6- or 8-mm diameter steel bars—the size needs to be small enough to be embedded into mortar bed joints.

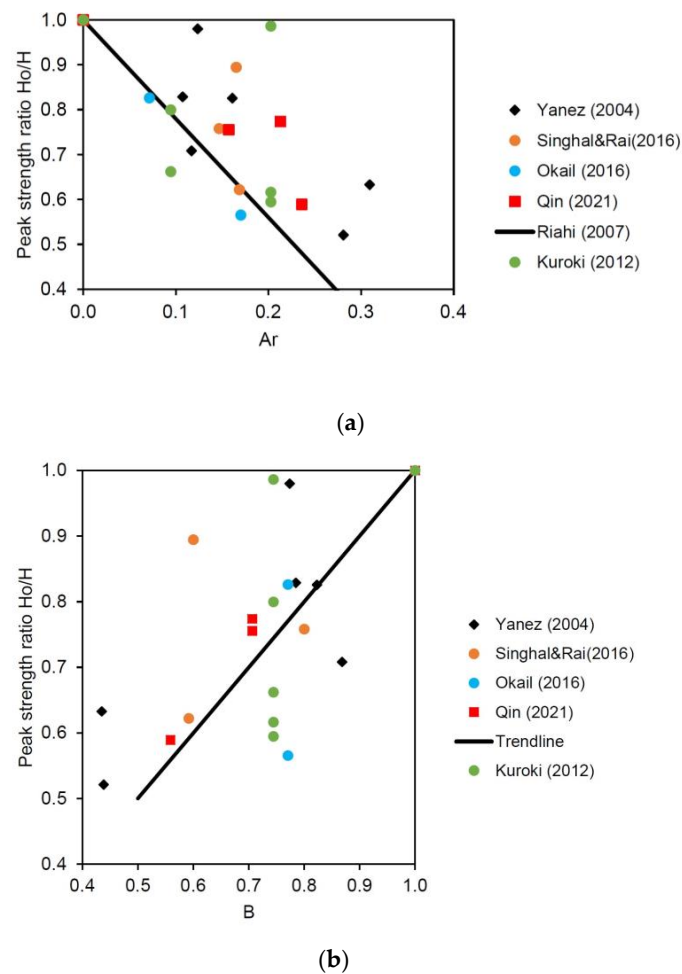


**Figure 32.** Effect of openings on the peak strength of CM walls (based on the database of 38 experimental specimens, see Table A4): (a) ratio of the opening area relative to the CM panel area and (b) ratio of the net wall cross-sectional area to the total wall area.

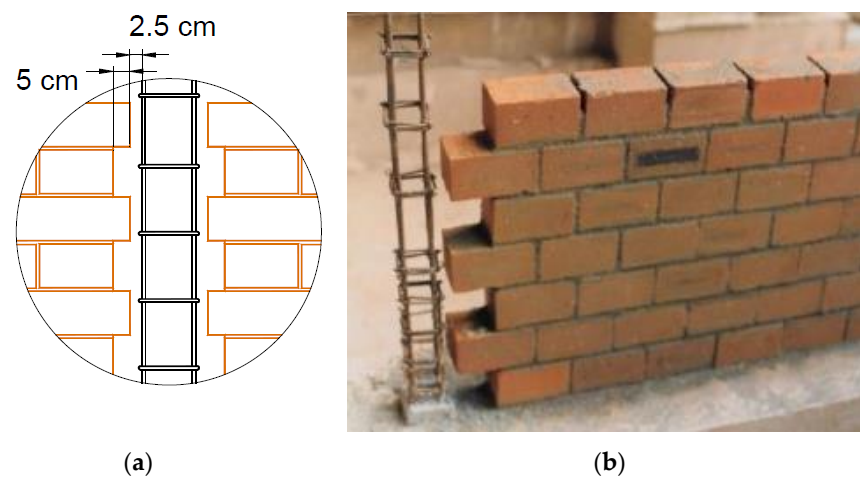


**Figure 33.** Toothed connection at the wall-to-tie-column interface: (a) recommended practice (reprinted from [3] with permission of the publisher, the Earthquake Engineering Research Institute) and (b) a field application (credit: C. Vegas).

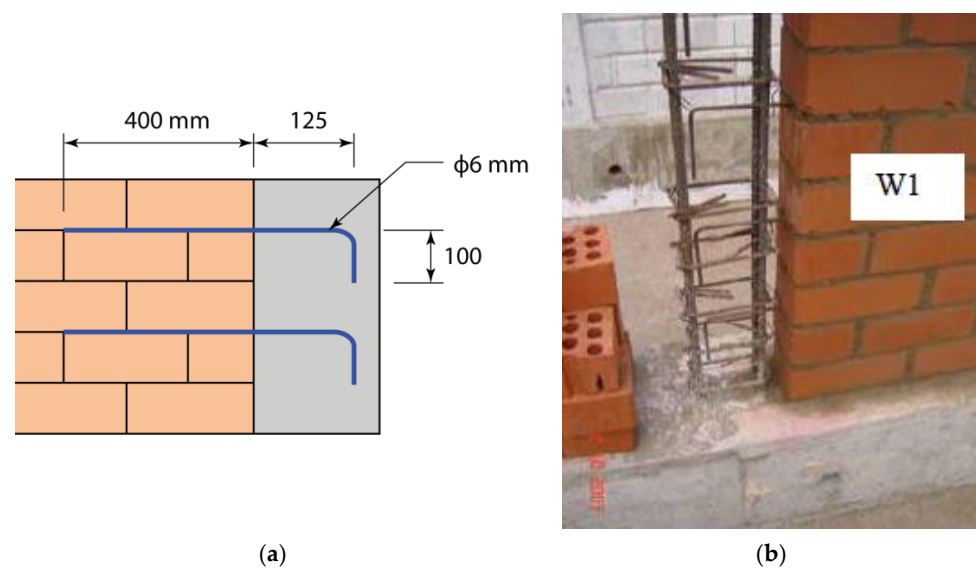


**Figure 34.** Connections at the wall-to-tie-column interface through dowels: (a) recommended practice and (b) a field application [144].

The minimum reinforcement ratio ( $\rho_{sh}$ ) for dowels is usually on the order of 0.1%, and vertical spacing between the dowels can therefore be calculated depending on the wall thickness. It is a common practice to provide a dowel every two or three courses along the wall height. For example, in a 140 mm thick masonry wall, a dowel with a diameter of 6 mm (28 mm<sup>2</sup> area) needs to be provided at a spacing of 200 mm; this is the equivalent of two courses of 90 mm high bricks with a 10 mm mortar joint thickness. The corresponding reinforcement ratio  $\rho_{sh}$  is equal to  $(28)/(140 \times 200) = 0.1\%$ .

Experimental evidence related to the study of toothed masonry connections and connections achieved through dowels is limited. A few pioneering experimental studies on the effect of different types of wall-to-tie-column connections in CM walls were performed at the PUCP, Peru [66,145,146]. An experimental study was performed on three half-scale CM walls subjected to reversed cyclic loading [145] (Figure 35). Wall 1 had a toothed connection and Wall 2 had a simple vertical wall-to-tie-column interface (no tothing or dowels). Wall 3 had an unusual construction sequence: initially, the tie-columns were constructed with the dowels, and subsequently the masonry wall was constructed. Walls 1 and 2 showed similar behaviour; however, in Wall 3, a tie-column separated from the masonry during an early stage, showing a flexural behaviour. All specimens experienced shear failure, characterised by multiple diagonal cracks, at a lateral drift level of approximately 1.0%. Subsequently, OOP testing of Wall 2 and Wall 3 was performed on the shaking table [146]. Under severe shaking, Wall 2 without tothing/dowels collapsed by overturning, while Wall 3 with dowels did not collapse. This study confirmed the importance of a wall-to-tie-column connection.

Gonzalez [66] performed an experimental study on two full-size CM wall specimens (Wall 1 and Wall 2) with both types of interface. First, the specimens were subjected to reversed cyclic lateral loading until shear failure took place; subsequently, an OOP test was performed on a shaking table. Wall 1 had a toothed connection between the masonry panel and adjacent RC tie-columns, with a tooth size equal to one-half of a brick. Wall 2 had a dowel connection in which the dowels were bars with a diameter of  $\frac{1}{4}$ " (6.3 mm) embedded into the mortar joints every two courses, and anchored into the adjacent RC tie-columns with 90-degree hooks at both ends. Under reversed cyclic loading, both walls showed similar behaviour during the testing (both in elastic and inelastic range). The cracking pattern, in the form of diagonal shear cracks, was similar in both walls. No visible cracks were observed along the wall-to-tie-column connection in Wall 2 with the dowels. In the second part of the experimental program, the same walls were subjected to OOP seismic

effects on a shaking table. The walls were anchored to the base of a shaking table, and the tie-beam was fixed to a horizontal actuator simulating the action of an RC floor slab, which in real buildings is horizontally restrained by other walls in the transverse direction. Both specimens experienced only minor additional cracks; therefore, it was concluded that the OOP vibrations did not aggravate damage in the walls.

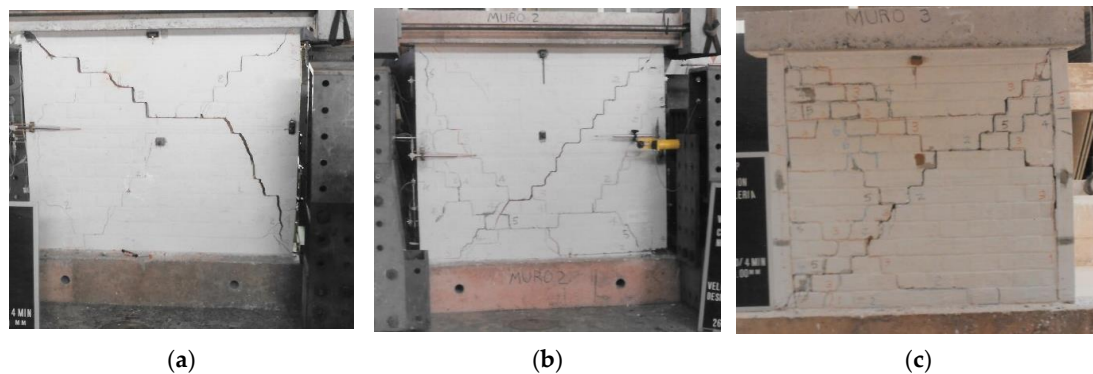


**Figure 35.** Walls with different interface arrangements: (a) Wall 1 (toothed connection); (b) Wall 2 (no tothing or dowels); and (c) Wall 3 (doweled connection) (credit: C. Vegas).

Singhal and Rai [147] investigated the effect of tothing on the stability of four wall specimens due to in-plane and OOP seismic loading. Of the four specimens, one was an RC frame with masonry infill (SI), and the remaining three specimens were CM panels: high-density tothing ( $SC_{FT}$ ), low-density tothing ( $SC_{CT}$ ), and no tothing ( $SC_{NT}$ ) (Figure 36). The design was performed in accordance with the Mexican masonry design code [32]. All specimens had an intermediate RC tie-column. The test program included in-plane reversed cyclic loading, followed by OOP simulated earthquake excitation induced by a shaking table. All specimens attained the required in-plane drift of 1.75%. The testing was discontinued when OOP displacement was large and collapse was imminent (specimen SI), or when longitudinal reinforcement in exterior tie-columns fractured (specimens  $SC_{FT}$  and  $SC_{CT}$ ), or when masonry experienced significant damage and cracking in intermediate tie-columns (specimen  $SC_{NT}$ ).

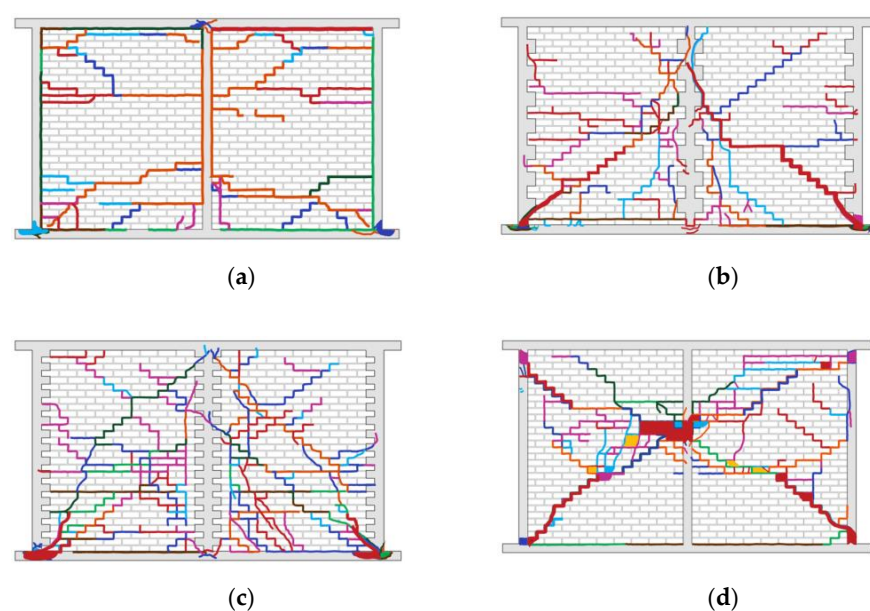


**Figure 36.** Comparison of cracking patterns for all specimens after 1.75% in-plane drift cycle (adapted from [147]): (a) SI (RC frame with infill); (b)  $SC_{CT}$  (with coarse tothing); (c)  $SC_{FT}$  (with fine tothing); and (d)  $SC_{NT}$  (without tothing).

It was also observed that separation of the masonry infill from the RC frame occurred in specimen SI at in-plane drift of 0.5%. CM wall panels maintained OOP stability and experienced low OOP displacements throughout the testing (up to the maximum drift of 1.75%). A variation in the fundamental period indicated a decrease in the wall stiffness with increasing in-plane drift. It was observed that the most significant decrease in stiffness occurred in the SI specimen (RC frame with infill). Finally, cracking distribution in the toothed specimens ( $SC_{FT}$  and  $SC_{CT}$ ) was similar (Figure 36). One of the main conclusions was that a composite action at the wall-to-tie-column interface in CM specimens reduced the OOP deflections and instability, as illustrated in Figure 37. With regard to in-plane loading, increased density of the tothing (fine tothing, specimen  $SC_{FT}$ ) resulted in improved post-peak behaviour, which was characterised by higher ductility and lower strength degradation.

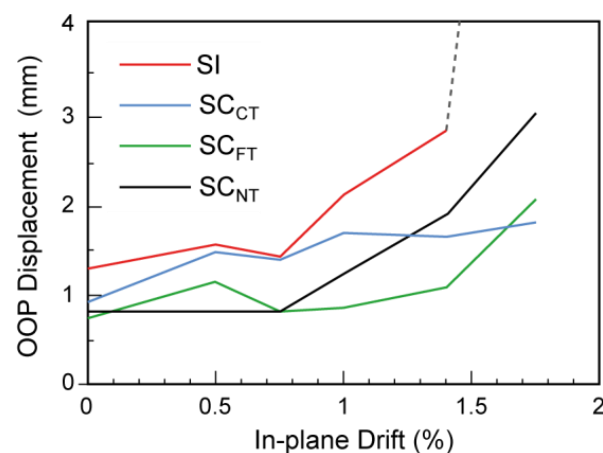


**Figure 37.** Variation in OOP displacements due to increasing in-plane drift demand (adapted from [147]).

Nguyen et al. [148] performed an experimental study on two CM wall specimens constructed with different wall-to-tie-column interface connections. The objective of the study was to compare the shear capacity, ductility and failure mechanisms for the test specimens subjected to in-plane cyclic loading. Wall 1 had a toothed connection, while the wall-to-tie-column connection in Wall 2 was achieved via steel dowels. The specimens were 200 mm thick squat walls (aspect ratio 0.83) and were constructed using clay brick masonry laid in a running bond. The tothing in Wall 1 extended by 10 cm (equivalent to one-half of the brick length), while the connection in Wall 2 was achieved via #3 (9.5 mm diameter) dowels with standard 90-degree hooks provided at a vertical spacing of 406 mm. Figure 38a,b show the specimens at the end of the test. Both specimens underwent shear failure and were severely damaged, but they did not collapse, even under high drift demands. These results indicated that Wall 1 had higher in-plane shear strength, while Wall 2 had a higher ductility (Figure 38c). It was concluded that tothing was more effective at establishing composite behaviour with the tie-column compared to an alternative doweled connection.

Castellano, Torrasi, and Crisafulli [149] reported a comparison between the performance of three wall specimens under reversed cyclic lateral load: an RC frame with infill (PR), a traditional CM wall (CM) according to the Argentinian practice, and a CM wall with a toothed connection (CMD). The traditional CM wall specimen had neither tothing nor dowels, while the CMD wall had a toothed connection over 1/5 of the length of the masonry unit (50 mm). The PR wall showed a separation along the wall-to-tie-column interface from the beginning of the test, and its lateral load capacity was lower compared to those of the CM and CMD walls. On the other hand, both the CM and CMD walls exhibited an adequate bond at the masonry-to-tie-column interface; however, both walls showed a separation along the interface due to diagonal cracking that extended up to the interface.

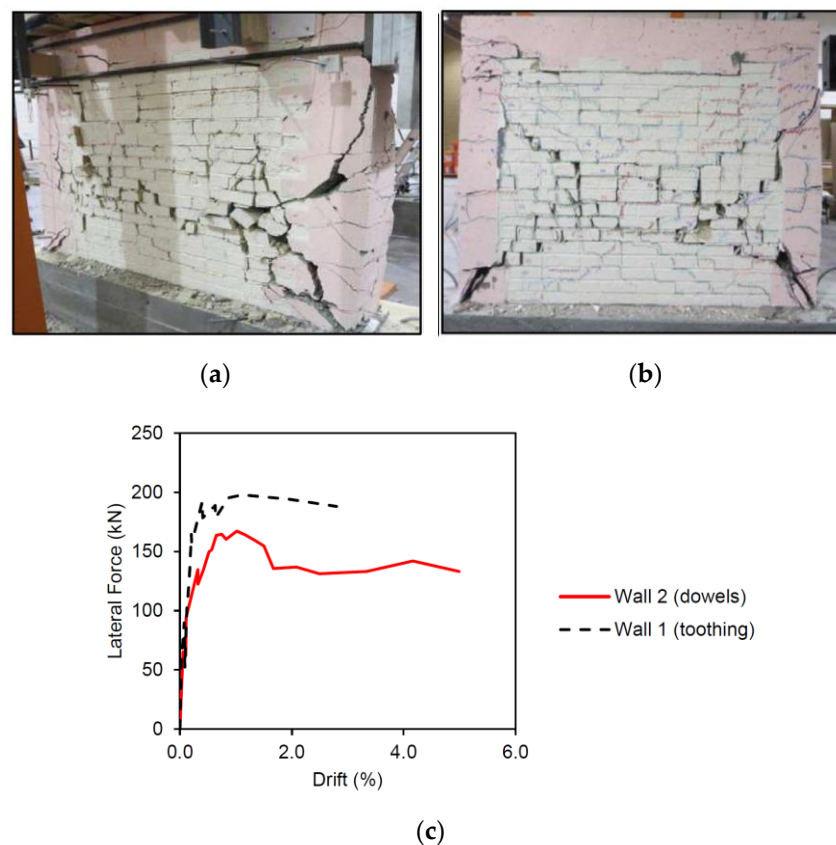


**Figure 38.** CM walls with different wall-to-tie-column interfaces: (a) failure of Wall 1 (toothed connection) at approximately 3.0% drift; (b) failure of Wall 2 (connection through dowels) at approximately 5.0% drift; and (c) lateral force versus drift ratio (images a) and b) from [148] reprinted with permission of the publisher: the Masonry Society, and c) was adapted from [148]).

Wiyaja et al. [150] reported an experimental study on four squat CM walls with a square shape. Wall A had no connection between masonry and tie-columns, Wall B was connected through dowels with a diameter of 8 mm every six courses, Wall C had a toothed connection, and Wall D had continuous 8 mm continuous horizontal reinforcing bars at a vertical spacing of 1 m (in addition to the same dowels as Wall B). The lateral force was applied via the top tie-beam, until the specimen either collapsed or 5.0% drift was reached. Compared to Wall A, the additional short anchor in Wall B slightly enhanced the lateral strength of the wall. Wall D, with continuous horizontal bars, had the highest lateral load capacity due to the shear contribution of horizontal reinforcement and enhanced confinement. The behaviour of Wall C showed that a toothed connection did not improve lateral load capacity, and it was characterised by the lowest capacity of all specimens.

The damage and failure of the walls was initiated by vertical cracking along the wall-to-tie-column interface. The final failure mode in the specimens with toothed and doweled connections was characterised by sliding shear patterns along the mortar bed joints, thus negatively affecting the structural performance. Conversely, Wall D, with continuous bars, strengthened the wall confinement and allowed the development of a diagonal cracking pattern; therefore, the best structural performance occurred in that wall.

A few relevant experimental research studies are summarised in Table A5, Appendix A. The results of these studies showed that the walls with toothed and doweled wall-to-tie-column connections had better in-plane seismic behaviour compared to the walls without connections; this is reflected in the reduced amount of cracking and the higher ductility, while possessing a similar shear capacity. Regarding the OOP effects, the majority of walls without connections either collapsed or experienced large deflections, while the walls with toothed or doweled connections sustained the OOP effects without failure.

### 5.3. Materials

Masonry is a composite material, composed of masonry units and mortar which binds the units together, and in some cases, reinforcement and grout. Mortar is a mix of cement, sand, lime, and water. The proportions of these materials vary significantly between various countries, and in some cases among different regions within the same country. Masonry units vary in terms of materials, dimensions, and design. Traditionally, masonry units are made of concrete, clay, fly ash, silicate, and Autoclaved Aerated Concrete (AAC), and are either in the form of bricks or blocks (based on the dimensions and proportions). Masonry units are typically classified into solid and hollow (based on the presence of perforations/cells). Hollow units have many variations related to the shape and size of perforations. For example, the types of masonry units used in Mexico, shown in Figure 39, include solid and hollow concrete blocks (with two cells) (Figure 39a), multi-perforated clay units (four types) (Figure 39b), multi-perforated concrete blocks (Figure 39c), hollow clay blocks (Figure 39d), solid clay and concrete bricks (Figure 39e), and traditional hand-made clay bricks (Figure 39f). It can be observed that some multi-perforated clay units have external vertical ribs that are intended for enhanced bonding with the mortar and/or plaster, while other units have smooth vertical faces.



**Figure 39.** Various types of masonry units used in Mexico (Credit: L. Flores).

Experimental studies have shown that hollow masonry units have a lower compressive strength compared to solid units [9]; this can be explained by a reduced net area for hollow units compared to otherwise similar solid units, and also relatively thin and brittle masonry face shells in hollow units. Several experimental research studies in different countries have been performed focusing on testing the mechanical properties of masonry materials, and their findings are relevant for all types of loadbearing masonry structures, including CM walls. Kaushik, Rai and Jain [151] performed a comprehensive experimental study on the mechanical properties of masonry materials used in India. They tested four different brick grades, with compressive strength ranging from 16.1 to 28.9 MPa. In total, 40 brick specimens were tested, and the average compressive strength was 20.8 MPa. Different mortar mix compositions (cement:lime:sand by volume) were used in the study, including 1:0:6 (weak), 1:0:3 (strong), and 1:½:4½ (intermediate). The corresponding compressive strengths, obtained by testing 27 mortar cubes in total, were 3.1, 20.6, and 15.2 MPa, respectively. The researchers tested 84 masonry prisms in total (28 prisms per mortar type). As expected, higher masonry compressive strength,  $f'_m$ , was obtained when a stronger mortar was used. The masonry compressive strength values increased with increasing brick compressive strength, but the difference was most pronounced for prisms constructed in weak mortar: the  $f'_m$  values ranged from 2.9 MPa to 5.1 MPa for the weakest and strongest bricks, respectively (the latter value is by 75% higher than the former one). On the other hand, the differences in  $f'_m$  values were less pronounced for prisms constructed in strong mortar, with the  $f'_m$  values ranging from 6.5 MPa to 8.5 MPa for the weakest and

strongest bricks, respectively (the latter value is higher than the former one by 31%). The average  $f'_m$  values for all prisms constructed using weak and strong mortar were 4.1 MPa and 7.5 MPa, respectively. It is noteworthy that, although the prisms constructed using intermediate mortar were not characterised by the highest  $f'_m$  (6.6 MPa), they attained the highest ultimate strain (0.008), while the other prisms attained only 0.006; this increased deformability can be attributed to the presence of lime in the intermediate mortar.

Zabala et al. [152] tested solid clay brick masonry used in Argentina and determined the compressive strength of the bricks (4.5 MPa) and masonry (2.9 MPa).

The type and mechanical properties of masonry units have a considerable effect on the behaviour of CM walls subjected to in-plane lateral loading. Figure 40 shows shear strength envelopes for three series of wall specimens (16 specimens in total), which were constructed using different masonry units and amounts of horizontal (joint) reinforcement [153]. The amount of joint reinforcement was quantified as a product of the reinforcement ratio and steel yield strength ( $\rho_h f_{yh}$ ), see Table 3. The specimens tested by Aguilar et al. [25] (M1 to M4) were constructed using traditional hand-made solid clay bricks. Although the bricks were characterised by low shear strength, the wall specimens exhibited a large displacement capacity (ductility); this can be attributed to use of solid masonry units. Note that the provision of joint reinforcement did not result in a significant increase in the shear strength; however, it did positively influence displacement capacity (ductility), see specimens M3 and M4. Alcocer et al. [27] tested CM walls N1 to N4, constructed using machine-made multi-perforated clay units with compression strength greater than 16.0 MPa, which exhibited significantly higher shear strength compared to walls constructed using traditional clay bricks. However, the displacement capacity of these walls was very limited, and the strength degradation rate was very rapid compared to other types of masonry units. Because the ratio of net/gross area of the units was about 60%, and the material failed in a brittle manner, post-peak behaviour was characterised by unit spalling. It was also observed that the gain in shear strength in specimens N2, N3, and N4 was very significant with joint reinforcement. The last set of CM walls (MB-0 to MB-5) tested by Cruz et al. [40] used multi-perforated concrete units, which resulted in CM walls with ductile behaviour and a slower strength degradation rate compared to the specimens constructed using machine-made solid clay bricks. However, the results showed that the behaviour was not as ductile as the specimens with the traditional solid clay units; this was probably due to the fact that the masonry units had 70% net/gross area ratio. The increase in strength was also very significant for wall specimens with joint reinforcement.

**Table 3.** CM wall specimens: horizontal reinforcement parameters.

Aguilar et al. [25]		Alcocer et al. [27]		Cruz et al. [40]	
Specimen ID	$\rho_h f_{yh}$	Specimen ID	$\rho_h f_{yh}$	Specimen ID	$\rho_h f_{yh}$
M1	0.89	N1	0	MB-0	0
M2	0	N2	0.30	MB-1	0.23
M3	0.43	N3	0.30	MB-2	0.62
M4	1.14	N4	1.14	MB-3	0.92
				MB-4	1.21
				MB-5	1.58

The critical parameters for characterising the mechanical behaviour of masonry are diagonal compression strength,  $v_m$ , and the masonry compression strength,  $f'_m$ ; however, a few additional parameters may be required as input for complex nonlinear analyses [44]. It is a common practice to use the compression strength of masonry,  $f'_m$ , to estimate its shear and tensile strengths. Although standardised tests for determining diagonal compression strength are well established (e.g., ASTM E-519), these tests are not required by the masonry design codes in the USA, Canada, or majority of other countries with a developed masonry construction practice; instead,  $f'_m$  is used as a measure of tensile strength. In Latin American countries, diagonal compression strength is used in Mexico as a material testing

requirement prescribed by the masonry design code (NTC-M) since 2004. The results of diagonal compression tests for masonry specimens gathered by Treviño et al. [64] are shown in Figure 41a. In total, 104 specimens were considered in this study, and four different types of masonry unit were used. The results showed that  $v_m$  values ranged from 2.5 to 11.0 MPa, with different upper/lower bounds for different types of masonry unit.

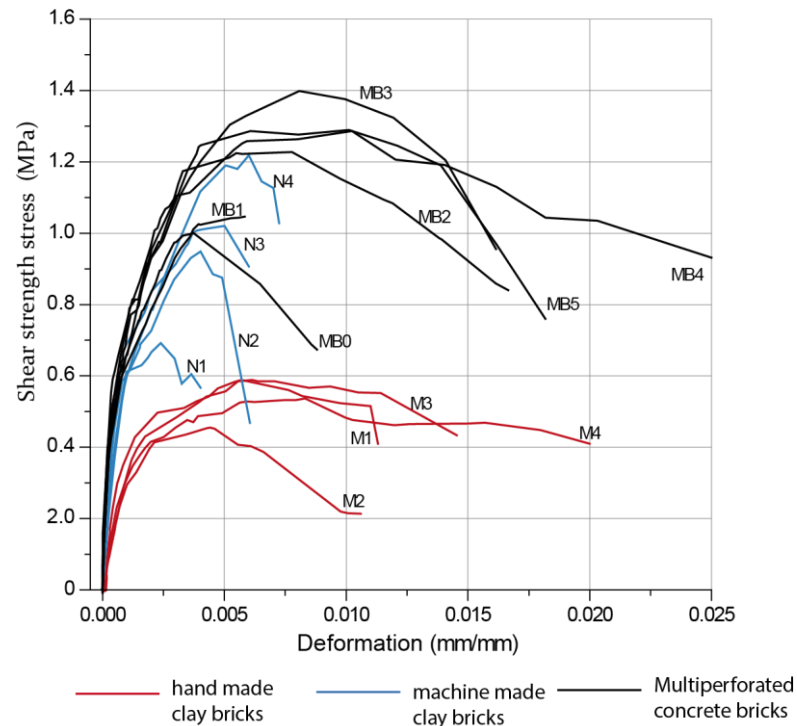


Figure 40. Shear strength envelopes for CM walls with different masonry units and amounts of joint reinforcement (adapted from [153]).

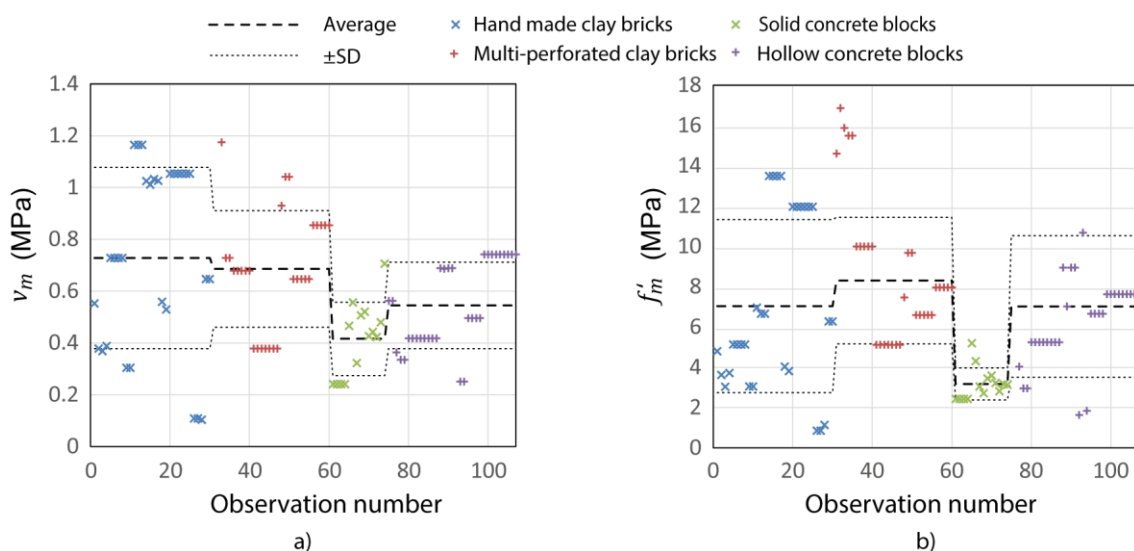
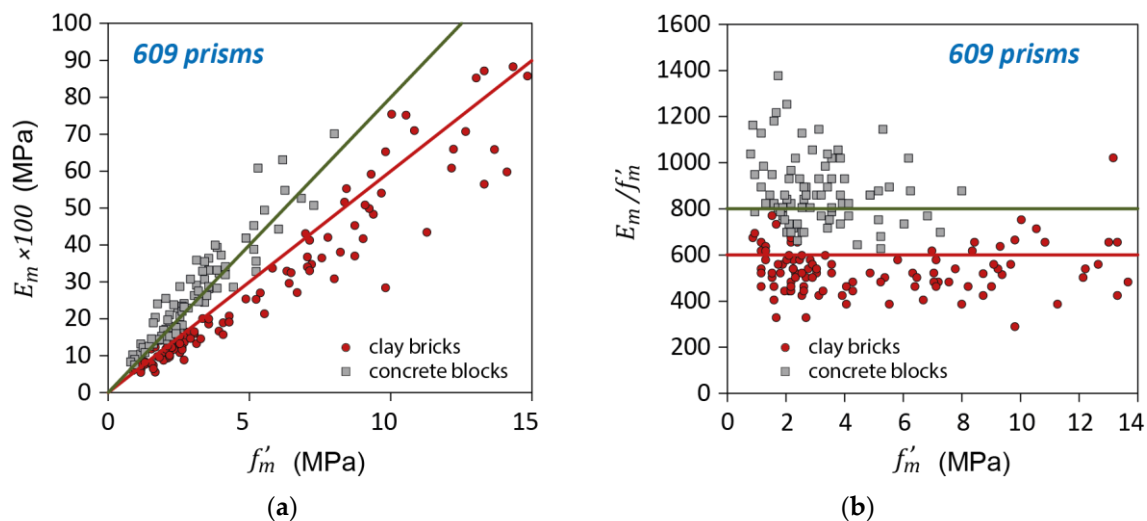


Figure 41. Masonry mechanical properties: (a) diagonal compression strength and (b) masonry compression strength (data from [64]).

Masonry compression strength,  $f_m$ , can be considered to be a measure of masonry quality, and it is used to estimate both the axial compression resistance and the flexural resistance of masonry walls. According to the Mexican masonry design code [33],  $f_m$  is also related to the maximum shear strength contributed by joint reinforcement. Figure 41b

shows masonry compression strength values for specimens gathered by Treviño et al. [64]. In total, 104 specimens were tested, and the  $f_m$  values ranged from 1.0 to 17.0 MPa. It can be seen that the largest variation in the results was obtained for specimens with hand-made clay bricks.

The masonry compression strength,  $f_m$ , is also related to the modulus of elasticity,  $E_m$ . Extensive testing was carried out in Mexico to establish this relationship for different types of masonry unit [14,154]. The relationship between  $f_m$  and  $E_m$  is shown in Figure 42a, while the  $E_m/f_m$  ratio is shown in Figure 42b. The horizontal lines show the code-prescribed ratios in Mexico, that is,  $E_m/f_m = 800$  for concrete blocks and  $E_m/f_m = 600$  for clay bricks. Masonry design codes in various countries have adopted different values for the  $E_m/f_m$  ratio based on the local data, but they usually fall in the range from 550 to 850.



**Figure 42.** Relationship between the masonry compression strength and modulus of elasticity: (a) experimental  $f_m$  and  $E_m$  values for clay bricks and masonry blocks; and (b)  $E_m/f_m$  ratio (data from [14]).

## 6. Conclusions and Research Gaps

The previous experimental research studies reviewed in this paper contain substantial evidence related to the seismic behaviour of CM walls. Based on the available experimental studies, relevant conclusions and future research needs (shown in *italics*) are summarised for each major topic.

### 6.1. In-Plane Shear

In most cases, CM shear walls subjected to in-plane seismic effects demonstrate a shear-dominant behaviour. An experimental database from several past research studies on CM wall specimens subjected to either monotonic or reversed cyclic lateral loading was used to establish critical parameters that influence the in-plane shear strength of CM walls. A statistical analysis of more than 100 experimental data points has confirmed that the masonry shear strength,  $v_m$ , is proportional to the square root of masonry compression strength,  $f_m$ ; however, the diagonal compression strength is a better indicator of the shear strength. Another influencing factor is the wall aspect ratio,  $H/L$ , which has been accounted for by the  $f$  factor, which was proposed as a result of an experimental research study. It was observed that shear–moment interaction due to the applied bending moment at the top of the wall causes a decrease in the masonry shear strength, particularly for walls characterised by a higher aspect ratio. The results of experimental studies have confirmed that masonry shear resistance is also proportional to the level of applied axial compression. The contribution of horizontal joint reinforcement to shear resistance of CM walls was shown to be proportional to the reinforcement ratio and steel yield strength. The results

of experimental studies indicated that the effectiveness of horizontal reinforcement in CM walls may be limited, that is, there exists a maximum limit for the amount of such reinforcement in the wall beyond which its effectiveness cannot be increased. The effect of RC tie-columns on masonry shear strength has been studied by several researchers, but the conclusions in terms of the effect of longitudinal reinforcement differ. A statistical analysis of experimental data performed by the authors indicated that the masonry shear strength is proportional to square root of the product of longitudinal reinforcement ratio, steel yield strength, and concrete compressive strength, and the results show that the amount of longitudinal reinforcement in RC tie-columns has a significant influence on the masonry shear strength.

*Further experimental research studies are needed on the following topics:*

- *Shear strength of walls under tension;*
- *The effect of the geometry of masonry units on masonry shear strength (bricks vs. blocks, perforated units);*
- *A rational mechanical model for understanding the shear contribution of horizontal reinforcement; and*
- *The interaction of in-plane shear and flexure.*

### 6.2. In-Plane Flexure

The flexural failure of CM shear walls subjected to combined axial load and in-plane lateral loading is less common than shear failure; therefore, the experimental research evidence related to in-plane flexural behaviour of CM walls is limited. In general, flexure-dominant behaviour is characterised by yielding of longitudinal reinforcement and crushing of concrete at the base of RC tie-columns. Vertical cracks develop along the masonry-to-tie-column interface in slender CM specimens with higher aspect ratios. A comprehensive experimental study on 28 CM walls performed in Japan [120] showed that the specimens with cantilevered boundary conditions experienced either a shear-dominant or sliding failure mechanism, while the specimens with fixed ends experienced a flexural failure. The study showed that horizontal dowels provided at the masonry-to-tie-column interface are effective at preventing the separation of RC tie-columns from masonry panels. Recent experimental research studies performed in Mexico on CM walls subjected to reversed cyclic loading [118] showed that the specimens with predominant flexural behaviour attained higher displacement ductility at the ultimate stage than the CM walls with predominant shear behaviour; this is a very important consideration for performance-based seismic design. The results of previous experimental studies performed in Mexico [13,122] indicated that the normalised moment resistance of CM walls increases with increasing axial stress level; however, it appears that the effect of higher axial stress level is more important for CM walls with an aspect ratio of 2.0 or higher.

The results of a parametric numerical study performed by the authors indicate that the key parameters influencing the type of failure mechanism (flexure or shear) in CM walls are: axial stress level, masonry shear strength, horizontal reinforcement ratio, wall aspect ratio, and tie-column longitudinal reinforcement ratio. The study showed that the walls with an aspect ratio higher than 1.0 and/or with higher masonry shear and compression strength can be expected to experience a flexural failure. The amount (ratio) of horizontal reinforcement in the masonry panel is probably the most important parameter: the higher the horizontal reinforcement ratio, the higher the chance of flexural failure. An increased amount of horizontal reinforcement leads to increased shear capacity of CM walls.

*Further experimental research studies are needed on the flexure-dominant behaviour of CM walls of all types, including different types of masonry units, wall aspect ratios, and axial load levels.*

### 6.3. Out-of-Plane (OOP) Behaviour

The OOP failure mechanism in CM walls subjected to seismic effects is complex, and depends on the type of loading, as shown by experimental studies. Arching mechanisms can be used to estimate the OOP resistance (ultimate pressure) for loadbearing masonry

walls, including CM walls. According to the concept of arching mechanism, two or more rigid segments will form in cracked masonry walls that are subjected to a combination of gravity loading and lateral pressure. This mechanism can culminate in masonry crushing, which is characteristic for walls with low slenderness ( $h/t$ ) ratios, but additional factors include masonry compressive strength and the stiffness of adjacent RC confining elements. An alternative failure mechanism is lateral instability due to excessive horizontal displacements, referred to as “snap-through” failure; this mechanism may be expected in slender CM walls and walls with flexible RC confining elements. Mechanical models based on a bi-directional arching mechanism are more accurate than those based on one-directional models, which tend to be conservative (i.e., predict lower resistance). It is important to note that bi-directional models consider the wall aspect ratio as an indicator of OOP resistance. Past studies indicated that the OOP resistance of CM walls depends on a few parameters, including the wall geometry (height, length, thickness), stiffness of adjacent RC confining elements, and masonry compression strength. A review of past experimental studies on CM walls subjected to monotonic OOP pressure [50,129–131,133,134] showed a significant scatter of ultimate pressure for specimens with different slenderness ratios; however, the results of a shaking table study [135] showed that less slender walls have higher OOP resistance, which is in line with the predictions obtained from analytical models [127]. The wall aspect ratio and axial stress level also influence the OOP behaviour of CM walls—experimental studies have shown that the ultimate pressure for CM walls increases with increasing aspect ratio and axial stress level. The stiffness of RC confining elements is a very important parameter that influences seismic response of CM walls. Experimental studies on CM walls showed that walls with stiff RC confining elements experience crushing failure in the masonry, while walls with flexible RC confining elements experience a “snap-through” failure.

*Further experimental research studies are needed on the following topics:*

- *The OOP response of CM walls constructed using clay bricks and multi-perforated clay blocks;*
- *The effect of the stiffness of the RC confining elements on the OOP behaviour of CM walls;*
- *A comparison of the OOP behaviour of masonry infills in RC frames and CM walls under reversed cyclic loading;*
- *The OOP response of CM walls subjected to reversed cyclic loading, and also dynamic loading (e.g., shaking table tests); and*
- *The effect of combined in-plane and OOP loading.*

#### 6.4. Openings in CM Walls

Openings in CM walls subjected to seismic effects cause a decrease in their peak strength and stiffness, as evidenced by several experimental studies, as well as reports from past earthquakes. The extent of the decrease in strength depends on the size of an opening relative to the size of a wall panel and the position of opening within the panel. A ratio of the area of an opening relative to the CM panel area,  $A_r$ , can be used to predict strength decrease in CM walls with openings. Experimental studies have confirmed a beneficial effect of vertical and horizontal RC confining elements around the openings, which are effective at reducing the extent of damage and maintaining the wall's strength, stiffness, and displacement/drift potential.

*Further experimental research studies are needed on the following topics:*

- *The in-plane and OOP behaviour of walls with openings, considering different sizes and locations of openings;*
- *The effect of the size and location of confining elements in walls with openings; and*
- *The behaviour of CM walls with openings in buildings with flexible floor/roof diaphragms.*

#### 6.5. Toothing

One of the key features of CM construction is the connection between the masonry panels and the adjacent RC confining elements. It is believed that such a connection is beneficial for enhancing the performance of CM walls subjected to in-plane and out-of-plane

seismic effects. The most common connection is in the form of tothing, and consists of a “zig-zag” edge created by masonry units along the masonry-to-tie-column interface. Subsequently, concrete is poured into RC tie-columns, and hence shear keys are formed along the interface. Alternatively, horizontal steel bars (dowels) may be embedded in mortar joints and extended on each side of a RC tie-column by a minimum length required for effective anchorage. The choice of connection depends on the type of masonry unit: tothing may be feasible when bricks are used, while dowelled connections are suitable for CM walls constructed using block units. In some countries, e.g., Argentina, CM walls are traditionally constructed without any connections (vertical edge). Although experimental research studies have been performed focusing on studying the performance of CM walls with different masonry-to-tie-column connections, the evidence is limited. Experimental studies have been performed to determine the effectiveness of the presence of toothed connections in CM walls. Singhal and Rai [147] tested CM walls under in-plane and OOP loading and concluded that tothing is particularly effective at controlling the damage due to OOP seismic effects, and that fine tothing (with smaller tooth sizes) is more effective than coarse tothing arrangements. Other research studies [66,145,146,149] showed that CM specimens with a toothed connection did not show superior performance compared to otherwise similar specimens without a toothed connection. A few researchers have performed comparisons between CM walls with toothed and dowelled connections [148,150], concluding that both connection types (tothing and dowels) are similar in terms of their effectiveness.

*Further experimental research studies are needed on the following topics:*

- *The tothing length and teeth spacing requirements for CM walls with different types of masonry units (bricks, blocks);*
- *A comparison of tothing effectiveness for CM walls constructed using brick and block masonry;*
- *The number (size and spacing) of steel dowels required for CM walls without tothing (a common situation in CM with block units); and*
- *The response of CM walls with/without tothing under reversed cyclic loading.*

#### 6.6. Materials

The mechanical characteristics of masonry materials influence the seismic behaviour of CM walls. Masonry materials, particularly masonry units, vary between countries, and also between different regions within the same country. In the past, solid clay bricks were used for CM wall construction; however, in the last few decades, multi-perforated clay blocks have been widely used, particularly in the Latin American and European countries. Masonry mortar, in terms of the mix proportion and constituent materials (cement, lime, sand), also has a significant effect on the masonry compressive and shear strength. An experimental study on 16 CM walls performed in Mexico [25,27,40] showed that the specimens constructed using traditional hand-made solid clay bricks had relatively low shear resistance, but at the same time a higher displacement capacity (ductility) than the specimens constructed using other types of masonry units. The results of another study on CM wall specimens constructed using machine-made clay bricks characterised by significantly higher compressive strength showed higher shear strength of CM walls, but a rapid post-peak strength degradation and a notably lower displacement ductility. Finally, the specimens constructed using multi-perforated concrete blocks demonstrated the highest strength and a gradual post-peak strength degradation, combined with a reasonably high ductility.

*Further experimental research studies should be directed towards masonry assemblage testing more than material testing. From a look at the available studies, the use of materials, clay or concrete, hollow or solid, is dependent on the in-situ availability of products. In addition, it would be interesting to establish how accurately results for the tested masonry assemblages compare to the as-built conditions.*

**Author Contributions:** Conceptualization, J.J.P.G.E., S.B. and M.T.R.; Methodology, J.J.P.G.E., S.B., E.F.E.C., S.G., D.Q. and M.T.R.; Software, J.J.P.G.E. and E.F.E.C.; Validation, E.F.E.C., S.G., D.Q. and M.T.R.; Formal analysis, J.J.P.G.E.; Investigation, J.J.P.G.E., S.B., E.F.E.C., S.G. and D.Q.; Resources, S.B.; Data curation, J.J.P.G.E.; Writing—original draft, J.J.P.G.E., S.B., E.F.E.C., S.G. and D.Q.; Writing—review & editing, M.T.R.; Visualization, E.F.E.C.; Supervision, S.B. All authors have read and agreed to the published version of the manuscript.

**Funding:** This research received no external funding.

**Data Availability Statement:** Research data is available in Appendix A.

**Acknowledgments:** The authors are grateful to Ernesto Treviño and Leonardo Flores for sharing the experimental data and agreeing to use experimental database which they created for this study, and to publish the data in Appendix A. This manuscript is a result of an initiative by the joint Confined Masonry working group formed by the Masonry Society and the Earthquake Engineering Research Institute, and the authors acknowledge the support of these two organizations.

**Conflicts of Interest:** The authors declare no conflict of interest.

## Appendix A. Database of Experimental Test Data Related to CM Walls

**Table A1.** A summary of experimental studies on in-plane shear testing of CM walls.

Reference	Country	Number of Walls	Type of Units
Aguilar et al. (2001) [65]	México	4	Hand-made clay bricks
Pineda (1996) [67]	México	4	Hand-made clay bricks
Mendoza (2006) [68]	México	1	Hand-made clay bricks
Vázquez (2005) [69]	México	1	Hand-made clay bricks
Arias (2005) [70]	México	1	Hand-made clay bricks
Barragán (2005) [71]	México	1	Hand-made clay bricks
Diez (1987) [72]	Chile	4	Hand-made clay bricks
San Bartolomé (1983) [73]	Perú	2	Hand-made clay bricks
San Bartolomé (-) [74]	Perú	6	Hand-made multiperforated clay bricks
San Bartolomé et al. (-) [75]	Perú	3	Hand-made soil sand and straw
González et al. (-) [66]	Perú	2	Hand-made clay bricks
Zepeda et al. (2001) [76]	México	4	Machine-made multiperforated bricks
Meli et al. (1969) [13]	México	5	Machine-made multiperforated bricks
Hernández et al. (1976) [16]	México	7	Machine-made multiperforated bricks
San Bartolomé (1983) [73]	Perú	3	Machine-made multiperforated bricks
Echevarría (-) [77]	Perú	5	Machine-made multiperforated bricks
Pastorutti et al. (-) [78]	Perú	5	Machine-made multiperforated bricks
Alcocer et al. (2003) [79]	México	4	Solid concrete bricks
Urzúa (1999) [80]	México	4	Solid concrete bricks
Cosío (2001) [81]	México	6	Solid concrete bricks
Meli et al. (1968) [82]	México	2	Hollow concrete blocks
Hernández et al. (1976) [16]	México	2	Hollow concrete blocks
Treviño et al. (2004) [83]	México	8	Hollow concrete blocks
Muñoz (1992) [84]	Chile	4	Hollow concrete blocks
Ramírez et al. (-) [85]	Perú	1	Hollow concrete blocks
Quiun et al. (2005) [86]	Perú	2	Hollow concrete blocks
Marinilli et al. (2007) [87]	Venezuela	4	Hollow concrete blocks
Castilla (1998) [88]	Venezuela	9	Hollow concrete blocks

**Table A2.** Database of experimental studies on in-plane shear testing of CM walls (selected data).

Num	Reference	Identification		Unit		Geometry			Masonry		Tie-Column		Shear Strength	
		Study ID	Specimen ID	Type (+)	$f_p$ (MPa)	$L$ (cm)	$H$ (cm)	$t$ (cm)	$f_m$ (MPa)	$p$ (%)	$f_y$ (MPa)	$f'_c$ (MPa)	$V_{ag+}$ (kN)	$V_{max+}$ (kN)
1	Aguilar et al. (2001) [65]	CEN08	M-3/8-Z6	1	11.8	250	250	12.5	4.8069	1.52%	447.3	27.0	147.2	174.1
2	Aguilar et al. (2001) [65]	CEN09	M-0-E6	1	11.8	250	250	12.5	3.6297	1.51%	447.3	27.5	98.1	133.9
3	Aguilar et al. (2001) [65]	CEN10	M-5/32-E20	1	11.8	250	250	12.5	3.0411	1.51%	447.3	22.6	127.5	174.6
4	Aguilar et al. (2001) [65]	CEN11	M-1/4-E6	1	11.8	250	250	12.5	3.7278	1.51%	447.3	24.0	103.0	158.9
5	Pineda (1996) [67]	CEN12	M-072	1	11.8	250	250	12.5	5.14044	3.17%	442.4	53.0	281.1	415.5
6	Pineda (1996) [67]	CEN13	M-147	1	11.8	250	250	12.5	5.14044	4.56%	442.4	53.0	291.4	374.3
7	Pineda (1996) [67]	CEN14	M-147R	1	11.8	250	250	12.5	5.14044	4.56%	453.2	53.0	196.7	382.1
8	Pineda (1996) [67]	CEN15	M-211	1	11.8	250	250	12.5	5.14044	6.84%	453.2	53.0	361.0	503.3
9	Mendoza (2006) [68]	CEN35	MV-2	1	10.4	230	250	12	3.05091	1.58%	418.0	13.9	51.6	101.5
10	Vázquez (2005) [69]	II-MV5	M1SRCC	1	11.8	508.92	120	6	6.9651	1.98%	455.9	26.2	182.5	264.9
11	Arias (2005) [70]	II-MV6	M3SRCC	1	11.8	508.92	120	6	6.6708	1.98%	455.9	23.2	227.6	288.4
12	Barragán (2005) [71]	II-MV7	M2SRCC	1	11.8	508.92	120	6	6.6708	1.98%	455.9	23.2	159.9	216.8
13	Diez (1987) [72]	CHILE4	MRE1	2	11.8	120	240	14	13.49856	1.62%	412.0	20.9	58.9	101.5
14	Diez (1987) [72]	CHILE5	MRE2	2	11.8	120	240	14	13.49856	1.62%	412.0	20.9	58.9	95.2
15	Diez (1987) [72]	CHILE9	MRG1	2	11.8	240	240	14	13.49856	1.62%	412.0	20.9	117.7	117.7
16	Diez (1987) [72]	CHILE1	MRG2	2	11.8	240	240	14	13.49856	1.62%	412.0	20.9	155.0	186.4
17	San Bartolomé (1983) [73]	PERU2	A-0-1	1	5.6	240	240	13.5	4.04172	1.49%	428.7	15.5	110.9	148.1
18	San Bartolomé (1983) [73]	PERU5	A-1-2	1	5.6	240	240	13.5	3.81609	1.49%	428.7	15.5	102.7	133.0
19	San Bartolomé (-) [74]	PERU14	M1	2	23.1	240	250	13	11.9682	1.09%	445.9	17.2	115.4	157.6
20	San Bartolomé (-) [74]	PERU15	M2	2	23.1	240	250	13	11.9682	0.91%	412.0	17.2	111.1	148.6
21	San Bartolomé (-) [74]	PERU16	M3	2	23.1	240	250	13	11.9682	1.94%	443.6	17.2	176.6	263.3
22	San Bartolomé (-) [74]	PERU17	M4	2	23.1	240	250	13	11.9682	1.64%	412.0	17.2	176.6	222.0
23	San Bartolomé (-) [74]	PERU18	M5	2	23.1	240	250	13	11.9682	3.05%	429.9	17.2	176.6	266.9
24	San Bartolomé (-) [74]	PERU19	M6	2	23.1	240	250	13	11.9682	2.55%	412.0	17.2	176.6	276.1
25	San Bartolomé et al. (-) [75]	PERU20	M1	1	5.9	274	245	25	0.861318	0.34%	418.2	10.2	36.7	37.2
26	San Bartolomé et al. (-) [75]	PERU21	M2	1	5.9	274	245	25	0.861318	0.17%	418.2	10.2	33.7	33.2
27	San Bartolomé et al. (-) [75]	PERU22	M3	1	5.9	274	245	25	1.141884	0.34%	418.2	10.2	42.3	42.9
28	González et al. (-) [66]	PERU23	M1	2	9.8	240	230	13	6.2784	1.95%	412.0	17.9	113.0	227.7
29	González et al. (-) [66]	PERU24	M2	2	9.8	240	230	13	6.2784	1.95%	412.0	17.9	123.3	188.8
30	Zepeda et al. (2001) [76]	CEN16	N1	2	22.0	240	230	12	14.6169	4.95%	459.1	26.0	180.0	203.6
31	Zepeda et al. (2001) [76]	CEN17	N2	2	22.0	240	230	12	16.8732	4.95%	459.1	26.0	172.7	279.1
32	Zepeda et al. (2001) [76]	CEN18	N3	2	22.0	240	230	12	15.8922	6.33%	451.3	31.9	192.3	300.2
33	Zepeda et al. (2001) [76]	CEN19	N4	2	22.0	240	230	12	15.4998	8.71%	467.1	26.0	175.6	358.6

(+) 1—Hand-made solid clay bricks; 2—Machine-made multiperforated clay bricks.

**Table A3.** Experimental database of CM walls subjected to OOP pressure.

Study	Specimen	Unit	$H$ (mm)	$L$ (mm)	$H/L$	$t$ (mm)	$H/t$	Axial Stress (MPa)	$f_m$ (MPa)	# of Supports	$W_{cr}$ (kPa)	$W_u$ (kPa)
Varela-Rivera et al. (2011) [129]	E-1	HCB	1760	3600	0.49	150	11.73		3.07	4	3.4	13.7
	E-2	HCB	1760	3600	0.49	150	11.73		3.07	4	3.4	13.6
	E-3	HCB	1760	3600	0.49	150	11.73		3.07	4	3.7	14.3
	E-4	HCB	1760	3600	0.49	150	11.73		3.07	3	3.4	13.1
	E-5	HCB	1760	3600	0.49	150	11.73		3.07	3	3.3	13.3
	E-6	HCB	1760	3600	0.49	150	11.73		3.07	3	3.1	13.1
Varela-Rivera, Moreno-Herrera, et al. (2012) [50]	E-1	HCB	2720	3670	0.74	150	18.13		2.84	4	2.63	8.79
	E-2	HCB	2880	3770	0.76	150	19.20		2.84	4	6.37	13.01
	E-3	HCB	2880	3770	0.76	120	24.00		2.85	4	4.81	12.01
	E-4	HCB	2720	2850	0.95	150	18.13		2.84	4	5.1	14.53
	E-5	HCB	2720	2950	0.92	150	18.13		2.84	4	5.1	17.83
	E-6	HCB	2720	2950	0.92	120	22.67		2.85	4	4.03	15.4
Varela-Rivera, Polanco-May, et al. (2012) [130]	S-1	HCB	2700	3700	0.73	150	18	0.000	2.840	4	2.63	8.79
	S-2	HCB	2700	3700	0.73	150	18	0.065	2.640	4	4.26	17.32
	S-3	HCB	2700	3700	0.73	150	18	0.196	2.640	4	6.22	18.91
Moreno-Herrera et al. (2015) [133]	W1	HCB2	2760	3770	0.73	113	24.42	0.079	3.72	4	-	8.81
	W2	MPB	2760	3770	0.73	115	24.00	0.082	6.48	4	-	10.49
	W3	MPB	2760	3770	0.73	120	23.00	0.079	6.17	4	-	11.06
	W4	SB	2760	3770	0.73	114	24.21	0.081	4.15	4	-	7.33
	W5	HCB2	2760	2950	0.94	113	24.42	0.088	3.72	4	-	13.44
	W6	MPB	2760	2950	0.94	115	24.00	0.092	6.48	4	-	17.61
	W7	MPB	2760	2950	0.94	120	23.00	0.078	6.17	4	-	18.06
	W8	SB	2760	2950	0.94	114	24.21	0.085	4.15	4	-	14.24
Navarrete-Marcias et al. (2016) [134]	M1	HCB	2550	3490	0.73	120	21.25	0.11	6.48	1	-	10.95
	M2	HCB	2550	3490	0.73	120	21.25	0.23	6.48	1	-	11.22
	M3	HCB	2550	3490	0.73	120	21.25	0.35	6.48	1	-	14.07
	M4	HCB	2550	2450	1.04	120	21.25	0.23	6.48	1	-	9.96
	M5	HCB	2550	1410	1.81	120	21.25	0.23	6.48	1	-	8.43
Varela-Rivera et al. (2020) [131]	M1	HCB	2710	1930	1.40	145	18.69	0	3.3	4	-	19.72
	M2	HCB	2710	1330	1.40	145	18.69	0.33	3.3	4	-	24.23
	M3	HCB	2710	1930	2.04	145	18.69	0.0	3.3	4	-	31.64
	M4	HCB	2710	1330	2.04	145	18.69	0.33	3.3	4	-	38.32

Table A4. Experimental database of CM walls with openings.

Study	Specimen	Peak Strength (kN)	$H/H_{ref}$	Opening Length Lop (m)	Opening Height Hop (m)	Panel Length $L$ (m)	Net Panel Length $L_n$ (m)	Panel Height $H_w$ (m)	Opening Area $A_o$ (m <sup>2</sup> )	Panel Area $A_p$ (m <sup>2</sup> )	$A_r$ Ratio	B Ratio
Yanez et al. (2004) [138]	Concrete Pattern 1	123.25	1.00	0.00	0.00	3.65	3.65	2.25	0.00	8.21	0.00	1.00
	Concrete Pattern 2	78.00	0.63	2.06	1.23	3.65	1.59	2.25	2.54	8.21	0.31	0.43
	Concrete Pattern 3	120.75	0.98	0.83	1.23	3.65	2.83	2.25	1.01	8.21	0.12	0.77
	Concrete Pattern 4	101.75	0.83	0.65	2.05	3.65	3.01	2.25	1.32	8.21	0.16	0.82
	Brick Pattern 1	176.50	1.00	0.00	0.00	3.65	3.65	2.25	0.00	8.21	0.00	1.00
	Brick Pattern 2	92.00	0.52	2.05	1.13	3.65	1.60	2.25	2.31	8.21	0.28	0.44
	Brick Pattern 3	146.25	0.83	0.79	1.13	3.65	2.87	2.25	0.88	8.21	0.11	0.78
	Brick Pattern 4	125.00	0.71	0.48	2.00	3.65	3.17	2.25	0.96	8.21	0.12	0.87
Singhal and Rai (2018) [141]	SI	84.25	1.00	0.00	0.00	2.50	2.50	1.50	0.00	3.75	0.00	1.00
	SI-O2WA	52.40	0.62	1.02	0.62	2.50	1.48	1.50	0.63	3.75	0.17	0.59
	SC-OW2B	75.35	0.89	1.00	0.62	2.50	1.50	1.50	0.62	3.75	0.17	0.60
	SC-OW2C	94.10	1.12	1.06	0.62	2.50	1.44	1.50	0.66	3.75	0.18	0.58
Okail (2016) [155]	SC-ODWB	63.85	0.76	0.50	1.10	2.50	2.00	1.50	0.55	3.75	0.15	0.80
	CLY S-CTRL	230.00	1.00	0.00	0.00	2.31	2.31	2.28	0.00	5.27	0.00	1.00
	CLY P-W	190.00	0.83	0.53	0.71	2.31	1.78	2.28	0.38	5.27	0.07	0.77
Qin (2021) [143]	CLY P-D	130.00	0.57	0.53	1.69	2.31	1.78	2.28	0.90	5.27	0.17	0.77
	S1	466.28	1.00	0.00	0.00	3.40	3.40	2.90	0.00	9.86	0.00	1.00
	O1	352.21	0.76	1.00	1.55	3.40	2.40	2.90	1.55	9.86	0.16	0.71
	O2	274.76	0.59	1.50	1.55	3.40	1.90	2.90	2.33	9.86	0.24	0.56
Kuroki (2012) [139]	O3	360.76	0.77	1.00	2.10	3.40	2.40	2.90	2.10	9.86	0.21	0.71
	CMWO-07	79.70	1.00	0.00	0.00	1.70	1.70	1.51	0.00	2.57	0.00	1.00
	CMWO-05	63.72	0.80	0.43	0.56	1.70	1.27	1.51	0.24	2.57	0.09	0.74
	CMWO-06	150.02	1.88	0.43	0.56	1.70	1.27	1.51	0.24	2.57	0.09	0.74
	CMWO-08	108.67	1.36	0.43	0.56	1.70	1.27	1.51	0.24	2.57	0.09	0.74
	CMWO-09	52.75	0.66	0.43	0.56	1.70	1.27	1.51	0.24	2.57	0.09	0.74
	CMWO-10	97.44	1.22	0.43	0.56	1.70	1.27	1.51	0.24	2.57	0.09	0.74
	CMWO-11	49.13	0.62	0.43	1.20	1.70	1.27	1.51	0.52	2.57	0.20	0.74
	CMWO-12	82.24	1.03	0.43	1.20	1.70	1.27	1.51	0.52	2.57	0.20	0.74
	CMWO-13	47.40	0.59	0.43	1.20	1.70	1.27	1.51	0.52	2.57	0.20	0.74
CMWO-14	78.61	0.99	0.43	1.20	1.70	1.27	1.51	0.52	2.57	0.20	0.74	

**Table A5.** Summary of experimental research studies on CM walls with toothed, doweled or no connections at the masonry-to-concrete interface.

Study	Type of Connection	# of Specimen	H/L	Masonry Unit	Max Drift (%)	In Plane Test	OPP Testing Included
						Failure Mechanism	
Vegas (1992) [145]	Toothing	1	1.2	Clay Brick 1/3	1.0	Shear	No
	Dowels	1	1.2	Clay Brick 1/3	1.0	Shear	
	None	1	1.2	Clay Brick 1/3	1.0	Shear	
San Bartolomé, Vegas, and Silva (1991) [146]	Dowels	1	1.2	Clay Brick 1/3	not available	OOP	Yes
	None	1	1.2	Clay Brick 1/3	not available	OOP	
Gonzalez (1993) [66]	Toothing	1	1	Clay Brick	0.65	Shear	Yes
	Dowels	1	1	Clay Brick	0.65	Shear	
Castellano et al. (2020) [148]	Toothing	1	0.74	Clay Brick	3.1	Shear cracking in masonry and RC tie-columns	No
	Dowels	0	-	-	-	-	
	None	1	0.74	Clay Brick	3.8	Shear cracking in masonry and RC tie-columns	
	Infill Frame	1	0.74	Clay Brick	5.0	Masonry shear cracking, and concrete crushing in RC tie-columns	
Singhal and Rai (2014) [147]	Toothing	2	1.1–1.2	Clay Brick	1.75	Shear cracking in masonry/reinforcement fracture in RC tie-columns	Yes
	Dowels	0	-	-	-	-	
	None	1	1.1	Clay Brick	1.75	Masonry shear cracking, and concrete crushing in RC tie-columns	
	Infill Frame	1	1.1	Clay Brick	1.75	Separation at the masonry wall and RC tie-beam interface at 0.5% drift	
Nguyen et al. (2017) [148]	Toothing	1	0.83	Brick/Double Wythe	3.0	Shear cracking in masonry and shear failure in RC tie-columns	No
	Dowels	1	0.83	Brick/Double Wythe	5.0	Shear cracking in masonry and shear failure in RC tie-columns	
Wijaya et al. (2011) [150]	Toothing	1	1	Clay Brick	2.46	Sliding Shear	No
	Dowels	1	1	Clay Brick	1.82	Shear	
	None	1	1	Clay Brick	1.08	Shear	
	Continuous Bar	1	1	Clay Brick	2.02	Shear	

## References

1. Brzev, S.; Mitra, K. *Earthquake-Resistant Confined Masonry Construction*, 3rd ed.; National Information Center on Earthquake Engineering: Kanpur, India, 2018.
2. Schacher, T.; Hart, T. *Construction Guide for Low-Rise Confined Masonry Buildings*; Earthquake Engineering Research Institute: Oakland, CA, USA, 2015.
3. Meli, R.; Brzev, S.; Astroza, M.; Boen, T.; Crisafulli, F.; Dai, J.; Farsi, M.; Hart, T.; Mebarki, A.; Moghadam, A.S.; et al. *Seismic Design Guide for Low-Rise Confined Masonry Buildings*; World Housing Encyclopedia Report, Earthquake Engineering Research Institute: Oakland, CA, USA, 2011.
4. Galvis, F.A.; Miranda, E.; Heresi, P.; Dávalos, H.; Ruiz-García, J. Overview of Collapsed Buildings in Mexico City after the 19 September 2017 (Mw7.1) Earthquake. *Earthq. Spectra* **2020**, *36*, 83–109. [[CrossRef](#)]
5. Astroza, M.; Moroni, O.; Brzev, S.; Tanner, J. Seismic Performance of Engineered Masonry Buildings in the 2010 Maule Earthquake. *Earthq. Spectra* **2012**, *28*, S385–S406. [[CrossRef](#)]
6. Confined Masonry Network | Promoting Seismically Safe, Economical Housing Worldwide. Available online: <https://confinedmasonry.org/> (accessed on 15 January 2023).
7. USCB. *U.S. and World Population Clock*. U.S. Census Bureau; U.S. Department of Commerce: Washington, DC, USA, 2018.
8. Brzev, S.; Reiter, M.; Pérez Gavilán, J.J.; Quiun, D.; Membreño, M.; Hart, T.; Sommer, D. Confined Masonry the Current Design Standards. In Proceedings of the 13 North American Masonry Conference, Salt Lake City, UT, USA, 16–19 June 2019.
9. Marques, R.; Lourenço, P. Structural Behaviour and Design Rules of Confined Masonry Walls: Review and Proposals. *Constr. Build. Mater.* **2019**, *217*, 137–155. [[CrossRef](#)]
10. Esteva, L. *Comportamiento de Muros de Mampostería Sujetos a Carga Vertical*; SID 46; Investigación, Instituto de Ingeniería, UNAM: Mexico City, Mexico, 1961. (In Spanish)
11. Madinaveitia, J. *Ensayes de Muros de Mampostería Con Cargas Excéntricas*; SID 296; Investigación, Instituto de Ingeniería, UNAM: Mexico City, Mexico, 1971. (In Spanish)
12. Madinaveitia, J.; Rodriguez, A. *Resistencia a Carga Vertical de Muros Fabricados Con Materiales Usuales En El Distrito Federal*; SID 261; Investigación, Instituto de Ingeniería, UNAM: Mexico City, Mexico, 1970. (In Spanish)
13. Meli, R.; Salgado, G. *Comportamiento de Muros de Mampostería Sujetos a Carga Lateral*; SID 237; Segundo Informe, Instituto de Ingeniería UNAM: Mexico City, Mexico, 1969. (In Spanish)
14. Meli, R.; Hernández, B. *Propiedades de Piezas Para Mampostería Producidas En El Distrito Federal*; Informe No. 297; Instituto de Ingeniería, UNAM: Mexico City, Mexico, 1971. (In Spanish)
15. Meli, R.; Hernández, O. *Efectos de Hundimientos Diferenciales En Construcciones a Base de Muros de Mampostería*; SID350; Instituto de Ingeniería UNAM: Mexico City, Mexico, 1975. (In Spanish)
16. Hernández, O.; Meli, R. *Modalidades de Refuerzo Para Mejorar El Comportamiento Sísmico de Muros de Mampostería*; SID382; Informe de Investigación, Instituto de Ingeniería, UNAM: Mexico City, Mexico, 1976. (In Spanish)
17. Meli, R. *Comportamiento Sísmico de Muros de Mampostería*, 2nd ed.; SID352; Corregida y Aumentada, Instituto de Ingeniería UNAM: Mexico City, Mexico, 1979. (In Spanish)
18. Bazán, E. *Muros de Mampostería Ante Cargas Laterales, Estudios Analíticos*. Ph.D. Thesis, UNAM, México City, Mexico, 1980. (In Spanish)
19. Hernández, O.; Guzmán, H. *Uso de Aceros de Alto Grado de Fluencia Para Confinar Muros de Tabique Rojo*; Laboratorio de Materiales, Instituto de Ingeniería, UNAM: Mexico City, Mexico, 1987. (In Spanish)
20. Hernández, O. *Mampostería Reforzada Con Acero de Alta Resistencia: Una Opción Segura y Económica Para La Vivienda de Bajo Costo*. In Proceedings of the Simposio Internacional Sobre Seguridad Sísmica en la Vivienda Económica, Mexico City, Mexico, 25–28 February 1991. (In Spanish)
21. Hernández, O.; Guzmán, H. *Ensaye Bajo Cargas Laterales Alternadas de Muros Construidos Con El Tabique MULTEX*; Laboratorio de Materiales, Facultad de Ingeniería, Universidad Nacional Autónoma de México: Mexico City, Mexico, 1996. (In Spanish)
22. Hernández, O. *Comportamiento de Muros Confinados Construidos Con Tabique TABIMAX Ante Cargas Laterales Alternadas*; Laboratorio de Materiales, Instituto de Ingeniería UNAM: Mexico City, Mexico, 1998. (In Spanish)
23. Hernández, O.; Basilio, I. *Comportamiento Ante Cargas Laterales Alternadas de Muros Construidos Con Tabique Multiperforado*. In Proceedings of the XII Congreso Nacional de Ingeniería Sísmica, Morelia, Michoacán, Mexico, 23–26 November 1999. (In Spanish)
24. Alcocer, S.; Meli, R. Test Program on the Seismic Behavior of Confined Masonry Structures. *Mason. Soc. J.* **1995**, *13*, 68–76.
25. Aguilar, G.; Díaz, R.; Vásquez del Mercado, A. Influence of Horizontal Reinforcement on the Behavior on Confined Masonry Walls. In Proceedings of the 11th World Conference of Earthquake Engineering, Acapulco, Guerrero, México, 23–28 June 1996.
26. Alcocer, S.; Zepeda, J.; Ojeda, M. *Estudio de La Factibilidad Técnica Del Uso de Tabique VINTEX y MULTEX Para Vivienda Económica*; Centro Nacional de Prevención de Desastres (CENAPRED): Mexico City, Mexico, 1997. (In Spanish)
27. Alcocer, S.; Zepeda, J. Behavior of Multi-Perforated Clay Brick Walls under Earthquake-Type Loading. In Proceedings of the 8th North American Masonry Conference, Austin, TX, USA, 3–6 June 1999.
28. Alcocer, S.; Ruiz, J.; Pineda, J.; Zepeda, J. Retrofitting of Confined Masonry Walls with Welded Wire Mesh. In Proceedings of the 11th World Conference on Earthquake Engineering, Acapulco, Guerrero, México, 23–28 June 1996.

29. Flores, L.; Alcocer, S. Calculated Response of Confined Masonry Structures. In Proceedings of the 11th World Conference on Earthquake Engineering, Acapulco, Guerrero, México, 23–28 June 1996.
30. Alcocer, S. Implications Derived from Recent Research in Mexico on Confined Masonry Structures. In *Proceedings of the Committee on Concrete and Masonry Structures (CCSM) Symposium*; American Society of Civil Engineers: Chicago, IL, USA, 1996.
31. Alcocer, S.; Muriá, D.; Peña, J. *Comportamiento Dinámico de Muros de Mampostería Confinada*; Universidad Nacional Autónoma de México: Mexico City, Mexico, 1999. (In Spanish)
32. NTC-M. *Normas Técnicas Complementarias Para Diseño y Construcción de Estructuras de Mampostería*; Gaceta Oficial del Distrito Federal: Mexico City, Mexico, 2004. (In Spanish)
33. NTC-M. *Normas Técnicas Complementarias Para Diseño y Construcción de Estructuras de Mampostería*; Gobierno de la Ciudad de México: Mexico City, Mexico, 2017. (In Spanish)
34. Pérez Gavilán, J.; Flores, L.; Jean, R.; Cesin, J.; Hernández, O. Relevant Aspects of the New Mexico City's Code for the Design and Construction of Masonry Structures. In Proceedings of the 16th World Conference on Earthquake Engineering, Santiago, Chile, 9–13 January 2017.
35. Pérez Gavilán, J.; Flores, L.; Alcocer, S. An Experimental Study of Confined Masonry Walls with Varying Aspect Ratios. *Earthq. Spectra* **2015**, *31*, 945–968. [[CrossRef](#)]
36. Pérez Gavilán, J.; Flores, L.; Manzano, A. A New Shear Strength Design Formula for Confined Masonry Walls: Proposal to the Mexican Code. In Proceedings of the Tenth U.S. National Conference on Earthquake Engineering, Anchorage, AL, USA, 21–25 July 2014.
37. Pérez Gavilán, J.; Cruz, A. Shear Strength of Confined Masonry Walls with Transverse Reinforcement. In *Brick and Block Masonry: Trends, Innovations and Challenges—Proceedings of the 16th International Brick and Block Masonry Conference, IBMAC 2016*; CRC Press: London, UK, 2016; pp. 2335–2344.
38. Leal, J.; Pérez Gavilán, J.; Castorena, G.; Velázquez, D. Infill Walls with Confining Elements and Horizontal Reinforcement: An Experimental Study. *Eng. Struct.* **2017**, *150*, 153–165. [[CrossRef](#)]
39. Pérez Gavilán, J. The Effect of Shear-Moment Interaction on the Shear Strength of Confined Masonry Walls. *Constr. Build. Mater.* **2020**, *263*, 120087. [[CrossRef](#)]
40. Cruz, A.; Pérez Gavilán, J.; Flores, L. Experimental Study of In-Plane Shear Strength of Confined Concrete Masonry Walls with Joint Reinforcement. *Eng. Struct.* **2019**, *182*, 213–226. [[CrossRef](#)]
41. Rubio, P. Contribución Del Refuerzo Horizontal a La Resistencia a Corte de Muros Confinados de Piezas de Arcilla Extruida. Master's Thesis, Instituto de Ingeniería UNAM, Mexico City, Mexico, 2017. (In Spanish)
42. Lizárraga, J.; Pérez Gavilán, J. Modelación No Lineal de Muros de Mampostería Empleando Elementos de Contacto. *Ing. Sísmica* **2015**, *93*, 41–59. (In Spanish) [[CrossRef](#)]
43. Lizárraga, J. Comportamiento de Muros de Mampostería Confinada Sobre Elementos Flexibles. Ph.D. Thesis, Instituto de Ingeniería UNAM, Mexico City, Mexico, 2017. (In Spanish)
44. Lizárraga, J.F.; Pérez-Gavilán, J.J. Parameter Estimation for Nonlinear Analysis of Multi-Perforated Concrete Masonry Walls. *Constr. Build. Mater.* **2017**, *141*, 353–365. [[CrossRef](#)]
45. Pérez Gavilán, J. *Análisis de Estructuras de Mampostería*, Sociedad Mexicana de Ingeniería Estructural; Sociedad Mexicana de Ingeniería Estructural A.C.: Mexico City, Mexico, 2015. (In Spanish)
46. Gómez, B.; Jean, P.; Pérez, A.; Treviño, E. *Edificaciones de Mampostería*; LIMUSA: Mexico City, Mexico, 2019. (In Spanish)
47. Alcocer, S.; Casas, N. Shake-Table Testing of a Small-Scale Five-Story Confined Masonry Building. In Proceedings of the Thirteenth North American Masonry Conference, Salt Lake City, UT, USA, 16–19 June 2019.
48. Flores, L.; Pérez Gavilán, J.; Alcocer, S. Displacement Capacity of Confined Masonry Structures Reinforced with Horizontal Reinforcement: Shaking Table Tests. In Proceedings of the 16th World Conference on Earthquake Engineering, Santiago, Chile, 9–13 January 2017.
49. Pérez Gavilán, J. Three Story CM Buildings with Joint Reinforcement: Shaking Table Tests. In Proceedings of the 17 Brick and Block Masonry Conference, Cracow, Poland, 5–8 July 2020.
50. Varela-Rivera, J.; Moreno-Herrera, J.; Lopez-Gutierrez, I.; Fernandez-Baqueiro, L. Out-of-Plane Strength of Confined Masonry Walls. *J. Struct. Eng.* **2012**, *138*, 1331–1341. [[CrossRef](#)]
51. Svojsik, M.; San Bartolomé, A. Relevant Masonry Projects Carried out in the Structures Laboratory at the Catholic University of Peru. In Proceedings of the 8th World Conference on Earthquake Engineering, San Francisco, CA, USA, 21–28 July 1984.
52. San Bartolomé, A.; Torrealva, D. A New Approach for Seismic Design of Masonry Buildings in Peru. In Proceedings of the Fifth North American Masonry Conference, Urbana-Champaign, IL, USA, 3–6 June 1990.
53. San Bartolomé, A. *Construcciones de Albañilería*; Fondo Editorial Pontificia Universidad Católica del Perú: Lima, Perú, 1994. (In Spanish)
54. San Bartolomé, A.; Quiun, D.; Torrealva, D. Seismic Behaviour of a Three-Story Half Scale Confined Masonry Structure. In Proceedings of the 10th World Conference on Earthquake Engineering, Madrid, Spain, 19–24 July 1992.
55. San Bartolomé, A.; Quiun, D.; Silva, D. *Diseño y Construcción de Estructuras Sismo-Resistentes de Albañilería*; Fondo Editorial de la Pontificia Universidad Católica del Perú: Lima, Perú, 2010. (In Spanish)
56. Quiun, D.; Santillán, P. Development of Confined Masonry Seismic Considerations, Research and Design Codes in Peru. In Proceedings of the 16th World Conference on Earthquake Engineering, Santiago, Chile, 9–13 January 2017.

57. Astroza, M.; Andrade, F.; Moroni, M.O. Confined Masonry Buildings: The Chilean Experience. In Proceedings of the 16th World Conference on Earthquake Engineering, Santiago, Chile, 9–13 January 2017.
58. Moroni, M.; Astroza, M.; Tavonatti, S. Nonlinear Models for Shear Failure in Confined Masonry Walls. *TMS J.* **1994**, *12*, 72–78.
59. Moroni, M.; Astroza, M.; Acevedo, C. Performance and Seismic Vulnerability of Masonry Housing Types Used in Chile. *J. Perform. Constr. Facil.* **2004**, *18*, 173–179. [[CrossRef](#)]
60. Moroni, M.; Astroza, M.; Caballero, C. Wall Density and Seismic Performance of Confined Masonry Buildings. *TMS J.* **2000**, *18*, 79–86.
61. Moroni, M.; Astroza, M.; Salinas, C. Seismic Displacement Demands in Confined Masonry Buildings. In Proceedings of the 8th North American Masonry Conference, Austin, TX, USA, 6–9 June 1999.
62. Tomaževič, M. Shear Resistance of Masonry Walls and Eurocode 6: Shear versus Tensile Strength of Masonry. *Mater. Struct.* **2009**, *42*, 889–907. [[CrossRef](#)]
63. Ministerio de Vivienda, Construcción y Saneamiento. *Norma Técnica E.070 Albañilería*; Servicio Nacional de Capacitación Para La Industria de La Construcción: Lima, Peru, 2018. (In Spanish)
64. Treviño, E.; Larrúa, R.; Flores, L.; Alcocer, S.; Cabrera, Y.; Acevedo, A. Evaluación de Técnicas de Inteligencia Artificial Para La Predicción de La Respuesta de Muros de Mampostería Confinada. In Proceedings of the XIX Congreso Nacional de Ingeniería Estructural, Puerto Vallarta, Jalisco, México, 13–15 November 2014. (In Spanish)
65. Aguilar, G.; Alcocer, S. *Efecto Del Refuerzo Horizontal En El Comportamiento de Muros de Mampostería Confinada Ante Cargas Laterales*; CI/IEG-10122011; CENAPRED: Mexico City, Mexico, 2001. (In Spanish)
66. González, I. Estudio de La Conexión Columna-Albañilería En Muros Confinados. Civil Engineer Thesis, Facultad de Ciencias e Ingeniería, Pontificia Universidad Católica del Perú, San Miguel, Peru, 1993. (In Spanish)
67. Pineda, J.A. Comportamiento ante Cargas Laterales de Muros de Mampostería Confinada Reforzados con Malla Electrosoldada. Master's Thesis, DEPI, Universidad Nacional Autónoma de México, México City, Mexico, 1996. (In Spanish)
68. Mendoza, J.A. Estudio Experimental de Muros de Mampostería Confinada con y Sin Refuerzo Alrededor de la Abertura. Professional Thesis, Universidad Nacional Autónoma de México, México City, Mexico, 2006. (In Spanish)
69. Vázquez, A. Ensayo Experimental de Viviendas de Mampostería Confinada de un Piso Mediante el Ensayo en Mesa Vibradora. Master's Thesis, Universidad Nacional Autónoma de México, México City, Mexico, 2005. (In Spanish)
70. Arias, J.G. Ensayos en Mesa Vibradora de un Modelo a Escala 1:2 de Edificio de Mampostería Confinada de Tres Niveles. Master's Thesis, Universidad Nacional Autónoma de México, México City, Mexico, 2005. (In Spanish)
71. Barragán, R. Ensayo de Una Vivienda a Escala de Dos Niveles de Mampostería Confinada. Master's Thesis, Universidad Nacional Autónoma de México, México City, Mexico, 2005. (In Spanish)
72. Díez, R.J. Estudio Experimental de Muros de Albañilería Sometidos a Carga Lateral Alternada. Bachelor's Thesis, Universidad de Chile, Santiago, Chile, 1987. (In Spanish)
73. San Bartolomé, A. Ensayos de Carga Lateral en Muros de Albañilería Confinados—Correlación de Resultados Entre Especímenes a Escala Natural y Probetas Pequeñas. In Proceedings of the XXII Jornadas Sudamericanas de Ingeniería Estructural, Santiago, Chile, 1–4 July 1983. (In Spanish)
74. San Bartolomé, A.; Comportamiento Sísmico de Muros de Albañilería Confinada Reforzados con Canastillas Dúctiles y Electrosoldadas. Blog de San Bartolomé, Pontificia Universidad Católica del Perú. Available online: <http://blog.pucp.edu.pe/blog/wp-content/uploads/sites/82/2007/09/Canastilla-Electrosoldada.pdf> (accessed on 28 June 2023). (In Spanish)
75. San Bartolomé, A.; Pehovaz, R.; Comportamiento a Carga Lateral Cíclica de Muros de Adobe Confinados. Blog de San Bartolomé, Pontificia Universidad Católica del Perú. Available online: <http://blog.pucp.edu.pe/blog/wp-content/uploads/sites/617/2007/04/Adobe-Confinado.pdf> (accessed on 28 June 2023). (In Spanish)
76. Zepeda, J.A.; Alcocer, S. Comportamiento Ante Cargas Laterales de Muros de Ladrillo de Arcilla Perforado y Multiperforado. Informe Técnico, CENAPRED: Mexico City, Mexico, 2001. (In Spanish)
77. Echevarría, G.; San Bartolomé, A. Ensayo de Carga Lateral en Muros de Albañilería Confinados—Efectos de la Carga Vertical. In Proceedings of the VI Congreso Nacional de Ingeniería Civil, Colegio de Ingenieros del Perú, Cajamarca, Perú, 1–3 May 1986. (In Spanish)
78. Pastorutti, O.; San Bartolomé, A. Ensayos de Carga Lateral en Muros de Albañilería Confinados—Efectos del Refuerzo. In Proceedings of the VI Congreso Nacional de Ingeniería Civil, Colegio de Ingenieros del Perú, Cajamarca, Perú, 24–26 November 1986. (In Spanish)
79. Alcocer, S.M.; Marcelino, J. *Factibilidad del Uso de Malla de Alambre Soldado y Recubrimiento de Mortero en Muros de Bloque Como Técnica de Rehabilitación, Conjunto Rancho Alegre*; Informe interno; Instituto de Ingeniería, UNAM: Mexico City, Mexico, 2003.
80. Urzúa, D.A. Investigación de la resistencia sísmica de muros de mampostería elaborados con materiales típicos de Guadalajara. Master's Thesis, Universidad de Guadalajara, Guadalajara, Mexico, 1999. (In Spanish)
81. Cosío, C.O. Influencia de la Relación de Aspecto y de la Carga Vertical en la Resistencia Sísmica de Muros de Mampostería Confinada Elaborados con Materiales Típicos de Guadalajara. Master's Thesis, Universidad de Guadalajara, Guadalajara, Mexico, 2001. (In Spanish)
82. Meli, R.; Zeevaert, A.; Esteva, L. *Comportamiento de Muros de Mampostería Hueca Ante Carga Lateral Alternada*; Informe No. 156; Instituto de Ingeniería, UNAM: Mexico City, Mexico, 1968.

83. Treviño, E.; Alcocer, S.M.; Flores, L.E.; Larrúa, R.; Zárate, J.M.; Gallegos, L. Investigación Experimental del Comportamiento de Muros de Mampostería Confinada de Bloques de Concreto Sometidos a Cargas Laterales Cíclicas Reversibles Reforzados con Acero Grados 60 y 42. In Proceedings of the Memorias XIV Congreso Nacional de Ingeniería Estructural, Acapulco, Mexico, 29 October–1 November 2004. (In Spanish)
84. Muñoz, F.W. Estudio Experimental del Comportamiento de Muros de Albañilería de Bloques de Hormigón Sometidos a Carga Lateral Alternada. Bachelor's Thesis, Universidad de Chile, Santiago, Chile, 1992. (In Spanish)
85. Ramírez, V.; Saavedra, C.; San Bartolomé, A. Ensayo a Carga Lateral en Muros con Bloques de Concreto Vibrado—Efectos del Refuerzo. In Proceedings of the V Congreso Nacional de Ingeniería Civil, Colegio de Ingenieros del Perú, Tacna, Perú, 1–3 September 1984. (In Spanish)
86. Quiun, D.; Alferez, K.; Quinto, D. Reforzamiento Estructural de Muros de Albañilería de Bloques Artesanales de Concreto. In Proceedings of the Congreso Chileno de Sismología e Ingeniería Antisísmica IX Jornadas, Concepción, Chile, 16–19 November 2005. (In Spanish)
87. Marinilli, A.; Castilla, E. *Evaluación Sismorresistente de Muros de Mampostería Confinada con Dos o Más Machones*; Boletín Técnico, Instituto de Materiales y Modelos Estructurales, Facultad de Ingeniería, Universidad Central de Venezuela (UCV): Caracas, Venezuela, 2007. (In Spanish)
88. Castilla, C.E. Evaluación de la Respuesta de Muros Confinados de Bloques de Concreto contra Ciclos Severos de Carga Lateral. Ph.D. Thesis, Universidad Central de Venezuela, Caracas, Venezuela, 1998. (In Spanish)
89. Turnšek, V.; Čačovič, F. Some Experimental Results on the Strength of Brick Masonry Walls. In Proceedings of the 2nd International Brick Masonry Conference, British Ceramic Society, Stoke-on-Trent, UK, 12–15 April 1971.
90. Matsumura, A. Shear Strength of Reinforced Masonry Walls. In Proceedings of the Ninth World Conference on Earthquake Engineering, Tokyo-Kyoto, Japan, 2–9 August 1988.
91. D'Amore, E.; Decanini, L. Shear Strength Analysis of Confined Masonry Panels under Cyclic Loads: Comparison between Proposed Expressions and Experimental Data. In Proceedings of the 9th International Seminar on Earthquake Diagnostics, San José, Costa Rica, 19–23 September 1994.
92. Álvarez, J. Some Topics of the Seismic Behavior of Confined Masonry Structures. In Proceedings of the 11th World Conference on Earthquake Engineering, Acapulco, México, 23–28 June 1996.
93. Zeballos, A.; San Bartolomé, A.; Muñoz, A. Efectos de la esbeltez sobre la resistencia a fuerza cortante de los muros de albañilería confinada, Análisis por elementos finitos. Blog de Angel San Bartolomé, Pontificia Universidad Católica de Perú. Available online: <http://blog.pucp.edu.pe/blog/wp-content/uploads/sites/82/2007/05/Esbeltez{-}{-}Elementos-finitos.pdf> (accessed on 28 June 2023). (In Spanish)
94. Seif Eldin, H.M.; Galal, K. In-Plane Seismic Performance of Fully Grouted Reinforced Masonry Shear Walls. *J. Struct. Eng.* **2017**, *143*, 04017054. [[CrossRef](#)]
95. Pérez Gavilán, J.; Cardel, J. Shear-Moment Interaction in Confined Masonry Walls: Is It Worth Considering? *Bridge Struct. Eng.* **2015**, *45*, 19–28.
96. Drysdale, R.G.; Hamid, A.A. *Masonry Structures: Behavior and Design*, 3rd ed.; The Masonry Society: Boulder, CO, USA, 2008; p. 750.
97. Voon, K.C.; Ingham, J.M. Experimental In-Plane Shear Strength Investigation of Reinforced Concrete Masonry Walls. *J. Struct. Eng.* **2006**, *132*, 400–408. [[CrossRef](#)]
98. Anderson, D.; Priestley, M. In Plane Shear Strength of Masonry Walls. In Proceedings of the 6th Canadian Masonry Symposium, Saskatchewan, SK, Canada, 15–17 June 1992.
99. Canadian Standards Association (CSA). *Design of Masonry Structures*; CSA: Toronto, ON, Canada, 2014.
100. Seif Eldin, H.M.; Galal, K. Influence of Axial Compressive Stress on the In-Plane Shear Performance of Reinforced Masonry Shear Walls. In Proceedings of the 11th Canadian Conference on Earthquake Engineering, Victoria, BC, Canada, 21–24 July 2015.
101. *NZS 4230:2004*; Design of Reinforced Concrete Masonry Structures. Standards Association of New Zealand (SANZ): Wellington, New Zealand, 2004.
102. Riahi, Z.; Elwood, J.; Alcocer, S. Backbone Model for Confined Masonry Walls for Performance-Based Seismic Design. *J. Struct. Eng.* **2009**, *135*, 644–654. [[CrossRef](#)]
103. *TMS 402-16 and TMS 602-16*; Masonry Designers' Guide: Based on Building Code Requirements and Specification for Masonry Structures. Masonry Society (U.S.): Longmont, CO, USA.
104. Wakabayashi, M.; Nakamura, T. Reinforcing Principle and Seismic Resistance of Brick Masonry Walls. In Proceedings of the 8th World Conference on Earthquake Engineering, San Francisco, CA, USA, 2–9 August 1988.
105. Tomažević, M.; Lutman, M. Seismic Resistance of Reinforced Masonry Walls. In Proceedings of the 9th World Conference on Earthquake Engineering, Tokyo-Kyoto, Japan, 2–9 August 1988.
106. Shing, B.P.; Member, A.; Noland, J.L.; Klamerus, E.; Spaeh, H. Inelastic Behavior of Concrete Masonry Shear Walls. *J. Struct. Eng.* **1989**, *115*, 2204–2225. [[CrossRef](#)]
107. Shing, B.P.; Member, A.; Schuller, M.; Hoskere, V.S. In Plane Resistance of Reinforced Masonry Shear Walls. *J. Struct. Eng.* **1990**, *116*, 619–640. [[CrossRef](#)]
108. Sanchez, T.; Flores, L.; Alcocer, S.; Meli, R. *Respuesta Sísmica de Muros de Mampostería Confinada Con Diferentes Tipos de Refuerzo*; TA658.44 R47; CENAPRED: Mexico City, Mexico, 1992. (In Spanish)

109. Pérez Gavilán, J. Ductility of Confined Masonry Walls: Results from Several Experimental Campaigns in Mexico. In Proceedings of the 13th North American Masonry Conference, Salt Lake City, UT, USA, 16–19 June 2019.
110. Borah, B.; Singhal, V.; Kaushik, H. Experimental Validation of a Design Methodology for Tie-Columns of Confined Masonry Buildings. In Proceedings of the 14th North American Masonry Conference, Omaha, NE, USA, 11–14 June 2023.
111. Meli, R. Behavior of Masonry Walls under Lateral Loads. In Proceedings of the 5th World Conference on Earthquake Engineering, Rome, Italy, 25–29 June 1973.
112. Gouveia, J.; Lourenço, P. Masonry Shear Strength Walls Subjected to Cyclic Loading: Influence of Confinement and Horizontal Reinforcement. In Proceedings of the 10th North American Masonry Conference, St. Luis, MI, USA, 3–6 June 2007.
113. El-Dakhkhni, W.W.; Banting, B.R.; Miller, S.C. Seismic Performance Parameter Quantification of Shear-Critical Reinforced Concrete Masonry Squat Walls. *J. Struct. Eng.* **2013**, *139*, 957–973. [[CrossRef](#)]
114. Voon, K.C.; Ingham, J.M.; Asce, M. Design Expression for the In-Plane Shear Strength of Reinforced Concrete Masonry. *J. Struct. Eng.* **2007**, *133*, 706–713. [[CrossRef](#)]
115. Applied Technology Council. *Seismic Design Guidelines for Highway Bridges, ATC-6*; Applied Technology Council: Berkeley, CA, USA, 1981.
116. Shing, P.B.; Schuller, M.; Hoskere, V.S.; Carter, E. Flexural and Shear Response of Reinforced Masonry Walls. *Struct. J.* **1990**, *87*, 646–656.
117. Sveinsson, B.I.; McNiven, H.D.; Sucuoglu, H. *Cyclic Loading Tests of Masonry Single Piers, Volume 4: Additional Tests with Height to Width Ratio of 1*; Report No UCB/EERC-85/15; University of California Berkeley: Berkeley, CA, USA, 1985.
118. Varela-Rivera, J.; Fernandez-Baqueiro, L.; Gamboa-Villegas, J.; Prieto-Coyoc, A.; Moreno-Herrera, J. Flexural Behavior of Confined Masonry Walls Subjected to In-Plane Lateral Loads. *Earthq. Spectra* **2019**, *55*, 405–422. [[CrossRef](#)]
119. Paulay, T.; Priestley, M. *Seismic Design of Reinforced and Masonry Buildings*; John Wiley & Sons, INC.: New York, NY, USA, 1992.
120. Yoshimura, K.; Kikuchi, K.; Kuroki, M.; Nonaka, H.; Kyong, K.; Wangdi, R.; Oshikata, A. Experimental Study for Developing Higher Seismic Performance of Brick Masonry Walls. In Proceedings of the 13th World Conference on Earthquake Engineering, Vancouver, BC, Canada, 1–6 August 2004.
121. Bustos, J.; Zabala, F.; Masanet, A.; Santalucía, J. Estudio Del Comportamiento Dinámico de Un Modelo de Mampostería Encadenada Mediante Un Ensayo En Mesa Vibratoria. In Proceedings of the Anales de las XXIX Jornadas Sudamericanas de Ingeniería Estructural, Punta del Este, Uruguay, 13–17 November 2000. (In Spanish)
122. Varela-Rivera, J.; Fernandez-Baqueiro, L.; Alcocer-Canche, R.; Ricalde-Jimenez, J.; Chim-May, R. Shear and Flexural Behavior of Autoclaved Aerated Concrete Confined Masonry Walls. *Struct. J.* **2018**, *115*, 1453–1462. [[CrossRef](#)]
123. Tomaževič, M. *Earthquake-Resistant Design of Masonry Buildings*; Imperial College Press: London, UK, 1999.
124. Brzev, S.; Astroza, M.; Moroni Yadlin, M.O. *Performance of Confined Masonry Buildings in the 27 February 2010 Chile Earthquake*; A Report Prepared for the Confined Masonry Network; Earthquake Engineering Research Institute: Oakland, CA, USA, 2010.
125. McDowell, E.; McKee, K.; Sevin, E. Arching Action Theory of Masonry Walls. *J. Struct. Div.* **1956**, *82*, 1–8. [[CrossRef](#)]
126. Anić, F.; Penava, D.; Abrahamczyk, L.; Sarhosis, V. A Review of Experimental and Analytical Studies on the Out-of-Plane Behaviour of Masonry Infilled Frames. *Bull. Earthq. Eng.* **2020**, *18*, 2191–2246. [[CrossRef](#)]
127. Angel, R.; Abrams, D.; Shapiro, D.; Uzarski, J.; Webster, M. *Behavior of Reinforced Concrete Frames with Masonry Infills*; Technical Report; University of Illinois Engineering Experiment Station, College of Engineering, University of Illinois at Urbana-Champaign: Champaign, IL, USA, 1994.
128. Moghaddam, H.; Goudarzi, N. Transverse Resistance of Masonry Infills. *ACI Struct. J.* **2010**, *107*, 461–467.
129. Varela-Rivera, J.L.; Navarrete-Macias, D.; Fernandez-Baqueiro, L.E.; Moreno, E.I. Out-of-Plane Behaviour of Confined Masonry Walls. *Eng. Struct.* **2011**, *33*, 1734–1741. [[CrossRef](#)]
130. Varela-Rivera, J.; Polanco-May, M.; Fernandez-Baqueiro, L.; Moreno-Herrera, J. Confined Masonry Walls Subjected to Combined Axial Loads and Out-of-Plane Uniform Pressures. *Can. J. Civ. Eng.* **2012**, *39*, 439–447. [[CrossRef](#)]
131. Varela-Rivera, J.; Moreno-Herrera, J.; Fernandez-Baqueiro, L.; Cacep-Rodriguez, J.; Freyre-Pinto, C. Out-of-Plane Behavior of Confined Masonry Walls with Aspect Ratios Greater than One. *Can. J. Civ. Eng.* **2020**, *48*, 89–97. [[CrossRef](#)]
132. Moreno-Herrera, J.; Varela-Rivera, J.; Fernandez-Baqueiro, L. Bidirectional Strut Method: Out-of-Plane Strength of Confined Masonry Walls. *Earthq. Spectra* **2014**, *41*, 1029–1035. [[CrossRef](#)]
133. Moreno-Herrera, J.; Varela-Rivera, J.; Fernandez-Baqueiro, L. Out-of-Plane Design Procedure for Confined Masonry Walls. *J. Struct. Eng.* **2015**, *142*, 04015126. [[CrossRef](#)]
134. Navarrete-Macias, D.; Varela-Rivera, J.; Fernandez-Baqueiro, L. Out-Of-Plane Behavior of Confined Masonry Walls Subjected to Concentrated Loads (One-Way Bending). *Earthq. Spectra* **2016**, *32*, 2317–2335. [[CrossRef](#)]
135. Tu, Y.H.; Chuang, T.H.; Liu, P.M.; Yang, Y.S. Out-of-Plane Shaking Table Tests on Unreinforced Masonry Panels in RC Frames. *Eng. Struct.* **2010**, *32*, 3925–3935. [[CrossRef](#)]
136. Komaraneni, S.; Rai, D.C.; Singhal, V. Seismic Behavior of Framed Masonry Panels with Prior Damage When Subjected to Out-of-Plane Loading. *Earthq. Spectra* **2011**, *27*, 1077–1103. [[CrossRef](#)]
137. Chopra, A.K. *Dynamic of Structures*, 5th ed.; Pearson Education: Upper Saddle River, NJ, USA, 2016.
138. Yáñez, F.; Astroza, M.; Holmberg, A.; Ogaz, O. Behavior of Confined Masonry Shear Walls with Large Openings. In Proceedings of the 13th World Conference on Earthquake Engineering, Vancouver, BC, Canada, 1–6 August 2004.

139. Kuroki, M.; Kikuchi, K.; Nonaka, H.; Shimosako, M. Experimental Study on Reinforcing Methods Using Extra RC Elements for Confined Masonry Walls with Openings. In Proceedings of the 15th World Conference on Earthquake Engineering, Lisbon, Portugal, 24–28 September 2012.
140. Eshghi, S.; Pourazin, K. In-Plane Behavior of Confined Masonry Walls with and without Opening. *Int. J. Civ. Eng.* **2009**, *7*, 49–60.
141. Singhal, V.; Rai, D.C. Behavior of Confined Masonry Walls with Openings under In-Plane and Out-of-Plane Loads. *Earthq. Spectra.* **2018**, *34*, 817–841. [[CrossRef](#)]
142. Tu, Y.; Hsu, Y.; Chao, Y. Lateral Load Experiment for Confined and Infilled Unreinforced Masonry Panels with Openings in RC Frames. In Proceedings of the 12th North American Masonry Conference, Denver, CO, USA, 17–20 May 2015.
143. Qin, C.; Gao, Z.; Wu, T.; Bai, G.; Fu, G. Shear Testing and Analysis of the Response of Confined Masonry Walls with Centered Openings Made with Innovative Sintered Insulation Shale Blocks. *Soil Dyn. Earthq. Eng.* **2021**, *150*, 106901. [[CrossRef](#)]
144. San Bartolomé, A.; Angles, P.; Quiun, D. Seismic Behavior Comparison Of Confined Masonry Walls Of Clay And Concrete Bricks. In Proceedings of the 15th International Brick and Block Masonry Conference, Florianópolis, Brazil, 3–6 June 2012.
145. Vegas, C. Efectos de la Conexión Albañilería—Columna en el Comportamiento Sísmico de Muros de Albañilería Confinada. Civil Engineering Thesis, Facultad de Ciencias e Ingeniería, Pontificia Universidad Católica del Perú, San Miguel, Peru, 1992. (In Spanish)
146. San Bartolomé, A.; Vegas, C.; Silva, W. Ensayo Dinámico Perpendicular al Plano de Muros de Albañilería Confinados, Previamente Agrietados Por Corte. Blog de Angel San Bartolomé, Pontificia Universidad Católica de Perú. Available online: <http://blog.pucp.edu.pe/blog/wp-content/uploads/sites/82/2007/06/Clelia-Wilson.pdf> (accessed on 28 June 2023). (In Spanish)
147. Singhal, V.; Rai, D.C. Role of Tothing on In-Plane and Out-of-Plane Behavior of Confined Masonry Walls. *J. Struct. Eng.* **2014**, *140*, 04014053. [[CrossRef](#)]
148. Nguyen, L.; Corotis, R.; Schuller, M.; Camata, G. Confined Masonry Shear Walls: Experimental Testing and Analysis. *TMS J.* **2017**, *35*, 1–18.
149. Castellano, W.; Torrisi, G.; Crisafulli, F. Experimental Behavior of Masonry Walls with Different Types of Interfaces. *Rev. Int. Ing. Estruct.* **2020**, *25*, 261–284.
150. Wijaya, W.; Kusumastuti, D.; Suarjana, M.; Rildova; Pribadi, K. Experimental Study on Wall-Frame Connection of Confined Masonry Wall. *Procedia Eng.* **2011**, *14*, 2094–2102. [[CrossRef](#)]
151. Kaushik, H.B.; Rai, D.C.; Jain, S.K. Stress-Strain Characteristics of Clay Brick Masonry under Uniaxial Compression. *J. Mater. Civ. Eng.* **2007**, *19*, 728–739. [[CrossRef](#)]
152. Zabala, F.; Bustos, J.; Masanet, A.; Santalucia, J. Experimental Behavior of Masonry Structural Walls Used in Argentina. In Proceedings of the 13th World Conference on Earthquake Engineering, Vancouver, BC, Canada, 1–6 August 2004.
153. Pérez Gavilán, J.; Gómez, G.; Jean, R.; Gomez, A.; Treviño, T. Capítulo 6. In *Edificaciones de mampostería*; Limusa: Mexico City, Mexico, 2019. (In Spanish)
154. Meli, R.; Reyes, G. *Propiedades Mecánicas de La Mampostería*; Reporte de Investigación; SID 288; Instituto de Ingeniería de la UNAM: Mexico City, Mexico, 1971. (In Spanish)
155. Okail, H.; Abdelrahman, A.; Abdelkhalik, A.; Metwaly, M. Experimental and Analytical Investigation of the Lateral Load Response of Confined Masonry Walls. *HBRC J.* **2016**, *12*, 33–46. [[CrossRef](#)]

**Disclaimer/Publisher’s Note:** The statements, opinions and data contained in all publications are solely those of the individual author(s) and contributor(s) and not of MDPI and/or the editor(s). MDPI and/or the editor(s) disclaim responsibility for any injury to people or property resulting from any ideas, methods, instructions or products referred to in the content.